Notification: An updated report will soon be available

Understanding the potential habituation of seabirds to offshore wind farms is key for the site selection and impact assessment of offshore wind farms.

The models used for data analysis in this report have been updated to improve the signal-to-noise ratio and better cope with different levels of patchiness across different surveys/species. This has resulted in new abundance estimates which are higher than the previously reported. The differences are primarily related to the degree of extrapolation from the survey data into areas unseen by the aerial surveys.

An updated report, with a complete analysis of all relevant data, will replace the previous report.

The updated version will be published by end of November 2025 and includes novel data from six aerial surveys in winter 2024/2025, which may also introduce some changes between the previous and the updated report.

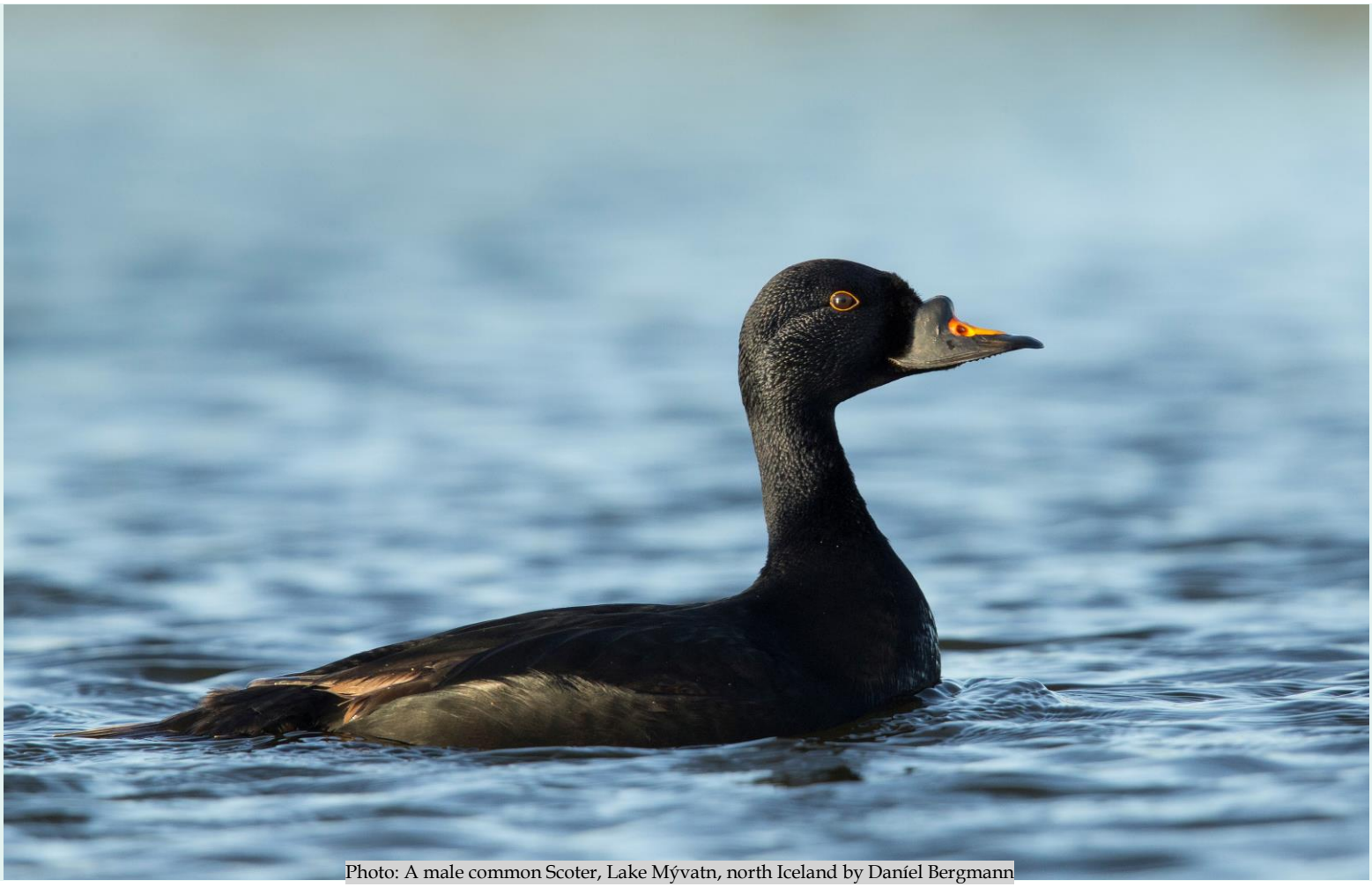

Photo: A male common Scoter, Lake Mývatn, north Iceland by Daníel Bergmann

Changes in the distribution and abundance of common scoter and diver species in the Horns Rev I, II and III offshore windfarm areas, Denmark

Bird distribution responses to wind farms, Horns Rev

Energinet Eltransmission A/S

Date: 15. November 2024

Rev. no.	Date	Description	Done by	Verified by	Approved by
3.0	15th November 2024	Horns Rev. Analyses of the distribution of common scoter and divers	Lindesay Scott-Hayward (CREEM) Ib Krag Petersen (DCE) Monique MacKenzie (CREEM) Claus Lunde Pedersen (DCE) Saana Isojunno (CREEM) Rasmus Due Nielsen (DCE) Jacob Sterup (DCE) Heidi Maria Thomsen (DCE) Rune Sø Neergaard (NIRAS)	Tony Fox (DCE) Rune Sø Neergaard (NIRAS)	Søren Granskov (NIRAS) Jesper Reinholt Fredshavn (DCE)

Contents

Preface

This report was commissioned by Energinet. It describes results obtained from the bird survey program in connection with the planned construction of the offshore wind farms (OWF's) area, and specifically addresses the distributional behaviour of divers (red-throated diver/black-throated diver) and common scoter within and around the Horns Rev I, the Horns Rev II and Horns Rev III offshore wind farms.

The report builds upon data collected under this project in combination with bird survey data from other previous projects within that same area between 2000 and 2012. The report has eight main chapters. Chapter 1 is Introduction and objectives of the report. Chapter 2 details the methods used. Chapter 3 describes the results of the work. Chapter 4 provides a discussion about the results. Chapter 5 provides conclusions from the work.

Front page illustration: An adult male common scoter at Lake Mývatn, north Iceland, photographed by Daníel Bergmann, Iceland.

Declaration

This report was prepared in close collaboration between CREEM, Univ. of St. Andrews, Aarhus University (DCE) and NIRAS. Aarhus University has been responsible for the data collection and data collation from survey data from 2000 to 2024 in the survey area. CREEM was responsible for statistical analyses of the data, encompassing Distance Sampling detection functions, spatial modelling of the survey data by survey and for the comparison of changes in distribution between phases of the OWF development in the survey area. NIRAS was responsible for project coordination.

The report was peer-reviewed by Tony Fox, Aarhus University, and quality assured by Jesper Fredshavn at DCE, Aarhus University and Rune Sø Neergaard, NIRAS. Søren Granskov, NIRAS gave final approval for publication of the report by NIRAS.

Energinet commented on a first and second draft of the report before the final version was published, the comments and author replies can be found here:

https://dce.au.dk/udgivelser/oevrige-dce-udgivelser/eksterne-udgivelser/2024.

The report is published by the Danish Energy Agency as part of the tender for OWF's in North Sea I.

The report and associated investigations were financed by Energinet. Energinet wrote the initial section of the Introduction chapter.

List of key terms

A list of terms (in English and Danish) and their explanations in relation to the Horns Rev study.

English (abbreviation)	Danish	Explanation
HR I	Horns Rev I havvindmøllepark	The Horns Rev I OWF
HR II	Horns Rev II havvindmøllepark	The Horns Rev II OWF
HR III	Horns Rev III havvindmøllepark	The Horns Rev III OWF
Phase 0	Før opførelse af HR I, HR II og HR III	The pre-construction phase of both the HR I, the HR II and the HR III OWF's
Phase 1	Efter opførelse af HR I, men før opførelse af HR II og HR III	The post-construction phase of HR I and pre-construction phase of both the HR II and the HR III OWF's
Phase 2	Efter opførelse af HR I og HR II, men før opførelse af HR III	The post-construction phase of HR I and HR II, and pre-construction phase of the HR III OWF
Phase 3	Efter opførelse af HR I, HR II og HR III	Post-construction of all three OWF's

Summary

Between February 2000 and April 2024, 56 observer-based aerial surveys of birds were conducted at Horns Rev, an area of the North Sea off central Jutland, using a Distance Sampling line transect survey design. The survey area covered the offshore wind farm (OWF) areas of Horns Rev I (HR I), Horns Rev II (HR II) and Horns Rev III (HR III). The surveys were classified into four phases according to the wind farm development stages. Phase 0 included 15 surveys prior to any wind farm construction, Phase 1 included 25 surveys post-construction HR I and pre-construction HR II and HR III, Phase 2 included 10 surveys post-construction HR I and HR II, but pre-construction HR III, while Phase 3 included six surveys post-construction of all three OWF's. These data in combination offers a unique opportunity to address the potential change in the displacement of birds over time, based on empirical data.

This report describes the changes in abundance and distribution of common scoter *Melanitta nigra* and divers (predominantly red-throated divers *Gavia stellata* but potentially including some black-throated divers *Gavia arctica*) over the period, based on the statistical analysis of visual aerial survey data in the Danish North Sea Horns Rev region gathered during the surveys described above. Species-specific distance analyses were conducted and pooled across surveys, followed by survey-specific spatial analyses with covariates including water depth (bathymetry), distance from the coast.

The outputs of the models were used to assess changes in distribution and abundance for common scoters and divers in relation to the three wind farms: Horns Rev I, II and III.

The number of common scoters in the survey area increased markedly from Phase 0 to Phase 2, then levelled off through Phase 3. Because of a general shift in the distribution of common scoter in the survey area over the first years of the survey period, with birds gradually moving further west into the area, it was difficult to assess the impact of the installation of the HR I. For the HR II area, there was evidence of a displacement between Phase 1 and Phase 2 in the footprint of the wind farm, which was out to a distance of 5 km. For the Phase 2 to Phase 3 period, the density increased significantly. Intriguingly, there seemed to be no displacement of common scoters after the construction of HR III.

While common scoters occurred at Horns Rev in high densities, diver densities were much lower. Diver abundance increased moderately between Phases 0 and 1 but then decreased through Phases 2 and 3. In the HR I area, diver density increased (but non-significantly) between Phases 0 and 1 and decreased through Phases 2 and 3. In the HR II area diver density increased between Phase 1 and Phase 2 and declined significantly after the construction of HR II. This decline continued into Phase 3. There was a significant decrease in density out to ca. 4 km from the periphery of the HR II wind farm between Phase 1 and 2, but significant decreases out to ca. 10 km when comparing Phase 1 to 3 or Phase 2 to 3. In the HR III area, diver density was stable through Phases 2 and 3, when HR III was operational.

We evaluated the long-term distribution of common scoter and diver species, bird species classified as sensitive to human disturbances, in and around the HR I, II and III OWF's at Horns Rev. We found that divers and common scoters decreased in and around the HR II wind farm after its construction. However, while common scoter densities increased in the HR II area between Phase 2 and 3, the reduction in diver density continued. Within the HR III area, with large and widely spaced turbines, no decline in the density of common scoter or divers was observed in the post-construction phase.

1 Introduction and Objective

The distributions of birds at sea have often been shown to be affected by human activities, for instance, by showing displacement activity caused by ship traffic (Schwemmer et al. 2011; Fliessbach et al. 2019; Petersen et al. 2017). A study in German waters ranking bird species disturbance vulnerability from approaching ships demonstrated that divers (red-throated diver, *Gavia stellata,* and black-throated diver *G. arctica*) showed the highest degree of disturbance effect, with 95% of the observed birds reacting to approaching ships. Common scoter, *Melanitta nigra,* ranked number six on that list, with 83% of the observed birds responding to the ship (Fliessbach et al. 2019). These two species have also shown avoidance behaviour in response to newly constructed OWF's. In the German North Sea, comparisons of 14 years of pre-construction data and ten post-construction surveys over two years showed marked displacements of divers, discernible out to ca. 16 km from the wind farms (Mendel et al. 2019). Another study from the same German North Sea area using a combination of aerial digital surveys and satellite telemetry data from 33 satellite telemetry-tagged red-throated divers showed 90 % reductions in density within the footprint of the OWF's and out to a distance of 5 km from the wind farm periphery, with significant displacement detectable out to a distance of 10-15 km (Heinänen et al. 2020).

Both red-throated diver (a specially protected species on Annex I of the Birds Directive) and common scoter (for which Denmark has special responsibility for the moulting and wintering distribution of the population) are numerous and relatively highly concentrated in Danish waters, especially in the North Sea. For this reason, and particularly for predicting the effects of future developments in offshore wind power, it is important to know if these major displacement responses are common to all types of OWF's and if there is any evidence for modification of these responses over time, i.e. whether birds have shown signs of moderating their responses as they have got used to initially unfamiliar and highly disturbing stimuli, which have potentially proved in the longer term not been a threat to their biological fitness.

In 2023 and 2024, aerial surveys to determine avian distribution and abundance at sea were conducted in relation to the environmental assessment of the North Sea 1 site, located in the eastern part of the Danish North Sea, commissioned by Energinet. The aerial survey and subsequent data analysis were conducted in collaboration between Aarhus University/DCE, the University of St. Andrews, Scotland and NIRAS A/S. The purpose of these surveys and the results of the analyses was to gather baseline information for future environmental impact assessments related to upcoming wind farm projects.

As a supplementary part of this project, Energinet commissioned the same consortium to conduct six aerial surveys of birds in the Horns Rev area between November 2023 and 2024, to determine potential changes in displacement shown by two specific key bird species, common scoter *Melanitta nigra* and red-throated diver *Gavia stellata* (by far the most numerous of the two diver species in the study area) in relation to constructed windfarms, supplementing a similar analysis undertaken in 2014. The main objective of this study was to assess the degree to which displacement responses to the wind turbines by the two bird species had changed over time; for instance, to see if initial avoidance response distances had been reduced (sometimes interpreted as potential habituation to the stimulus of the constructed wind turbines).

At Horns Rev, a shallow sand bar extending ca. 40 km west of Blåvandshuk in west Jutland, the Horns Rev I OWF first became operational in 2002. In the autumn of 2009, the Horns Rev II OWF was completed and became operational, followed by the Horns Rev III OWF in the same general area in 2019.

In relation to environmental assessments of these specific wind farm developments, a series of aerial surveys of birds have been conducted in the general Horns Rev area. These included 19 aerial surveys between February 2000 and April 2003, followed by seven additional surveys between September 2003 and September 2004 to monitor post-construction effects in relation to the construction of the Horns Rev I OWF. Fourteen further surveys were conducted from March 2005 to April 2007 in the Horns Rev area to contribute to Environmental

Assessments prior to the construction of the Horns Rev II OWF. Between March 2011 and April 2012, a further ten aerial surveys were conducted in the Horns Rev area as post-construction surveys in relation to the Horns Rev II OWF. As part of this present project, six aerial surveys were conducted between November 2023 and April 2024. A total of 56 aerial surveys over 24 years provide the background data for assessing potential changes in bird distributions in relation to the presence of the turbines undertaken here. All aerial surveys were conducted by Aarhus University/DCE under a series of different contracts using the same survey protocol.

A previous analysis of changes in distributions of common scoter and red-throated diver from pre- and post-construction bird survey data was performed for the Horns Rev II OWF (Petersen et al. 2014). The conclusion was that common scoters were displaced around the Horns Rev II wind farm. The present report re-analyses the data from the previous report and includes the 2023-2024 surveys to assess whether there have been changes in common scoter and red-throated diver distribution in relation to all three wind farms over time. The following sections describe the surveys, the distance sampling methods applied and the spatial analysis framework, which comprises model selection, diagnostics, inference and outputs. The results are presented for each species, while the appendices contain an executive summary of the methods and a description of the associated data files

1.1 Study area

The overall survey area covers an area of 2,818 km^2 and extends from the west Jutland coastline westwards to ca. 50 km west of Blåvandshuk. It extends a maximum of ca. 50 km from south to north, from an east-west line drawn from the southern point of Fanø, northwards (Figure 1.1).

The area contains three OWF's of different turbine configurations. The Horns Rev I wind farm consists of 80 turbines, spaced regularly 560 meters apart. Horns Rev II comprises 91 turbines in arcs spaced 693 meters apart in the inner arc and 905 meters in the outer arc. Horns Rev III has 49 turbines arranged in a more irregular design, generally comprising 1,105 meters between columns and 1,751 meters between rows (Figure 1.1).

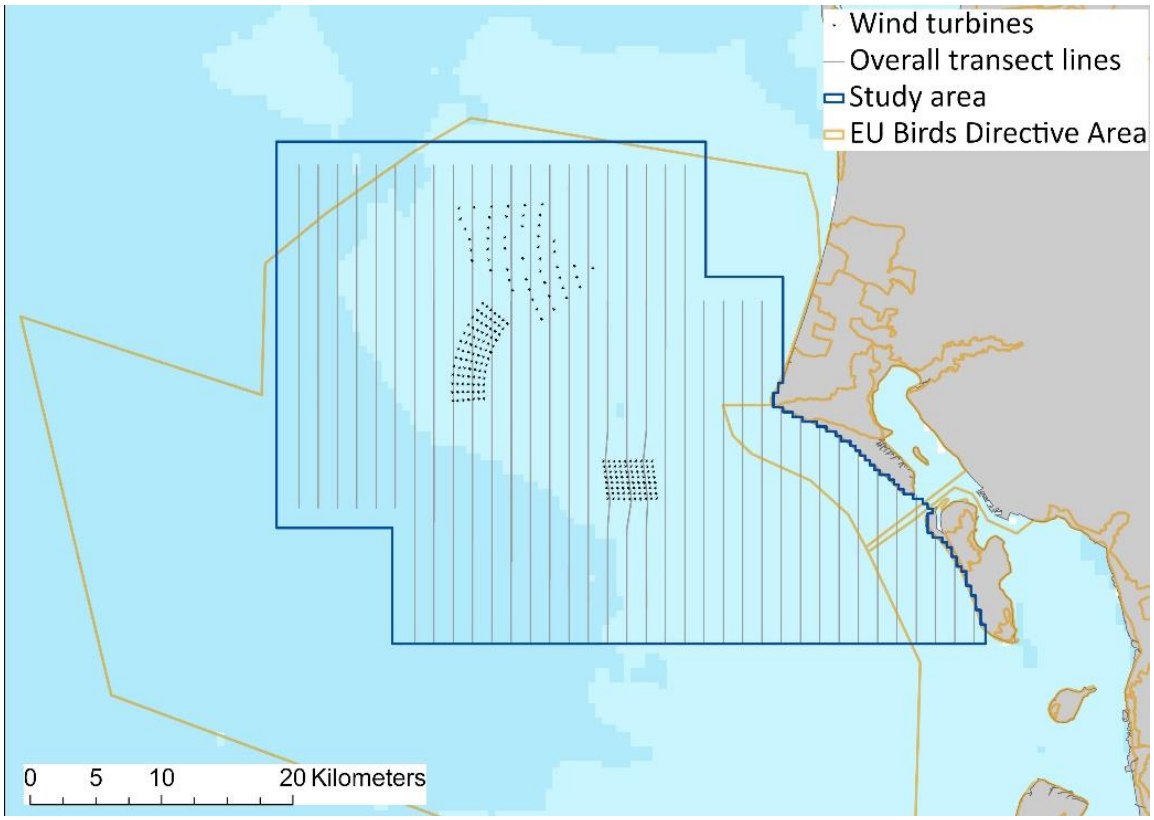

Figure 1.1. The Horns Rev OWF study area (dark blue line). The general survey transect lines are shown (grey lines). The turbine positions of the three OWF's, Horns Rev I (southeast), Horns Rev II (southwest) and Horns Rev III (north), are indicated. The extent of the EU Birds Directive Special Protection Area (ochre line) is shown.

The survey coverage changed over time between February 2000 and April 2024 with different projects and covered different sub-areas within the overall study area (Figure 2.3, Table 1-1). The survey coverage for each of the 56 aerial surveys can be found in Appendix 8.1 (Figure 8.1 to Figure 8.10 and Table 8-1). One of the 57 surveys was omitted from these analyses as none of the target species were present in the area at this time of year.

Table 1-1. The number of aerial surveys performed and the area covered (in square kilometers) for each of six surveys campaigns in the Horns Rev area between 2000 and 2024. In total, 57 surveys.

Period	Number of surveys	Km²
February 2000 to August 2005	30	1,911
November 2005	1	2,697
February 2006 to May 2006	6	2,035
January 2007 to April 2007	4	1,873
March 2011 to April 2012	10	2,337
November 2023 to April 2024	6	2,122

These surveys covered the time prior to any wind farm construction, post-construction of Horns Rev I, post-construction of Horns Rev II and post-construction of Horns Rev III (Table 1-2).

Table 1-2. Table detailing the construction phases, time frame and survey effort. The number of surveys from which data was used for the present analysis is given (Number of surveys).

Phase	Phase number	Date range	Number of surveys
Pre-construction	0	Feb 2000 - Apr 2002	15
Post HR I	1	Aug 2002 - Apr 2007	25
Post HR I & II	2	Mar 2011 - Apr 2012	10
Post HR I, II & III	3	Nov 2023 - Mar 2024	6

The bathymetry of the study area reaches from 0 to 35 meters depth. Horns Rev is a shallow sand bar extending west from Blåvandshuk, westwards to just west of the Horns Rev II OWF. Due to current and wave action, the sandy seabed is subject to turbulent movement and substrate instability.

Most of the study area falls within the "southern Danish North Sea" EU Bird Directive area (SPA113), which was enlarged from its original geographical extent by a revision in 2023. The southeastern part of the study area also falls within the "Vadehavet" Bird Directive area (SPA57).

This report describes the distribution and abundance of birds in the four construction phases shown in Table 2-1 and assess the results for significant changes in and around the three wind farm footprints. One of the objectives of the analyses in this report is to assess whether, and to what degree, a species might be showing distributional changes that suggest a return to areas within and around an OWF (or not) after a redistribution or decline post-construction (a sort of "re-habituation"). Therefore, to meet this objective, various outputs were produced, and a range of comparisons were made, including those that tested changes in density with distance from a wind farm footprint.

2 Methods

Visual aerial surveys were used to collect seabird data using line transect distance sampling methods (Buckland et al. 2001). During these surveys, trained observers searched for and recorded birds in distance bands in addition to environmental conditions at the time (e.g. sea state or sun glare).

2.1 Data collection

Data on bird abundance and distribution were collected using standard methods; human observers visually gathered data during aerial surveys, flying transects between designated GPS waypoints at a regular speed of 100 knots and an altitude of 76 meters (Figure 1-1). Twin-engine Partenavia P-68 and Cessna 337 high-wing aircraft were used for the surveys. Observations were recorded within distance bands parallel to the aircraft to allow for the modelling of differential detectability at increasing distances from the observers (Petersen & Sterup 2019, NOVANA Technical Specification TA A188), following standard Distance Sampling line transect survey methods (Buckland et al. 2001, 2015).

Two trained observers recorded birds from either side of the aircraft. The bird species or species group was noted for each record, along with information on flock size, behaviour, perpendicular distance from the survey track and time. In addition, the environmental conditions at the time (e.g. sea state or sun intensity) were registered. The perpendicular distance was classified in predefined distance bands with increasing distance from the survey track line out to 1.5 km on either side of the aircraft (Figure 2.1).

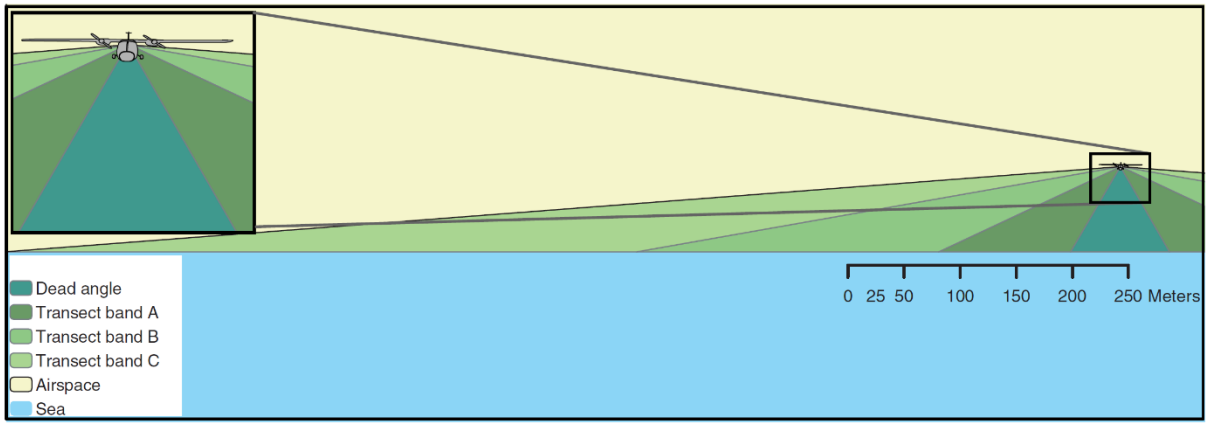

Figure 2.1. The transect band definitions for aerial line transect surveys. From the survey altitude of 76 m, there is a dead area extending to 44 m on each side of the survey track under the aircraft that the observers could not cover.

The survey transect lines were designed as parallel north-south oriented lines, covering the survey area. The transect lines were separated by 2 km for most transects, although in parts of the area, the distance between transects was 4 km (Figure 2.1).

At Horns Rev, a total of 56 aerial surveys of birds were conducted between 2000 and 2024. The precise survey coverage area differed slightly between the different projects and contracts. The coverage per survey is presented in Appendix 8.1, with the precise survey track lines covered during each survey and the numbers of both species encountered.

2.2 Survey data

The data used for this analysis consists of 56 surveys from February 2000 to April 2024. The transect lines for each survey were split into segments of approximately 500 m long up to 1000 m wide. Birds were detected in four distance bins perpendicular to the flight direction (A-D) with categories 0 m-119 m (A), 119 m-388 m (B), 388 m-956 m (C) and 956 m-1456 m (D), and detections were mostly observed from both sides of the plane. A band out to 44 m under both sides of the plane was visible to observers and, therefore, did not contribute to the dataset. Band D was removed from analysis for all species owing to very few or no observations.

All latitude/longitude locations were converted to UTMs using UTM Zone 32N. The transects for the surveys are shown in Figure 2.2. The number of segments per survey is presented in Table 2-1.

Table 2-1. Table detailing the survey effort (number of segments) for each survey and the number of segments in each wind farm footprint.

Survey date	Phase	Area covered (km^2)	Number of segments	HR I segments	HR II segments	HR III segments
2000-02-17	0	1581	1688	24	30	6
2000-02-21	0	1098	1184	24	0	0
2000-03-19	0	1525	1680	24	32	6
2000-04-27	0	1377	1514	24	32	6
2000-08-21	0	1388	1539	24	34	6
2000-10-06	0	1307	1472	24	22	6
2000-12-22	0	1171	1251	24	0	6
2001-02-09	0	1443	1540	24	32	6
2001-03-20	0	1564	1687	24	33	6
2001-04-21	0	1319	1691	24	32	6
2001-08-22	0	1566	1677	24	32	6
2001-09-26	0	1456	1550	24	28	6
2002-01-07	0	1274	1401	24	7	6
2002-03-12	0	1393	1478	16	32	4
2002-04-09	0	1296	1402	24	33	6
2002-08-08	1	1310	1404	24	30	5
2003-02-13	1	1218	1433	24	15	6
2003-03-16	1	1622	1741	24	32	12
2003-04-23	1	1606	1758	24	31	12
2003-09-05	1	1440	1722	24	32	6
2003-12-04	1	1295	1440	24	16	3
2003-12-30	1	1162	1290	24	14	6
2004-02-29	1	1562	1784	24	33	6
2004-03-26	1	1607	1782	24	31	6
2004-05-10	1	1599	1779	24	32	6
2004-09-09	1	1503	1632	24	14	6
2005-03-08	1	1676	1788	24	23	6
2005-04-02	1	1177	1775	24	31	5
2005-05-14	1	1666	1781	24	35	6
2005-08-17	1	1660	1776	24	33	6
2005-11-18	1	2198	2454	24	30	84
2006-02-02	1	1621	1712	24	33	88
2006-02-25	1	1622	1713	24	29	87
2006-03-12	1	1433	1714	24	34	87
2006-04-15	1	1616	1708	24	32	88

Survey date	Phase	Area covered (km^2)	Number of segments	HR I segments	HR II segments	HR III segments
2006-05-11	1	1484	1720	24	25	88
2007-01-25	1	1378	1470	24	30	31
2007-02-15	1	1190	1385	24	32	28
2007-03-03	1	1308	1399	24	32	35
2007-04-01	1	1464	1639	24	34	21
2011-03-01	2	1133	1216	24	37	81
2011-03-26	2	1200	1311	24	36	80
2011-04-11	2	1172	1305	24	46	79
2011-10-13	2	952	1297	24	35	81
2011-11-17	2	1184	1256	24	36	80
2012-01-15	2	1260	1336	24	36	81
2012-02-08	2	813	1294	24	36	80
2012-03-02	2	1155	1227	24	37	82
2012-03-22	2	1166	1271	24	37	81
2012-04-11	2	1171	1282	24	35	81
2023-11-17	3	1117	1213	24	36	81
2023-12-27	3	1017	1079	24	36	81
2024-01-09	3	1127	1194	24	36	81
2024-02-27	3	1127	1192	24	36	81
2024-04-08	3	1133	1201	24	36	81
2024-04-22	3	1099	1198	24	38	81

Figure 2.2. All survey data by survey. The coloured dots represent non-zero segment counts for the two species groups. The pale purple dots are zero segments.

2.3 Distance Sampling Analysis

All survey data were collected using visual aerial methods and so correction for declining detectability with increasing distance from the plane was accounted for using Distance sampling methodology (Multiple Covariate Distance Sampling, MCDS) (Marques and Buckland 2004; Marques et al. 2007; Buckland et al. 2001). Analyses were conducted for each of the common scoter and divers datasets by pooling the information across all surveys. The distance analysis models the decreased probability of detecting a bird or group of birds with increased distance away from the track line of the survey aircraft.

To allow for the detectability of birds varying due to external factors (not just distance from observer) other covariates were included in the distance model. The candidate variables trialled were bird group size, behaviour, observer and sea state (Table 2-2). For some observers there were too few observations so in those cases, the observers' observations were combined with the next smallest. Observations with sea states greater than four were removed. For scoters, which were occasionally seen in very large numbers (up to 20,000), any segments with birds were assumed to have perfect detection and omitted from the detection analysis. The observed values for these segments were used in the spatial analysis. Both half-normal and hazard rate detection functions were trialled (allowing different steepness/shape of the decline in detectability with distance) and the best of all competing models chosen using BIC. The effects of glare, and any mitigations as a result, was

approached using a dedicated analysis. Further details on this and the distance analysis can be found in Appendix 8.2.

Table 2-2. Table detailing the covariates used in the detection function fitting.

Covariates	Values
Behaviour	S (sitting or diving) and F (flying or flushing)
Observer	17 Observers
Sea State	0, 0.5, 1, 1.5, 2, 2.5, 3, 3.5 (calm to rough)

2.4 Spatial Analysis

The following sections describe the modelling methods employed for this analysis and a description of the outputs which follow. The following sections describe the spatial modelling methods employed and a description of the outputs which follow. For a more detailed look at the methods, see Appendix 8.2.

The outputs from the detection function analysis give a detectability corrected count (abundance) in a small area (segment of approximately 500 m). Spatial models are used to turn the distance corrected counts along transect lines into spatial distribution maps, whilst accounting for data characteristics and modelling assumptions. The spatial modelling process was undertaken using a Generalised Additive Model framework (GAM) with an error family suitable for count per unit area response data, the Tweedie distribution. The effort associated with each observation varied depending on the associated segment length and width. Segment area was therefore included as a log-scale offset term in the model. Additionally, the survey coverage was not constant throughout, and particularly in the early years did not fully overlap the prediction area of interest (Figure 2.3). Due to this potentially causing extrapolation artefacts, a model framework was extended to use the principle of quadrature points (Berman and Turner 1992). These points were generated on a 1 x 1 km grid in the combined prediction-survey area for each survey to provide a data reference for the model in areas that have not been surveyed. Therefore, the model framework used was weighted Tweedie GAM.

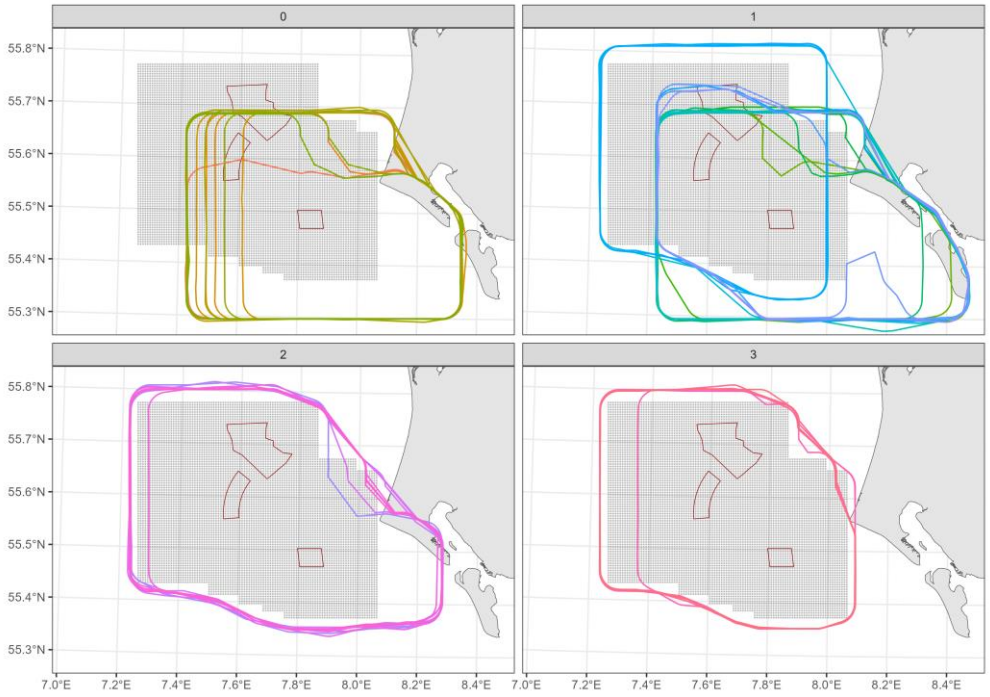

Figure 2.3. Figure showing the survey coverage (coloured polygons with multiple surveys in each phase) in relation to the prediction region (grey dots). The wind farm footprints are outlined in red.

As each survey was analysed separately, only spatial explanatory variables were considered. The candidate variables for inclusion in the spatial model were a set of one-dimensional terms, water depth (Figure 8.21) and distance to coast (Figure 8.22), that were permitted to change linearly or non-linearly with the response and a two-dimensional term using geographic coordinates to account for surface patterns, which could be a result of unmodelled environmental variability. The flexibility of any smooth functions (1D or 2D) was determine using BIC, whilst the more computationally intensive 5-fold cross-validation was used to choose between competing models (inclusion or exclusion of variables).

The response data were collected along survey lines in sequence, and so consecutive observations were likely to be correlated in space and time. With a spatial term included, any resulting temporal auto-correlation in model residuals was accounted for by using robust standard errors as part of the modelling framework. These essentially inflate the standard errors in relation to the positive correlation observed within pre-specified blocks (here, transects) of residuals.

Uncertainty in the outputs was estimated using both the detection model and spatial model in a process called bootstrapping. This involves repeatedly sampling from the parameter distributions of each model and obtaining a new set of predicted abundances across the spatial grid. From this process, we have 500 sets of plausible predictions for every grid cell. These may be used in a variety of ways to estimate uncertainty and answer questions such as "does the spatial distribution vary between two surveys or phases".

All models were fitted using the MRSeaPP R package (Scott-Hayward et al., 2023; R Core Team, 2024) and subjected to various diagnostic checks (e.g. assessment of the assumed mean-variance relationship, a key assumption check).

Further methodological details on model specification, fitting, and diagnostics are available in Appendix 8.2.

2.4.1 Model Framework

The response variable for the spatial models under analysis here, are bird counts in a small area (segment) which have been corrected for detectability. This response was modelled using a Tweedie framework, which includes an estimated dispersion parameter (ϕ) and Poisson-Gamma mixing parameter (ξ) to return an appropriate mean-variance relationship in each case. The mixing parameter takes on values from 1 (equivalent to quasi-Poisson) and 2 (equivalent to Gamma). If the estimated parameter was close to 1, the models were considered quasi-Poisson. A set of candidate explanatory variables were associated with each segment to model the signal, and in this study each of the 56 surveys was analysed separately, including covariate selection, for each species. The candidate environmental covariate was water depth (bathymetry, Figure 8.21) while distance from coast (Figure 8.22) (as a one-dimensional term) was also considered in each model, in the unlikely case there was compelling evidence for consistent spatial patterns with distance from coast which were the same in all directions. Additionally, to account for more realistic (and localised) surface patterns (due to perhaps unmeasured covariates) a spatial surface was also fitted to each model. Specifically, a two-dimensional CReSS-based surface using a Gaussian radial basis function was included in the model (Scott-Hayward, Oedekoven, et al. 2014).

As an illustration, the following equation represents an example of a Tweedie model with log link function and fitted with a one-dimensional smooth term (e.g., bathymetry) alongside a two-dimensional spatial smooth:

$$y_{ij} \sim Tw(\mu_{ij}, \phi, \xi)$$

$$\mu_{ij} = e^{\left(\beta_0 + s_1\left(\text{Bathymetry}_{ij}\right) + s_2\left(\text{XPos}_{ij}, \text{YPos}_{ij}\right)\right)}$$

where y_{ij} is the estimated count for transect i segment j and s_1 represents either a quadratic B-spline or natural cubic spline smooth of depth. Here, s_2 is a two dimensional smooth of space (with coordinates XPos and YPos in UTMs). Implicit in this model are also coefficients for the intercept (β_0) and any spline-based coefficients associated with the smooth terms. The effort associated with each observation varied depending on the associated segment area and so segment area was included as an offset term (on the log scale).

A globally applicable depth or distance to coast term and a more flexible spatial term were trialed for inclusion in each model, to indicate how best to model spatial patterns in each case. In particular, this quantifies if any spatial patterns are sufficiently described by the one-dimensional covariates (which applies the same across the surface) or if a more considered approach to spatial patterns was required for each survey and for each species. For example, if depth was selected and a two-dimensional spatial element was not deemed necessary (as determined by the model selection procedure governed by objective fit criteria) then this signals that any spatial patterns are primarily a function of the depth, regardless of the geographical location of this depth in the survey area.

If the two-dimensional spatial term was selected for inclusion in a model, then the spatial density patterns (over and above any environment-related terms) were accommodated using a spatially adaptive term which permits different amounts of flexibility across the surface in a targeted and yet parsimonious way (hence, relatively complex spatial patterns can be accommodated with very few parameters).

Selection between competing models was undertaken using an information criterion metric, BIC, which has a penalty related to the extent of the data supporting the model.

2.5 Model specifics

More specifically, the MRSea package CReSS-SALSA based spatially adaptive generalized additive models, with targeted flexibility, were fitted to data from each survey to allow for non-linear relationships between the one-dimensional and two-dimensional covariates and the response (Scott-Hayward, Mackenzie, et al. 2014, 2014; Scott-Hayward et al. 2023; Walker et al. 2010).

CReSS is a complex-region spatial smoother, whilst SALSA is a Spatially Adaptive Local Smoothing Algorithm both developed to examine animal survey data for signs of changes in animal abundance and distribution following marine renewables development. However, the methods are suitable for a wide range of applications.

The degrees of freedom for these terms determine the flexibility of these smooth (and nonlinear) relationships the more degrees of freedom, the more flexible the relationship can be.

The spatial patterns in each analysis were based on a two-dimensional Gaussian radial basis function (*df* = [2,100]). The flexibility of both the spatial and 1D elements constituted part of the model selection procedure and, for each survey, was determined using SALSA and the BIC measure of fit.

Uncertainty about model parameter estimates proceeded via robust standard errors due to the nature of the survey procedure. These essentially work by inflating the standard errors (normally obtained under traditional approaches) in relation to the positive correlation observed within pre-specified blocks of residuals. In cases where this residual correlation is minimal, the adjustments are small, and when the correlation is more extreme, the inflation is larger.

A transect-based blocking structure was used to reflect potential correlation within blocks while independence (i.e., no correlation) between blocks was assumed. To ensure this assumption was realistic, the decay of any residual correlation to zero (i.e., independence) with the distance between points (within blocks along transects) was assessed visually. Specifically, transects in each survey were used as the blocking structure. An Auto Correlation Function (ACF) plot was used to check the suitability of this blocking structure via a 'decay to zero' trend within blocks.

2.5.1 Modelling diagnostics

For all modelling there are assumptions made and the violation of these can lead to spurious results. To assess the adequacy of model fit and assumptions a range of diagnostic measures were used.

- ACF plot: A blocking structure was used to account for potential residual non-independence for each model and a robust standard error approach was based on unique transects. Figure 2.4 shows an example ACF plot with the temporal correlation within each transect shown in grey and the average in red. The plot shows a mean lag one correlation of approximately 0.25 followed by a reassuring decay to zero. This indicates that the robust standard errors were necessary for this model (no residual correlation is indicated by a lag 1 correlation of near zero) and that the blocking structure is appropriate.

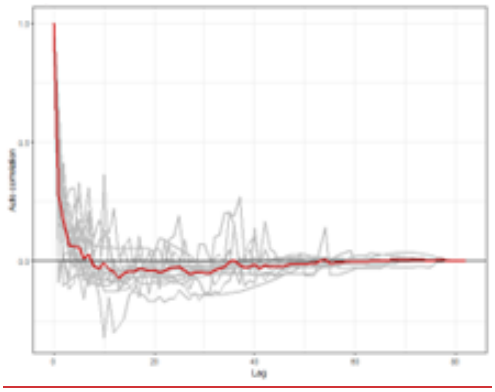

Figure 2.4. Example ACF plot: the grey lines represent the residual correlation observed in each transect and the red line the average of these values across transect.

- Mean-Variance plot: The assumed mean-variance relationship under the model was assessed visually using plots of the model's fitted values against the residuals' variance. In this analysis, Tweedie models were employed, which assume a nonlinear mean-variance relationship. Figure 2.5 shows an example plot. The observed residual variance is calculated in bins relating to quantiles of the fitted values (hence the irregular spacing). These are plotted as the black dots and agreement between these and the assumed relationship (Tweedie, dotted blue line) indicates the mean-variance assumption is appropriate. As the Quasi-Poisson and Poisson families are special cases of the Tweedie, these are included on the plot for comparison.

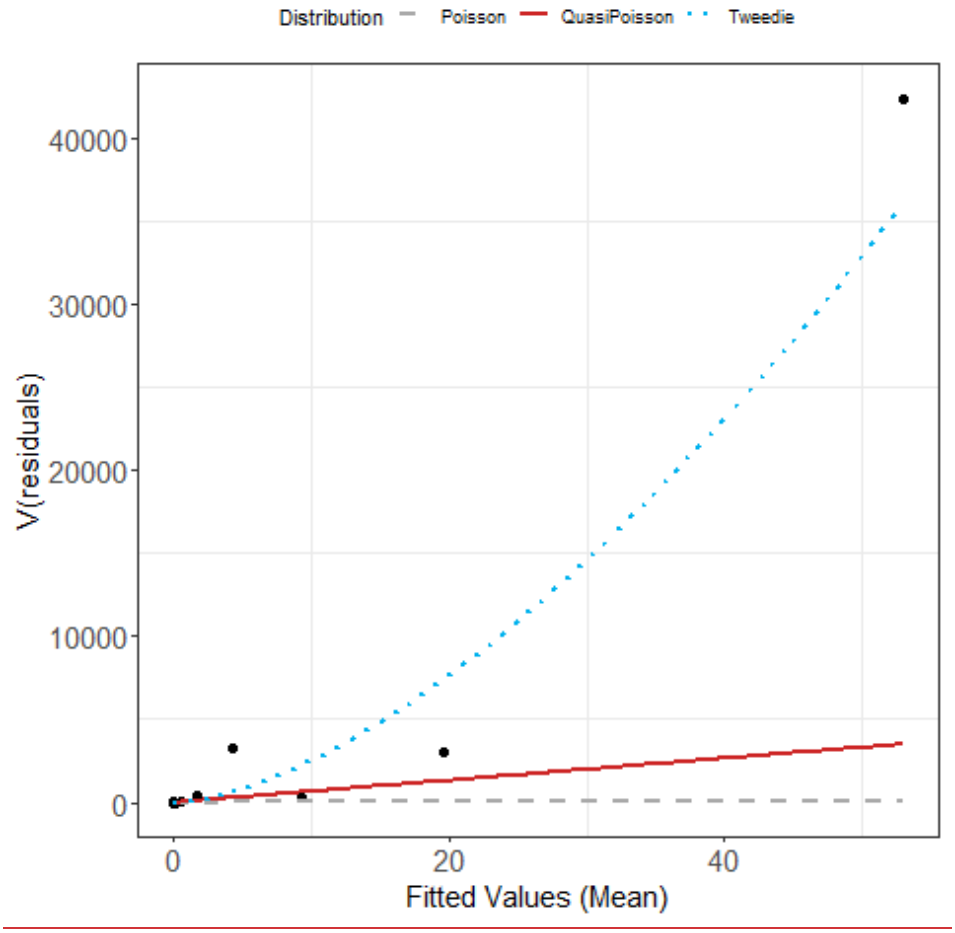

Figure 2.5. Plot showing the estimated Tweedie mean-variance relationship (blue dashed line). The red line shows the $V(\mu) = \Phi\mu$ relationship and the grey line the 1:1 relationship. The black dots are the observed residual variances.

- DHARMa diagnostic plots: QQ plots and residuals against predicted values plots were assessed to ascertain the level of agreement between the data and the model (Figure 2.6). These plots were created using the *DHARMa R* package and using simulated residuals. Given these outputs, we would expect that a correctly specified model shows:

  a) a straight 1-1 line, and no compelling evidence against the null hypothesis of a correct overall residual distribution, as indicated by the *p*-values for the associated tests in the QQ-plot.

  b) visual homogeneity of residuals in both the vertical and horizontal directions, in the residuals against predictor plot.

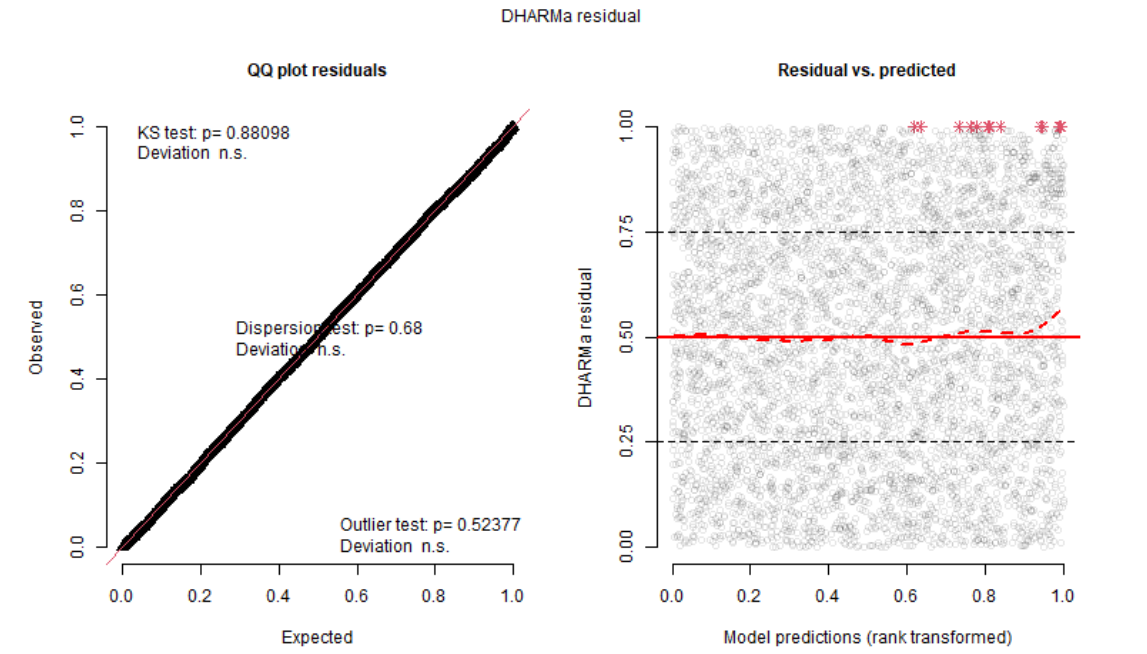

Figure 2.6. Example DHARMa plots: QQplot (left) and residuals against predicted values (right). The red stars are outliers and the red line is a smooth spline around the mean of the residuals.

- Pearson residuals for each model were also spatially visualised to ensure no areas of consistent bias across the survey area. This would be indicated by clusters of negative or positive residuals in spatially similar locations.

Diagnostic outputs are not shown in the results chapter, but a full set (all 56 models for both species) is available on request.

2.5.2 Model Predictions and estimates of uncertainty

Based on each selected model, predictions of counts were made to a grid of points (each point representing a 1km^2 grid cell) across the study region. Additionally, abundances within the survey-based prediction region were obtained by summing the grid cell counts across the relevant areas. A key output of any statistical modelling process is the incorporation of uncertainty from all steps and the presentation of this uncertainty alongside estimates (e.g. an abundance estimate with 95% confidence interval).

The uncertainty in the detection function was reflected using a parametric bootstrap ($n = 500$) of the fitted distance sampling model to obtain new estimated counts for each segment. The selected spatial model was then re-fitted to each of the new datasets to obtain a new set of parameter estimates for the model. The final output of this process was a parametric bootstrap procedure using the robust variance-covariance matrix from each parametric bootstrap model. These were used to calculate 500 sets of plausible model predictions, for every grid cell in the study area. To obtain 95% percentile-based confidence intervals and a coefficient of variation for each grid cell, the 2.5% and 97.5% quantiles of the 500 bootstrap predictions were taken along with the standard deviation. Using the bootstrap predictions, we can create a number of other outputs to assist in assessing consistency of distributional patterns (persistence) and distributional changes over time.

A calculation of 'persistence' was also undertaken across surveys within phases and across all surveys considered together, within species, using the geo-referenced estimates of density (abundance/associated area) across the survey area. Distributional persistence allows the reader to get a measure of intra/inter-annual

variability across multiple surveys. For example, there may be areas of consistent usage, despite survey-to-survey variability, which can provide context to the ability to detect post-construction changes. A persistence score of 1 indicates that the density in that grid cell was estimated to be above average in every bootstrap replicate in every survey (so uniformly above the mean; high persistence), while a value of 0.1 indicates that just 10% of the estimates were above the estimated mean, and thus indicates low persistence in that location. Persistence scores were calculated for every grid cell in the following way: Each bootstrap replicate was allocated a binary value based on whether or not the estimate in each location was above the mean estimated density (1) throughout the survey area or below this mean estimated density (0). This was performed for all sets of plausible predictions in each grid cell (based on the bootstrap replicates), and the proportion of these bootstrap predictions over the mean (indicated by the value of 1) was calculated for each grid cell to give a persistence score for that location. A zero would result from the density in every survey and every bootstrap being below average.

Distributional changes over time were evaluated by comparing the estimated distributions from the four phases. Any changes during this time in and around the three wind farm footprints could also be observed. Difference plots were used to visualise any spatially explicit changes in the distribution of birds. The bootstraps from the modelling process described above were used to generate a 95% interval for the difference in abundance in each grid cell. If the interval contained zero, it was deemed not to indicate a statistically significant difference in abundance between the two comparison years. If the range of plausible values for the difference (indicated by the 95% confidence interval) did not include zero, then the change was deemed significantly positive or negative. These bootstrap-based cell-wise differences between phases were also viewed in concentric rings that were within distance of the Horns Rev II footprint.

3 Results

3.1 Common scoter - Distance Analysis

The average probability of sighting common scoter was estimated to be 0.29 (CoV=0.01). This probability was estimated using a hazard rate detection function and group size as a covariate (*Figure 3.1*). As might be expected, the larger the group size, the higher the probability of detection.

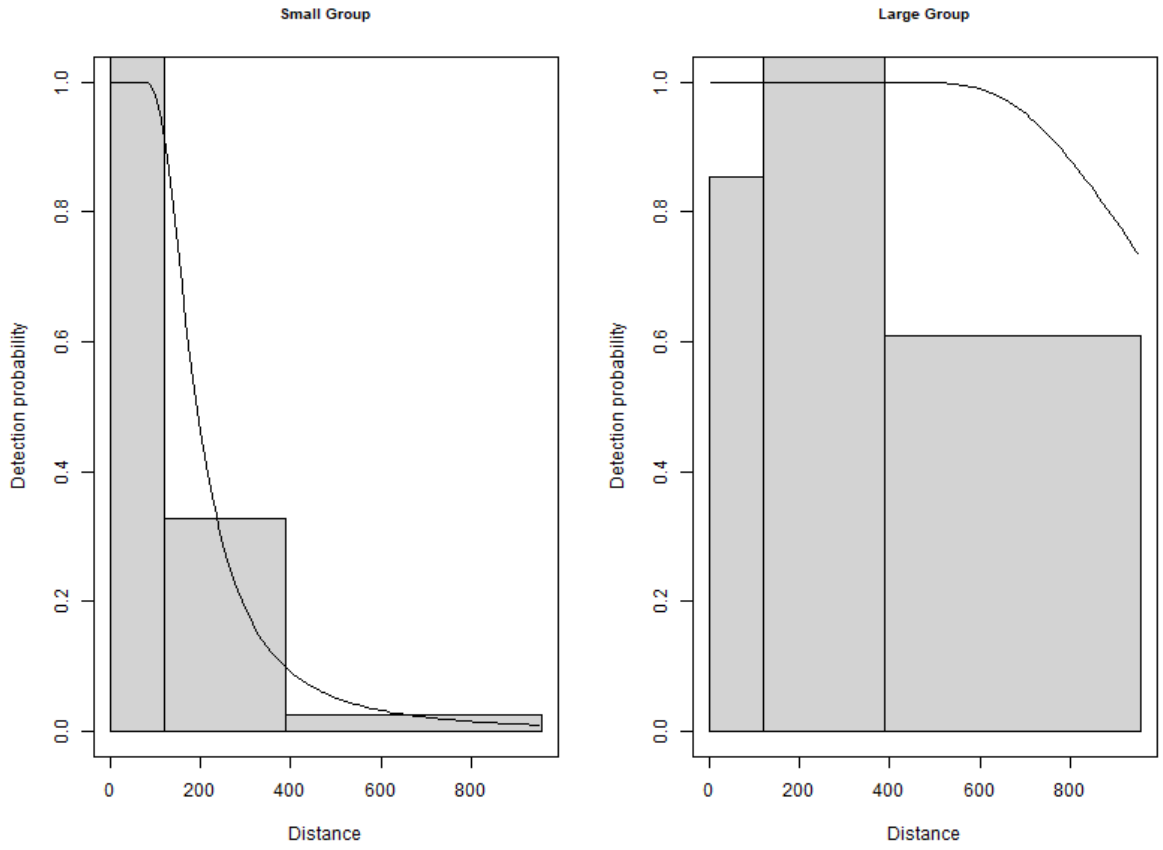

Figure 3.1. Figure showing the estimated detection function of common scoter in small and large groups. The histograms represent the distances (m) of the observed sightings across observers.

3.2 Common scoter Spatial Results by Survey

Figure 3.2 shows the distribution of the distance corrected counts for each of 56 surveys.

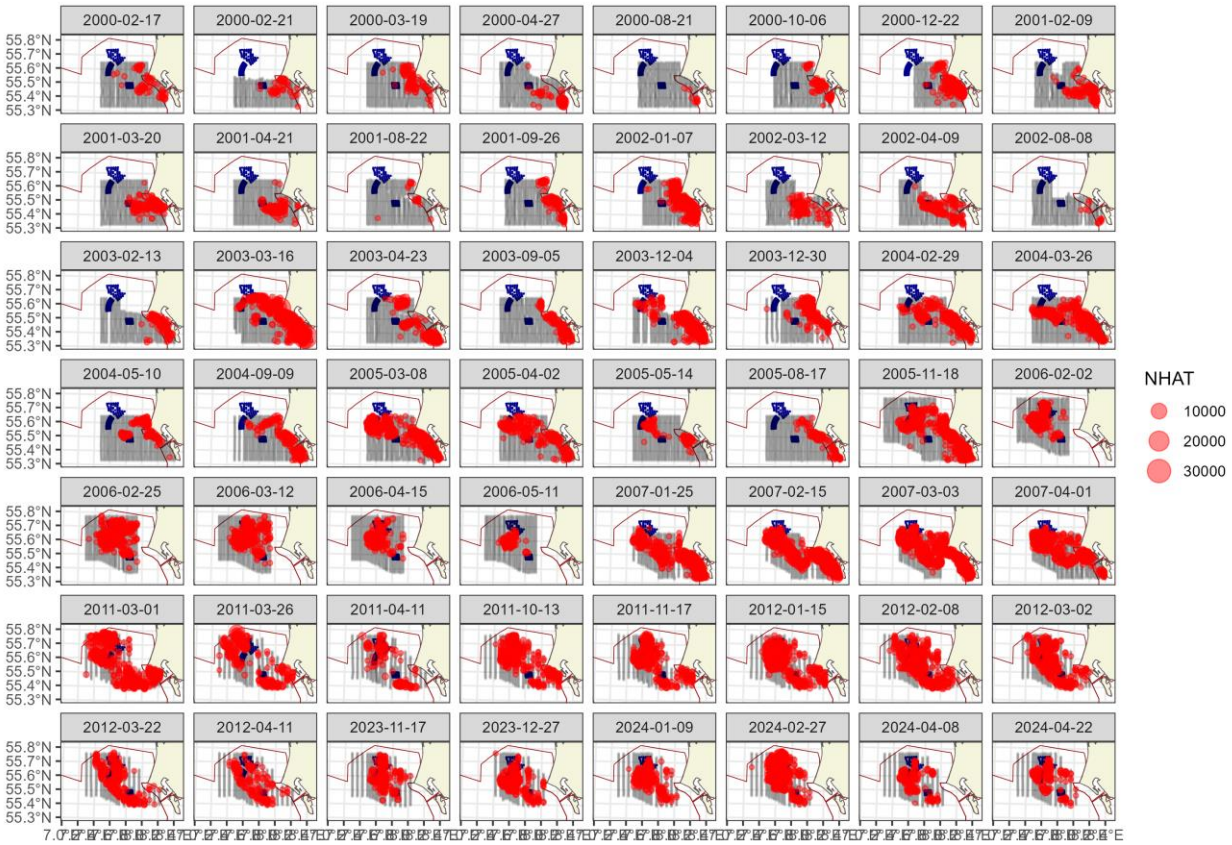

Figure 3.2. Distance-corrected counts for the common scoters across the 56 surveys. The red circles indicate the distance-corrected counts along the transect lines. The grey dots are segments with a count of zero.

3.2.1 Model Selection

For 42 of the 56 surveys, the models selected included a spatial term (of varying complexity) while the depth covariate (as a non-linear term) was selected for eight of the surveys – in five of these models however, the spatial term was also included. The distance to coast covariate was selected as a non-linear term in seven of the 56 models, which demonstrates compelling evidence for non-uniform spatial patterns in all but one survey, given all but one also included a spatial term. The spatial surfaces selected ranged from 2 to 10 parameters for the spatial term (Table 3-1). The estimated abundances and associated 95 percentile confidence intervals for each survey are given in Table 3-2, illustrated in Figure 3.3 for all surveys combines and Figure 3.4 combined for each of the phases.

Table 3-1. Model selection results for common scoter for each survey. The model column represents the terms in the model.

Survey	Model	Distribution	Variable 1D	Variable 2D	Number of parameters	Dispersion parameter	Tweedie parameter
2000-02-17	Best 1D2D	Tweedie	s(distcoast, df=2)	s(x,y, df=5)	8	46.4	1.61
2000-02-21	2D Only	Tweedie	NA	s(x,y, df=2)	3	130.3	1.58
2000-03-19	Best 1D2D	Tweedie	s(distcoast, df=2)	s(x,y, df=2)	5	46.2	1.61
2000-04-27	2D Only	Tweedie	NA	s(x,y, df=2)	3	195.6	1.53
2000-08-21	Intercept only	Tweedie	NA	NA	1	263.0	1.35
2000-10-06	Best 1D2D	Tweedie	s(depth, df=2)	s(x,y, df=4)	7	28.8	1.53
2000-12-22	2D Only	Tweedie	NA	s(x,y, df=6)	7	35.0	1.57
2001-02-09	2D Only	Tweedie	NA	s(x,y, df=6)	7	33.2	1.60

Survey	Model	Distribution	Variable 1D	Variable 2D	Number of parameters	Dispersion parameter	Tweedie parameter
2001-03-20	2D Only	Tweedie	NA	s(x,y, df=6)	7	78.7	1.61
2001-04-21	Best 1D2D	Tweedie	s(distcoast, df=2)	s(x,y, df=2)	5	40.7	1.61
2001-08-22	Intercept only	Tweedie	NA	NA	1	299.3	1.46
2001-09-26	2D Only	Tweedie	NA	s(x,y, df=6)	7	24.1	1.58
2002-01-07	2D Only	Tweedie	NA	s(x,y, df=5)	6	52.2	1.58
2002-03-12	Intercept only	Tweedie	NA	NA	1	1207.1	1.61
2002-04-09	Best 1D2D	Tweedie	s(distcoast, df=2)	s(x,y, df=4)	7	29.7	1.53
2002-08-08	2D Only	Tweedie	NA	s(x,y, df=2)	3	18.4	1.43
2003-02-13	2D Only	Tweedie	NA	s(x,y, df=3)	4	71.7	1.61
2003-03-16	2D Only	Tweedie	NA	s(x,y, df=13)	14	106.3	1.61
2003-04-23	Distance to coast	Tweedie	s(distcoast, df=2)	NA	3	151.4	1.56
2003-09-05	2D Only	Tweedie	NA	s(x,y, df=5)	6	7.5	1.50
2003-12-04	2D Only	Tweedie	NA	s(x,y, df=4)	5	418.3	1.53
2003-12-30	2D Only	Tweedie	NA	s(x,y, df=6)	7	50.9	1.61
2004-02-29	Best 1D2D	Tweedie	s(distcoast, df=2)	s(x,y, df=9)	12	84.8	1.59
2004-03-26	2D Only	Tweedie	NA	s(x,y, df=11)	12	44.8	1.56
2004-05-10	Intercept only	Tweedie	NA	NA	1	334.7	1.57
2004-09-09	Best 1D2D	Tweedie	s(distcoast, df=2)	s(x,y, df=6)	9	22.1	1.50
2005-03-08	2D Only	Tweedie	NA	s(x,y, df=13)	14	34.8	1.55
2005-04-02	Depth	Tweedie	s(depth, df=2)	NA	3	213.7	1.52
2005-05-14	2D Only	Tweedie	NA	s(x,y, df=6)	7	24.8	1.60
2005-08-17	2D Only	Tweedie	NA	s(x,y, df=3)	4	29.1	1.57
2005-11-18	Depth	Tweedie	s(depth, df=2)	NA	3	684.2	1.61
2006-02-02	2D Only	Tweedie	NA	s(x,y, df=9)	10	22.6	1.58
2006-02-25	2D Only	Tweedie	NA	s(x,y, df=9)	10	56.1	1.56
2006-03-12	Intercept only	Tweedie	NA	NA	1	148.3	1.51
2006-04-15	2D Only	Tweedie	NA	s(x,y, df=8)	9	38.6	1.53
2006-05-11	Intercept only	Tweedie	NA	NA	1	254.1	1.51
2007-01-25	2D Only	Tweedie	NA	s(x,y, df=13)	14	48.0	1.59
2007-02-15	Best 1D2D	Tweedie	s(depth, df=2)	s(x,y, df=9)	12	90.1	1.56
2007-03-03	2D Only	Tweedie	NA	s(x,y, df=14)	15	46.5	1.56
2007-04-01	Best 1D2D	Tweedie	s(depth, df=2)	s(x,y, df=9)	12	49.9	1.57
2011-03-01	2D Only	Tweedie	NA	s(x,y, df=12)	13	181.7	1.61
2011-03-26	Intercept only	Tweedie	NA	NA	1	564.6	1.61
2011-04-11	2D Only	Tweedie	NA	s(x,y, df=5)	6	146.6	1.61
2011-10-13	Intercept only	Tweedie	NA	NA	1	388.1	1.54
2011-11-17	2D Only	Tweedie	NA	s(x,y, df=8)	9	41.4	1.57

Survey	Model	Distribution	Variable 1D	Variable 2D	Number of parameters	Dispersion parameter	Tweedie parameter
2012-01-15	Depth	Tweedie	s(depth, df=2)	NA	3	299.3	1.56
2012-02-08	Intercept only	Tweedie	NA	NA	1	149.2	1.60
2012-03-02	2D Only	Tweedie	NA	s(x,y, df=10)	11	64.7	1.59
2012-03-22	Best 1D2D	Tweedie	s(depth, df=2)	s(x,y, df=5)	8	70.7	1.58
2012-04-11	Intercept only	Tweedie	NA	NA	1	162.3	1.57
2023-11-17	2D Only	Tweedie	NA	s(x,y, df=4)	5	66.3	1.59
2023-12-27	2D Only	Tweedie	NA	s(x,y, df=4)	5	83.6	1.55
2024-01-09	2D Only	Tweedie	NA	s(x,y, df=9)	10	44.9	1.61
2024-02-27	2D Only	Tweedie	NA	s(x,y, df=9)	10	158.1	1.56
2024-04-08	2D Only	Tweedie	NA	s(x,y, df=8)	9	29.6	1.53
2024-04-22	Best 1D2D	Tweedie	s(depth, df=2)	s(x,y, df=5)	8	35.9	1.60

3.2.2 Abundance Estimates by Survey

The estimated abundances, densities and associated 95 percentile confidence intervals for each survey are given in Table 3-2.

Table 3-2. Estimated abundance and density of common scoter for each survey. The 95% CI are percentile-based confidence intervals.

Month	Area (km^2)	Estimated count	95% CI count	Estimated density	95% CI density
2000-02-17	2019	2923	(1048, 9089)	1.4	(0.5, 4.5)
2000-02-21	2019	1841	(859, 4291)	0.9	(0.4, 2.1)
2000-03-19	2019	5109	(2479, 10551)	2.5	(1.2, 5.2)
2000-04-27	2019	889	(277, 3219)	0.4	(0.1, 1.6)
2000-08-21	2019	230	(57, 820)	0.1	(0, 0.4)
2000-10-06	2019	605	(237, 1803)	0.3	(0.1, 0.9)
2000-12-22	2019	968	(324, 3108)	0.5	(0.2, 1.5)
2001-02-09	2019	1862	(577, 6077)	0.9	(0.3, 3)
2001-03-20	2019	4579	(1750, 13232)	2.3	(0.9, 6.6)
2001-04-21	2019	10524	(4900, 23037)	5.2	(2.4, 11.4)
2001-08-22	2019	386	(151, 1067)	0.2	(0.1, 0.5)
2001-09-26	2019	1351	(640, 2830)	0.7	(0.3, 1.4)
2002-01-07	2019	10661	(6102, 19326)	5.3	(3, 9.6)
2002-03-12	2019	5676	(1753, 17596)	2.8	(0.9, 8.7)
2002-04-09	2019	4150	(2423, 7598)	2.1	(1.2, 3.8)
2002-08-08	2019	0	(0, 6)	0.0	(0, 0)
2003-02-13	2019	12	(5, 38)	0.0	(0, 0)
2003-03-16	2019	53268	(23688, 126656)	26.4	(11.7, 62.7)
2003-04-23	2019	9103	(4601, 17015)	4.5	(2.3, 8.4)
2003-09-05	2019	1607	(562, 5291)	0.8	(0.3, 2.6)
2003-12-04	2019	9497	(4320, 20929)	4.7	(2.1, 10.4)
2003-12-30	2019	16924	(7447, 40418)	8.4	(3.7, 20)
2004-02-29	2019	9614	(4332, 22612)	4.8	(2.1, 11.2)
2004-03-26	2019	19139	(9447, 40648)	9.5	(4.7, 20.1)
2004-05-10	2019	7765	(3044, 18870)	3.8	(1.5, 9.3)
2004-09-09	2019	1711	(772, 4337)	0.8	(0.4, 2.1)

Month	Area (km^2)	Estimated count	95% CI count	Estimated density	95% CI density
2005-03-08	2019	25431	(12427, 53627)	12.6	(6.2, 26.6)
2005-04-02	2019	5780	(3484, 9992)	2.9	(1.7, 4.9)
2005-05-14	2019	8370	(4620, 14542)	4.1	(2.3, 7.2)
2005-08-17	2019	1903	(838, 4758)	0.9	(0.4, 2.4)
2005-11-18	2019	30926	(16100, 62946)	15.3	(8, 31.2)
2006-02-02	2019	26731	(12545, 60918)	13.2	(6.2, 30.2)
2006-02-25	2019	30889	(16753, 60362)	15.3	(8.3, 29.9)
2006-03-12	2019	13429	(7448, 23564)	6.7	(3.7, 11.7)
2006-04-15	2019	17628	(7656, 40837)	8.7	(3.8, 20.2)
2006-05-11	2019	2631	(1225, 6267)	1.3	(0.6, 3.1)
2007-01-25	2019	25145	(11765, 55017)	12.5	(5.8, 27.2)
2007-02-15	2019	55356	(25410, 121823)	27.4	(12.6, 60.3)
2007-03-03	2019	56780	(27126, 127078)	28.1	(13.4, 62.9)
2007-04-01	2019	34426	(17141, 72305)	17.0	(8.5, 35.8)
2011-03-01	2019	99824	(36662, 280932)	49.4	(18.2, 139.1)
2011-03-26	2019	32270	(17233, 60985)	16.0	(8.5, 30.2)
2011-04-11	2019	22055	(8451, 61187)	10.9	(4.2, 30.3)
2011-10-13	2019	11428	(5846, 20614)	5.7	(2.9, 10.2)
2011-11-17	2019	23603	(11813, 51294)	11.7	(5.8, 25.4)
2012-01-15	2019	68332	(39397, 119141)	33.8	(19.5, 59)
2012-02-08	2019	37881	(22702, 63735)	18.8	(11.2, 31.6)
2012-03-02	2019	40807	(18688, 97569)	20.2	(9.3, 48.3)
2012-03-22	2019	27405	(13411, 56338)	13.6	(6.6, 27.9)
2012-04-11	2019	7145	(4112, 12153)	3.5	(2, 6)
2023-11-17	2019	13669	(5798, 32285)	6.8	(2.9, 16)
2023-12-27	2019	22766	(12220, 43434)	11.3	(6.1, 21.5)
2024-01-09	2019	27840	(11892, 65485)	13.8	(5.9, 32.4)
2024-02-27	2019	70062	(32485, 158317)	34.7	(16.1, 78.4)
2024-04-08	2019	9816	(4065, 27688)	4.9	(2, 13.7)
2024-04-22	2019	11183	(4649, 30427)	5.5	(2.3, 15.1)

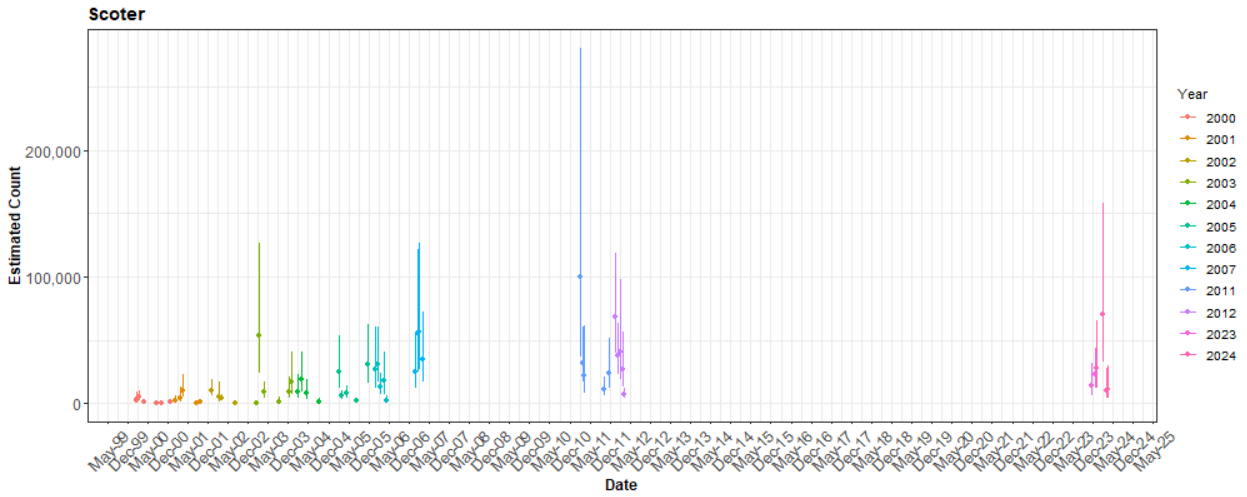

Figure 3.3. The estimated count of common scoter for each survey. The 95% CI are percentile-based confidence intervals are from a parametric bootstrap with 500 replicates. As the analysis area has the same extension between surveys, the estimated abundances are comparable.

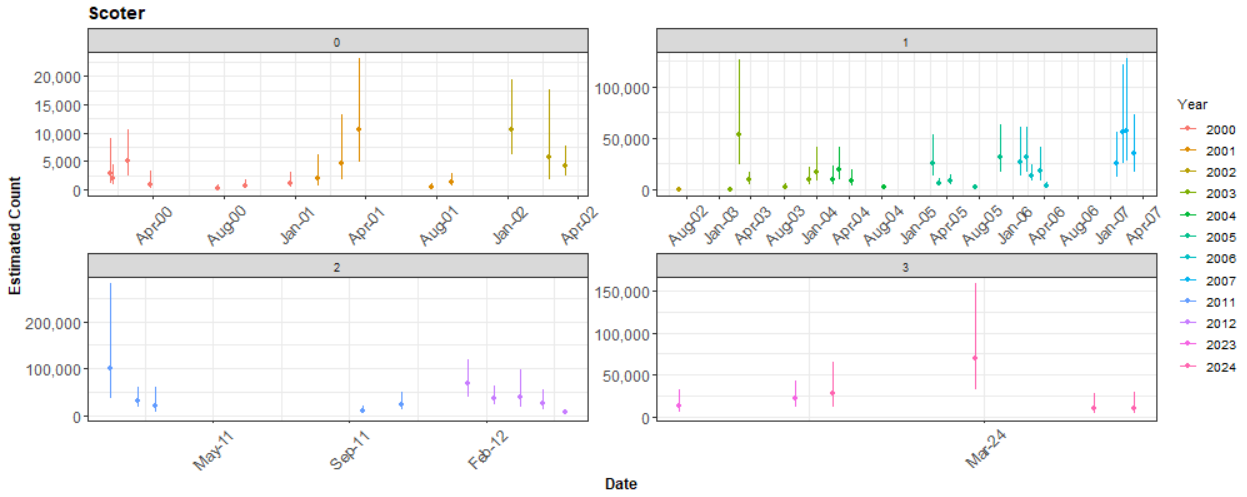

Figure 3.4. The estimated count of common scoter for each survey by phase. The 95% CI are percentile-based confidence intervals are from a parametric bootstrap with 500 replicates. To show more detail the y-axis is different for each phase.

3.2.3 Density Distributions

Figure 3.5 to Figure 3.8 show the estimated counts of common scoter in each 500 m x 500 m grid cells for each survey in each of the four phases. Generally, the estimated abundances fitted well to the raw data and there were no notable misalignments. In areas where the estimated counts were systematically higher, the abundances were also relatively high and there were no areas with large, estimated abundances unsupported by the data.

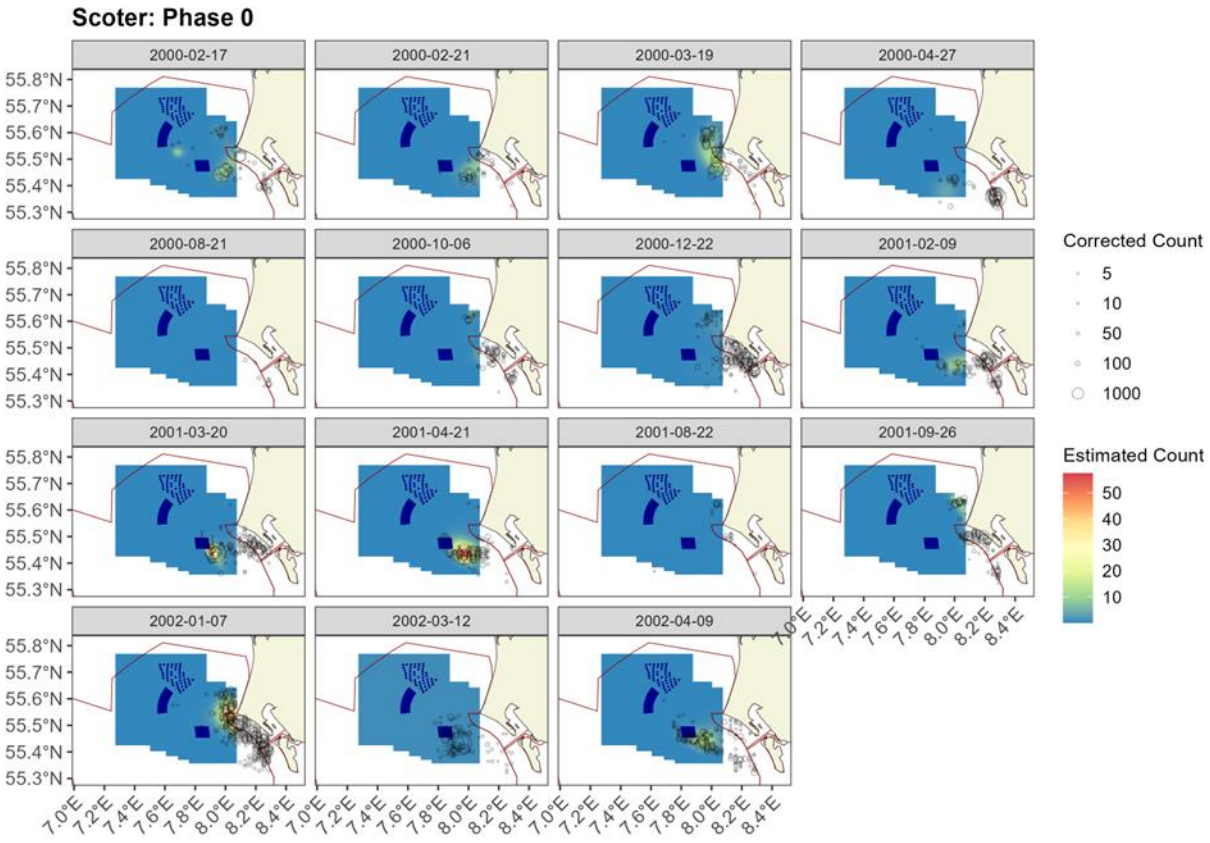

Figure 3.5. Figure showing the estimated common scoter abundance across the study site for each of the surveys in Phase 0. The estimated counts are per 500 m x 500 m grid cell. The open circles show the corrected counts. The coloured graphics represent the predicted counts in each location.

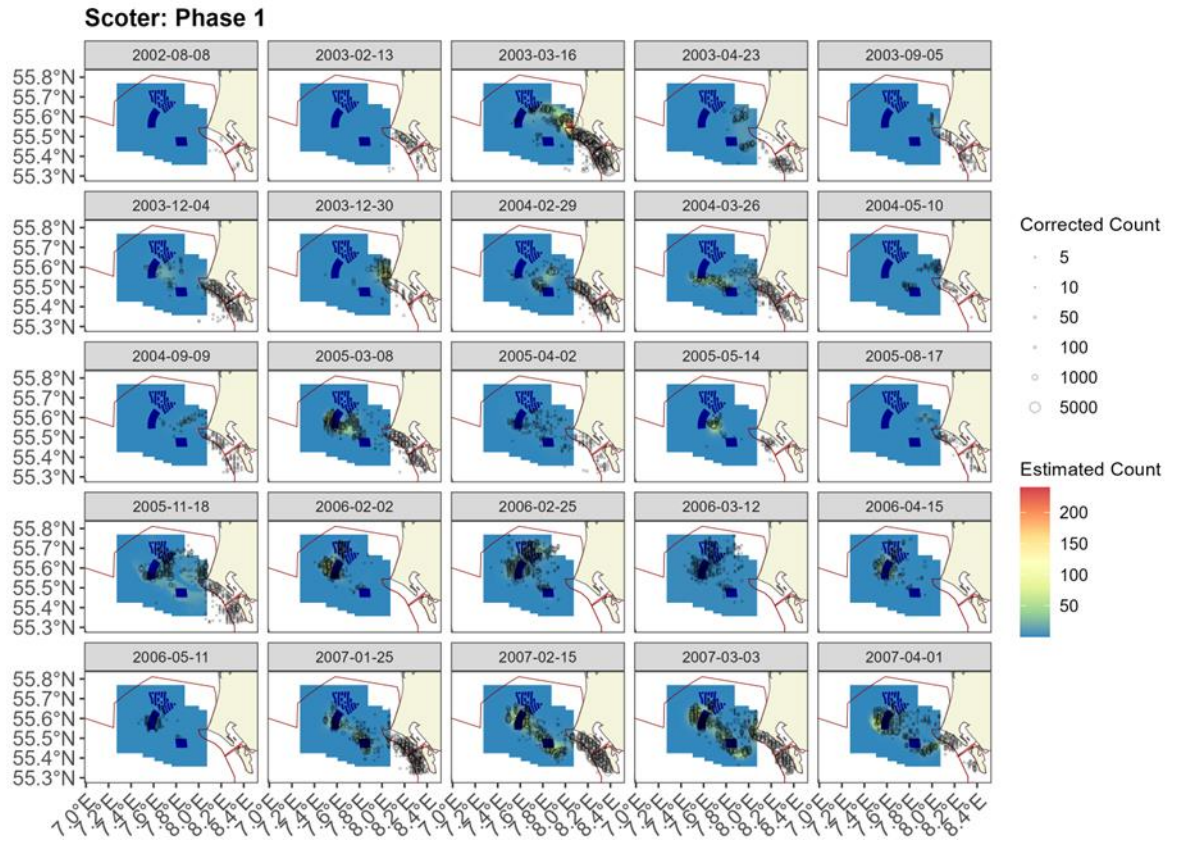

Figure 3.6. Figure showing the estimated common scoter abundance across the study site for each of the surveys in Phase 1. The estimated counts are per 500 m x 500 m grid cell. The open circles show the corrected counts. The coloured graphics represent the predicted counts in each location.

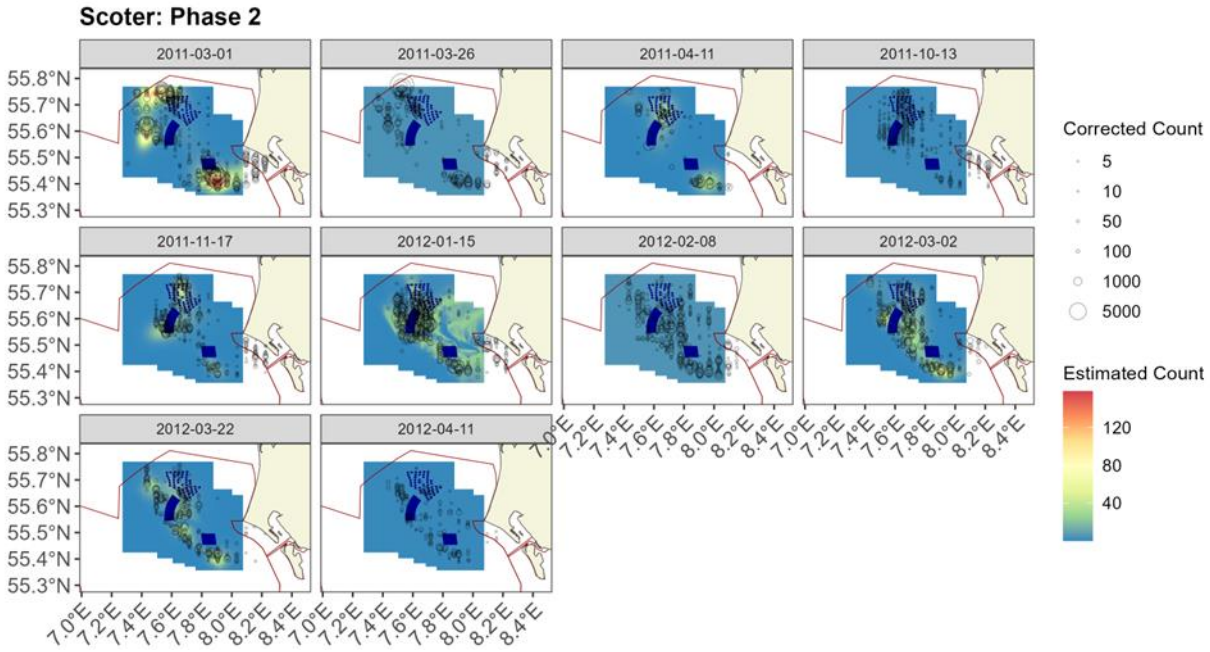

Figure 3.7. Figure showing the estimated common scoter abundance across the study site for each of the surveys in Phase 2. The estimated counts are per 500 m x 500 m grid cell. The open circles show the corrected counts. The coloured graphics represent the predicted counts in each location.

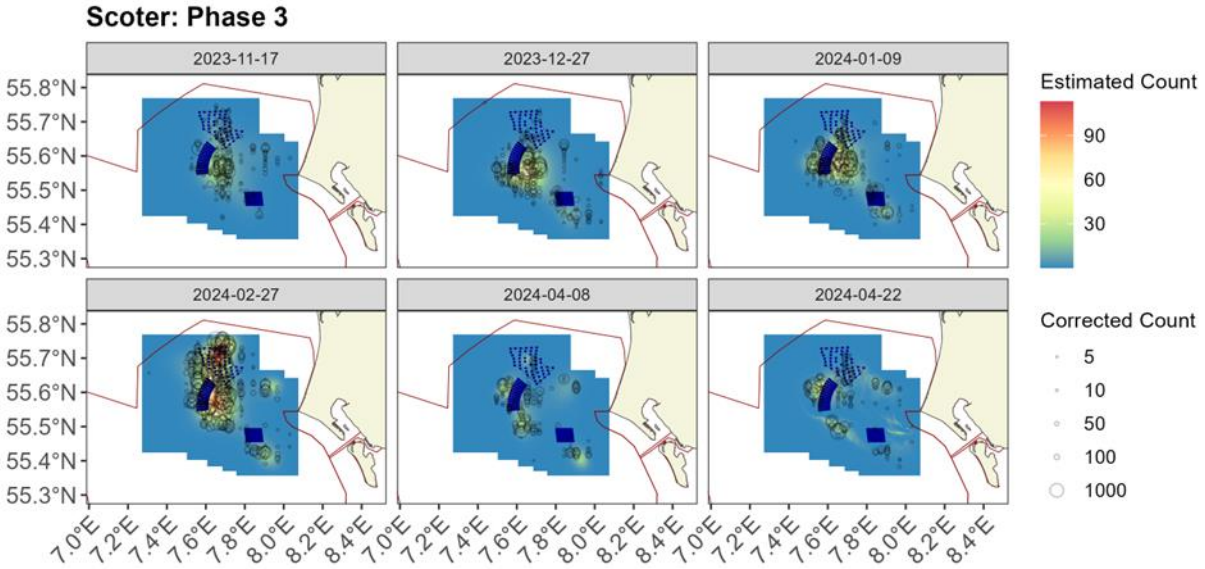

Figure 3.8. Figure showing the estimated common scoter abundance across the study site for each of the surveys in Phase 3. The estimated counts are per 500 m x 500 m grid cell. The open circles show the corrected counts. The coloured graphics represent the predicted counts in each location.

3.2.4 Uncertainty in spatial predictions

Broadly, the highest coefficient of variation (CoV) scores were associated with the `almost zero' predictions and it is known that the CoV metric is highly sensitive to any uncertainty for very small predictions. There was no material overlap between high values of the CoV metric and the transect lines/locations with non-zero counts. Therefore results can be considered to be valid i.e. they do not compromise the model (Figure 3.9).

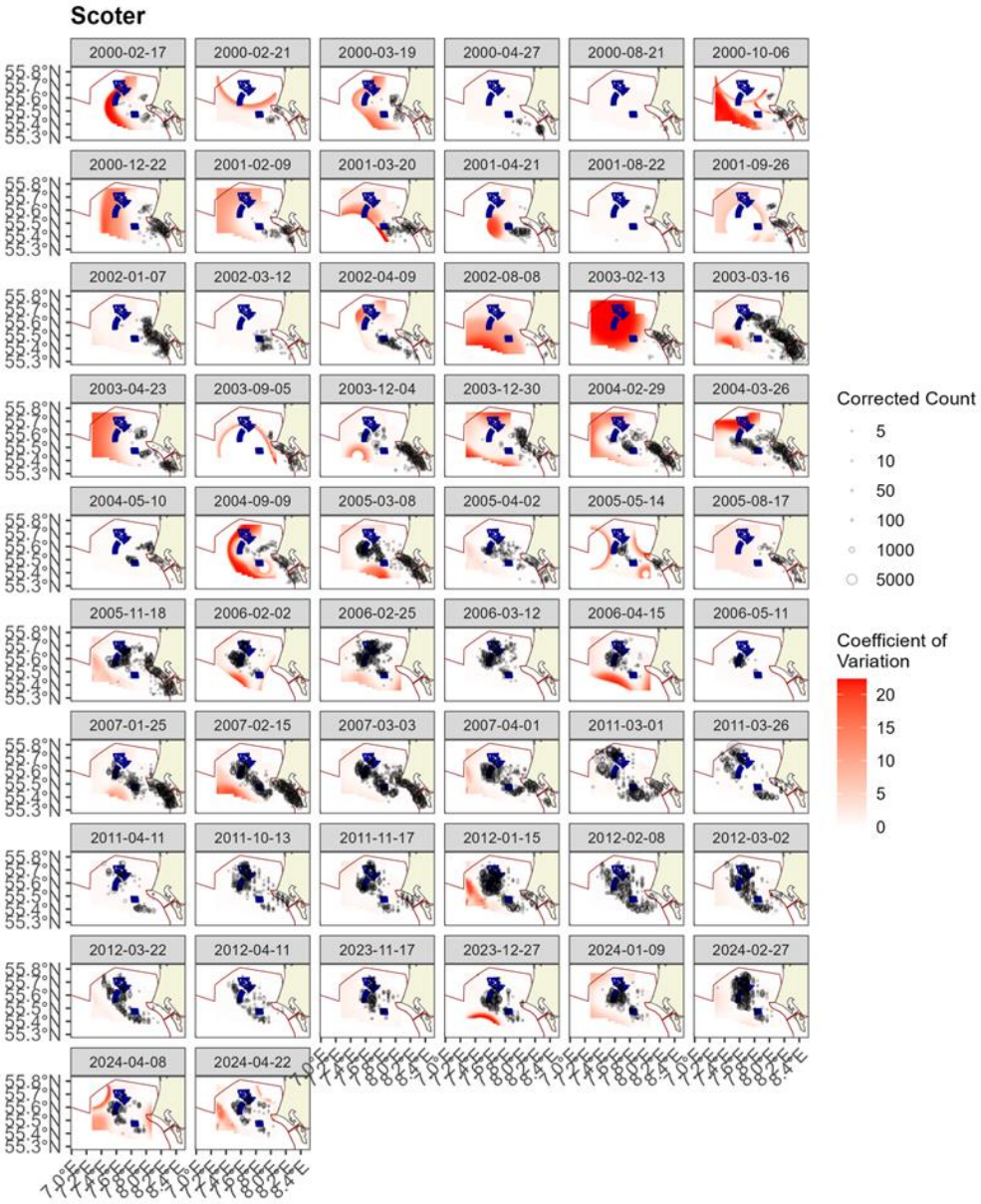

Figure 3.9. Figure showing the coefficient of variation across the study region for each of the surveys for common scoter. The open circles show the distance corrected counts. The presence of dark red CV scores in areas with virtually zero predictions are an artifact of the very small prediction rather than of any notable concern.

In the case, when the very small predicted values were excluded (Figure 3.10) there were some small red areas indicating high uncertainty but predominantly, these were in areas of very low predicted abundance.

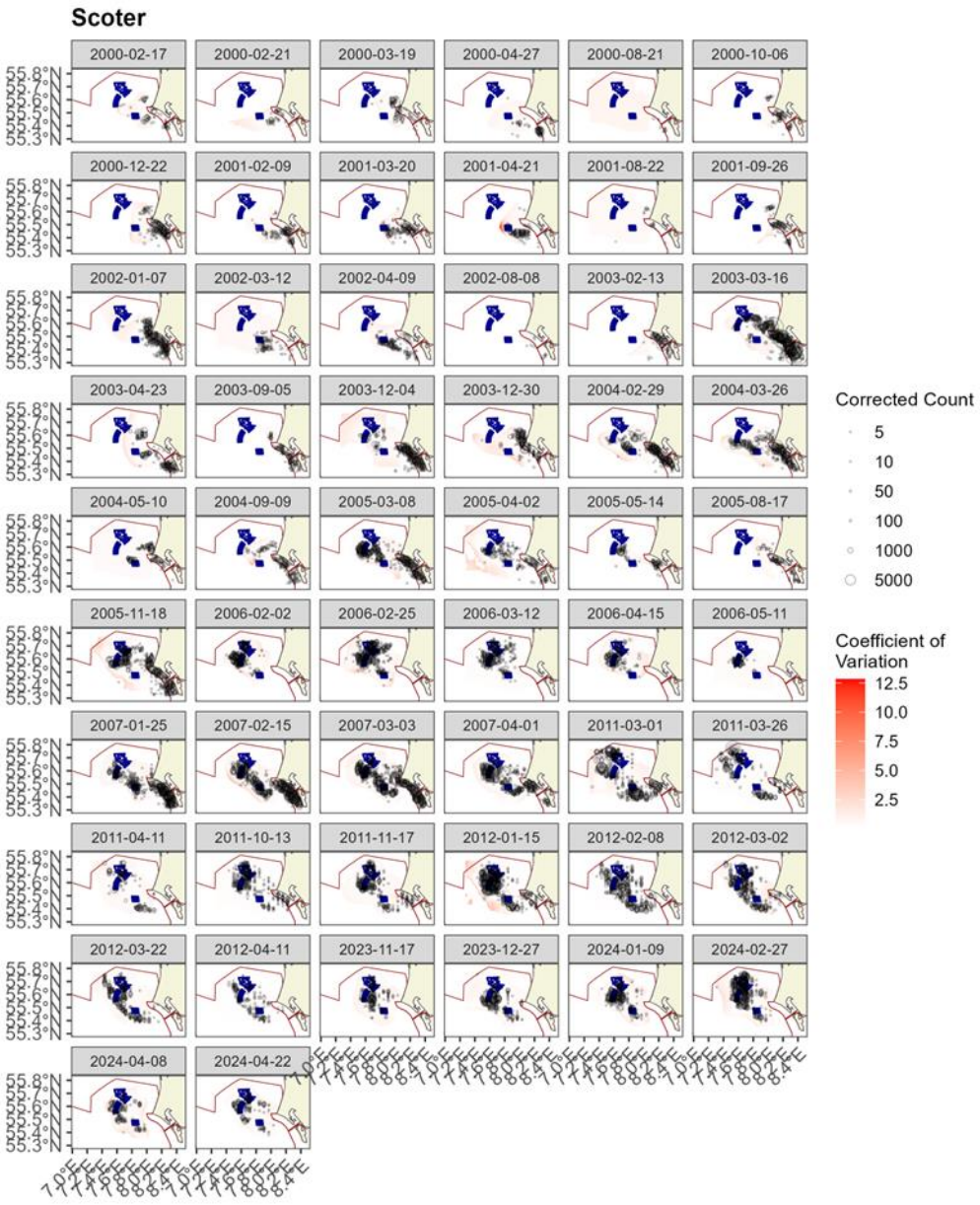

Figure 3.10. Figure showing the coefficient of variation across the study region for each of the surveys for common scoter. The open circles show the distance corrected counts. The presence of dark red CV scores in areas with virtually zero predictions are an artifact of the very small prediction rather than of any notable concern.

3.3 Common scoter Spatial results by Phase

3.3.1 Phase-specific spatial patterns

The mean distribution map in Phase 0 (Figure 3.11) illustrates the lack of common scoter in the majority of the study area, with the highest density of birds to the south east of the area. the distribution for Phase 1 shows the expansion of the geographic range to the north and west.

The abundance in Phase 1 appears to be higher than in Phase 0, which is true for the predicted area, however the majority of bird sightings in Phase 0 were to the east and so the change is not necessarily an indication of an increase in overall abundance of the species.

Phase 2 indicates a more uniform distributional pattern with the highest concentration of common scoter numbers to the south of the HR I footprint. Phase 3 has a much more concentrated abundance in the centre of the survey area, covering the HR II footprint to some extent but with a notable concentration to the east of this footprint. Phase 3 also demonstrates a non-trivial concentration in the footprint of the HR III footprint, even after its relatively recent construction.

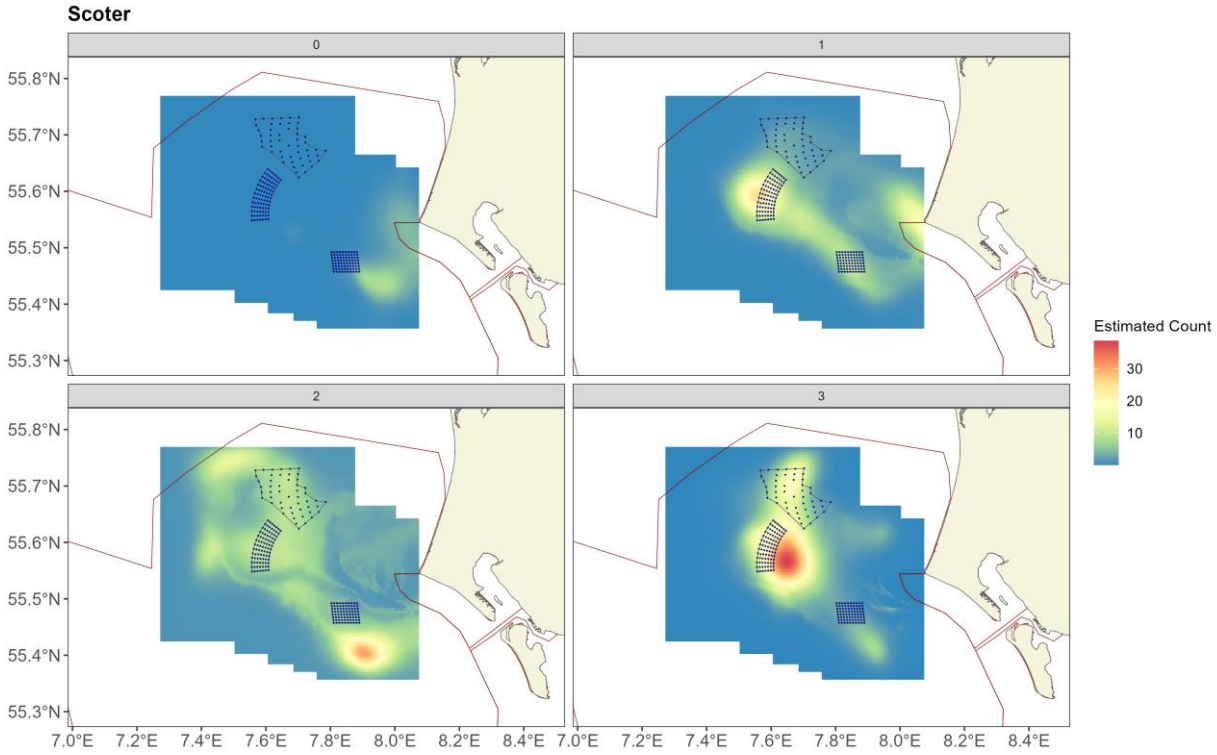

Figure 3.11. Figure showing the estimated common scoter abundance across the study site for each of the surveys from Phase 0 to Phase 3. The estimated counts are per 500 m x 500 m grid cell. The open circles show the corrected counts. The coloured graphics represent the predicted counts in each location.

3.3.2 Persistence

As well as looking at the mean distribution of birds in each phase, which may be influenced by a few surveys with large numbers of birds, we can assess the persistence of birds in each grid cell overall and by phase. The persistence analysis describes, at a fine geographical scale, areas of higher or lower usage by the species, evaluated over many surveys.

Across the 56 surveys (spanning 24 years) there is moderate to low persistence across the predicted area (Figure 3.12). The highest persistence (~ 50%) occurs in the central and south-eastern parts of the study area, along the extent of the Horns Rev sandbar.

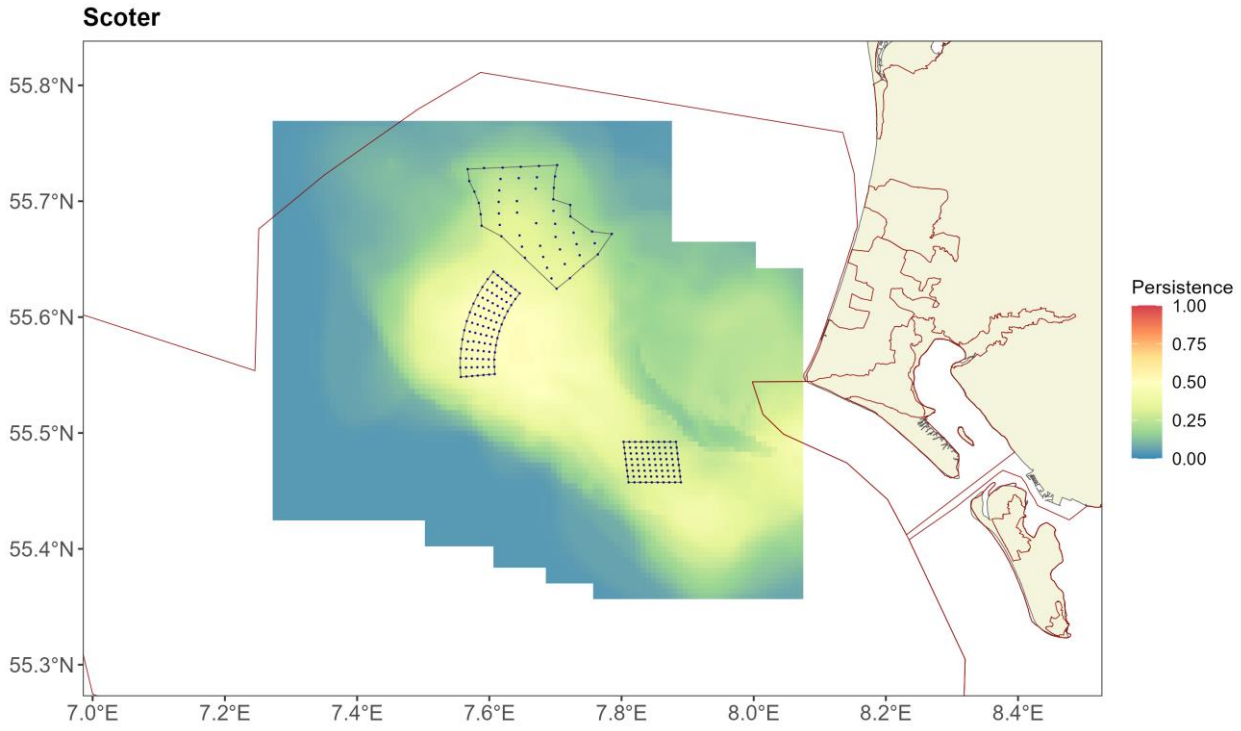

Figure 3.12. Persistence scores across the 56 surveys. The polygons represent the windfarms Horns Rev I, II and III (black line) with turbine locations indicated by the black dots.

Figure 3.13 to Figure 3.16 show the persistence of birds within each phase.

In Phase 0, prior to any construction, the birds show persistently high numbers to the east of the study region (Figure 3.13). After the construction of HR I (Phase 1), the birds became more prevalent offshore and more central in the study region, just to the east of where HR II would be constructed (at that time). The distribution in Phase 1 is also more widespread compared with Phase 0 which has a more focused distribution, nearer to shore (Figure 3.14).

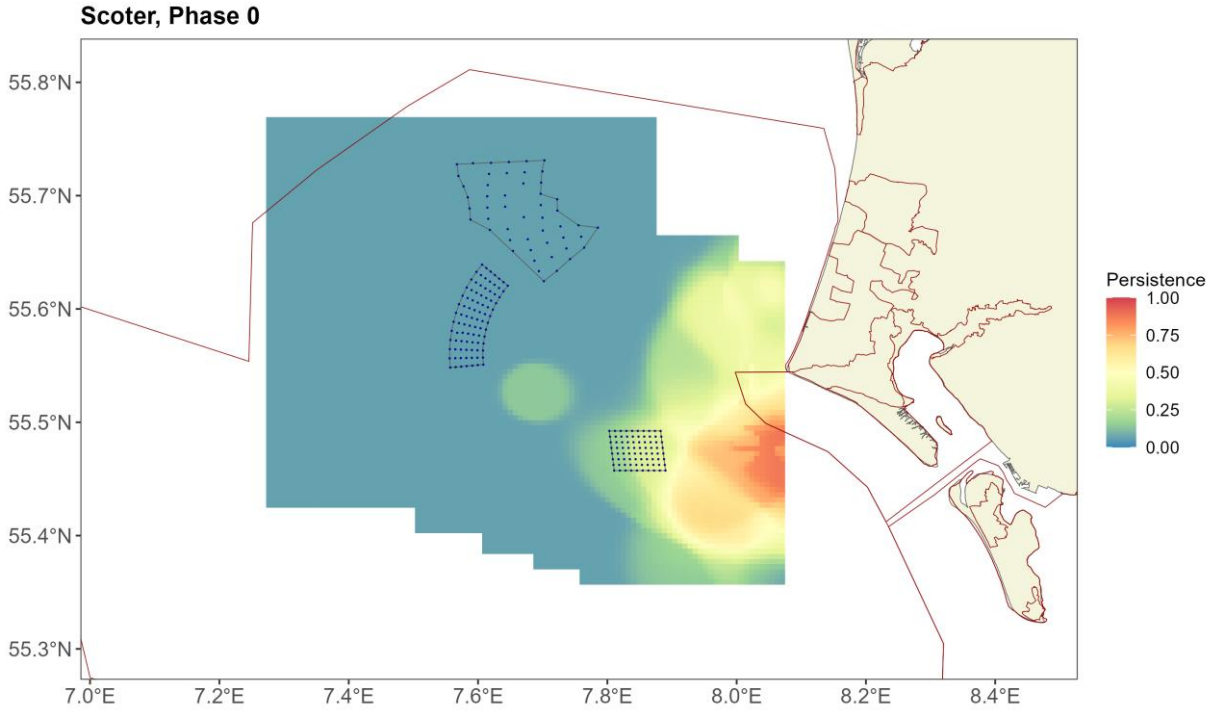

Figure 3.13. Persistence scores across the 15 surveys in Phase 0. The polygons represent the windfarms Horns Rev I, II and III (black line) with turbine locations indicated by the black dots.

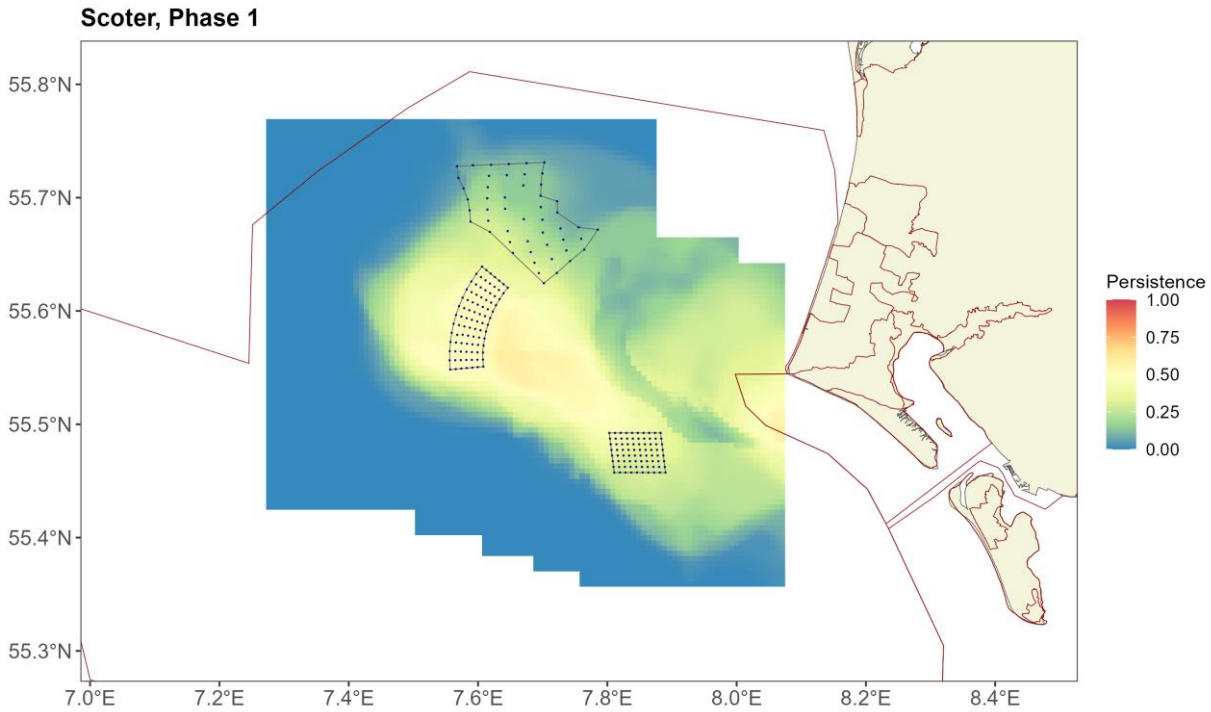

Figure 3.14. Persistence scores across the 25 surveys in Phase 1. The polygons represent the windfarms Horns Rev I, II and III (black line) with turbine locations indicated by the black dots.

Phase 2 is 2-5 years post-construction of HR II and 9-10 years post-construction of HR I. In this phase, the birds are persistently found to the south of HR I and on the eastern edge and north of HR II, and notably into the area where HR III was yet to be constructed (Figure 3.15).

The most recent surveys, in Phase 3, were carried out 5-6 years post-construction of HR III, 11-12 years post-construction of HR II and 21-22 years post-construction of HR I. During the Phase 3 surveys, the birds were persistently found in and around the HR II footprint. Additionally, while the persistence is relatively concentrated in and around HR II, some persistence was still seen to the south of HR I and to a lesser extent in the southern part of HR III (Figure 3.16).

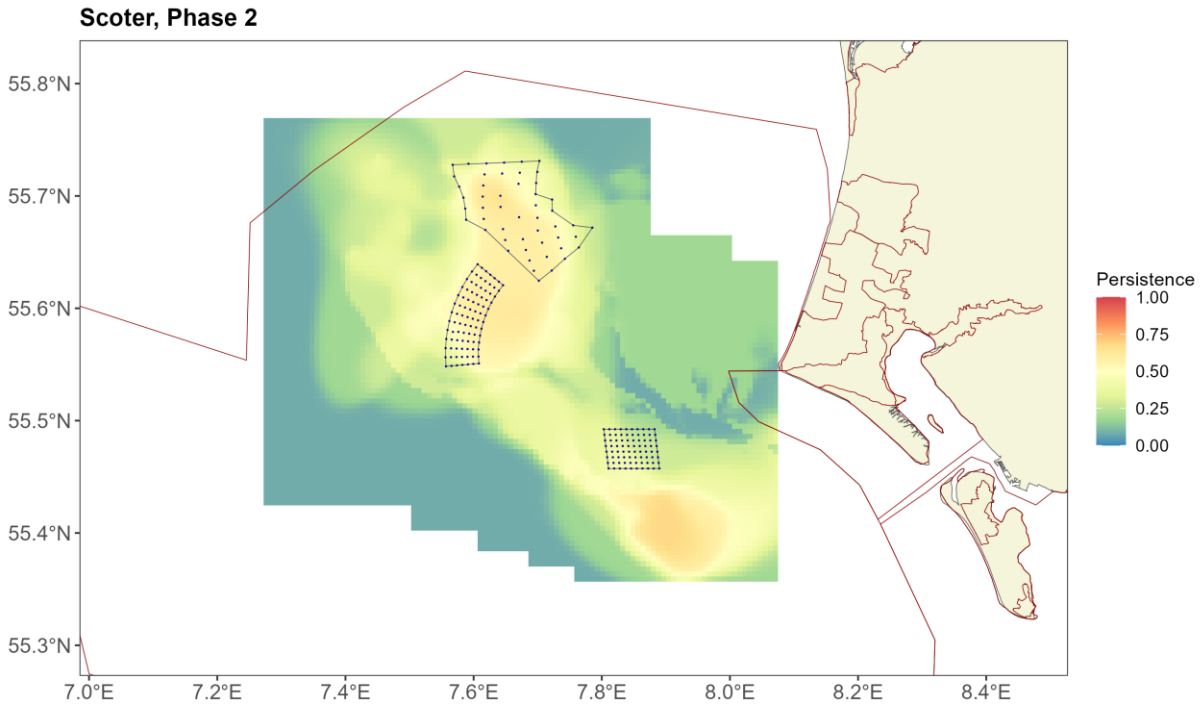

Figure 3.15. Persistence scores across the 10 surveys in Phase 2. The polygons represent the windfarms Horns Rev I, II and III (black line) with turbine locations indicated by the black dots.

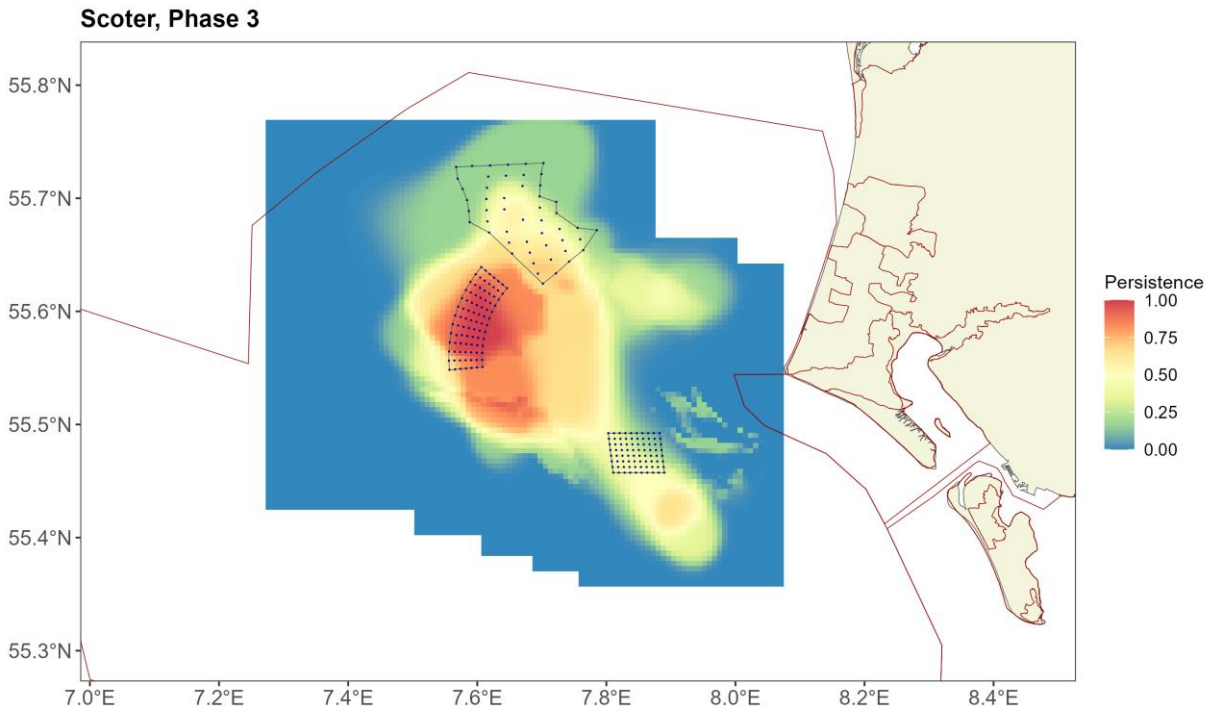

Figure 3.16. Persistence scores across the 6 surveys in Phase 3. The polygons represent the windfarms Horns Rev I, II and III (black line) with turbine locations indicated by the black dots.

3.3.3 Phase-specific windfarm footprint densities

Closer inspection of the estimated density of birds within windfarm-based footprints at various spatial scales was carried out to better understand any windfarm related changes (Figure 3.17 and Table 3-3). For instance, if there were no changes in common scoter density across the 24 years in this figure: either inside the footprint or up to 1 km or 2 km from the footprint then we would expect to see horizontal lines for all four colours in Figure 3.17. However, the likelihood of changes in bird density across this time frame is incredibly high, regardless of windfarm construction, and so any changes must be examined from several perspectives.

There has been a general increase in common scoter density from Phase 0-2 with some levelling off in Phase 3 (indicated by the black lines in Figure 3.17), providing a backdrop of variable abundances during the 24 years across the survey area.

Inside the footprint of each of the three windfarms (HR I, HR II and HR III) we see different patterns as each windfarm is constructed. Post-construction of HR I (Phase 1) we see an increased density within the footprint in compared with Phase 0. It is difficult to associate this change with the wind farm construction owing to the co-incident expansion of the geographic range of common scoter between those two phases throughout the survey area. The density in the HR I footprint drops off back to Phase 0 levels by Phase 3.

For HR II we see something different however, with a significant reduction of density inside the footprint after its construction (compared to pro-construction) with some recovery in Phase 3 (after HR III was constructed), to around Phase 1 density levels.

For HR III, we see increasing density from Phases 0 to 2, which is in line with the study wide increase in density and the geographic range expansion. From Phase 2 to 3 (pre- to post-construction of HR III) there is no significant change in footprint densities.

Within one and two kilometers of each windfarm footprint we also saw very similar patterns to those observed inside the footprint in each case.

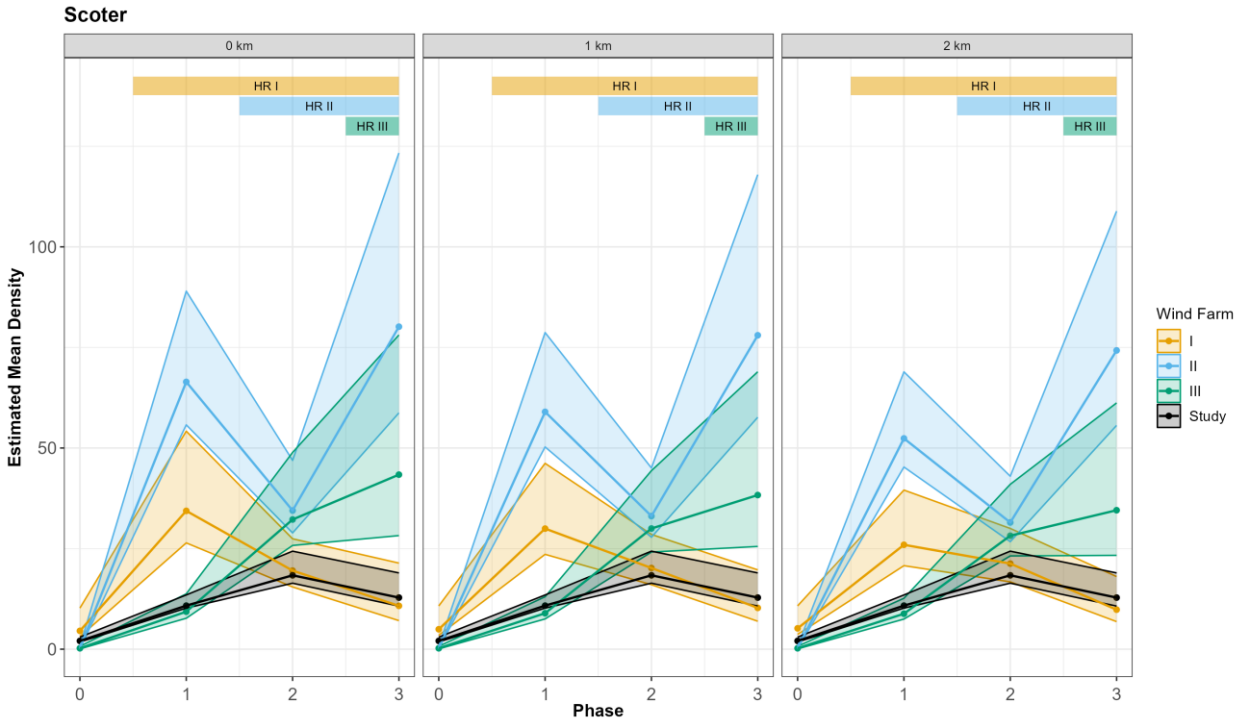

Figure 3.17. Figure showing the estimated mean density inside the footprint (indicated by 0 km from the footprint), footprint including a 1 km buffer (indicated by 1 km from the footprint) and footprint including a 2 km buffer (indicated by 2 km) of each windfarm for all phases. The bars at the top show the post-construction periods for each wind farm. Note that survey coverage in HR III during Phase 0 was limited.

Table 3-3. Table of abundance estimates and 95 percentile-based confidence intervals for each wind farm footprint and phase.

Phase	HR I	HR II	HR III
0	92.2 (63.4, 207)	7.28 (2.38, 22.4)	20.1 (6.24, 62.3)
1	697 (535, 1100)	2030 (1700, 2720)	797 (658, 1180)
2	396 (313, 556)	1050 (882, 1430)	2760 (2210, 4180)
3	218 (144, 434)	2450 (1790, 3760)	3710 (2420, 6680)

3.3.4 Phase-specific spatial differences

The shift in spatial patterns from Phase 0 to Phase 1 can be seen in Figure 3.18, which clearly illustrates a shift in common scoter numbers from the southeastern edge of the area of interest into the centre in Phase 1 and towards the HR II footprint before its construction. The increase in bird numbers in Phase 1, compared to Phase 0, is also evident here with significant increases in most locations in Phase 1 compared with Phase 0, and some higher than 20 birds/km^2 in many locations. While there is an abundance shift into the centre in Phase 1 (compared with Phase 0), there is also an increase on the eastern edge of the survey area in Phase 1, evidencing higher numbers than in Phase 0. There is a small, yet statistically significant, decrease in the south-eastern edge of the survey area, too, in Phase 1 compared with Phase 0.

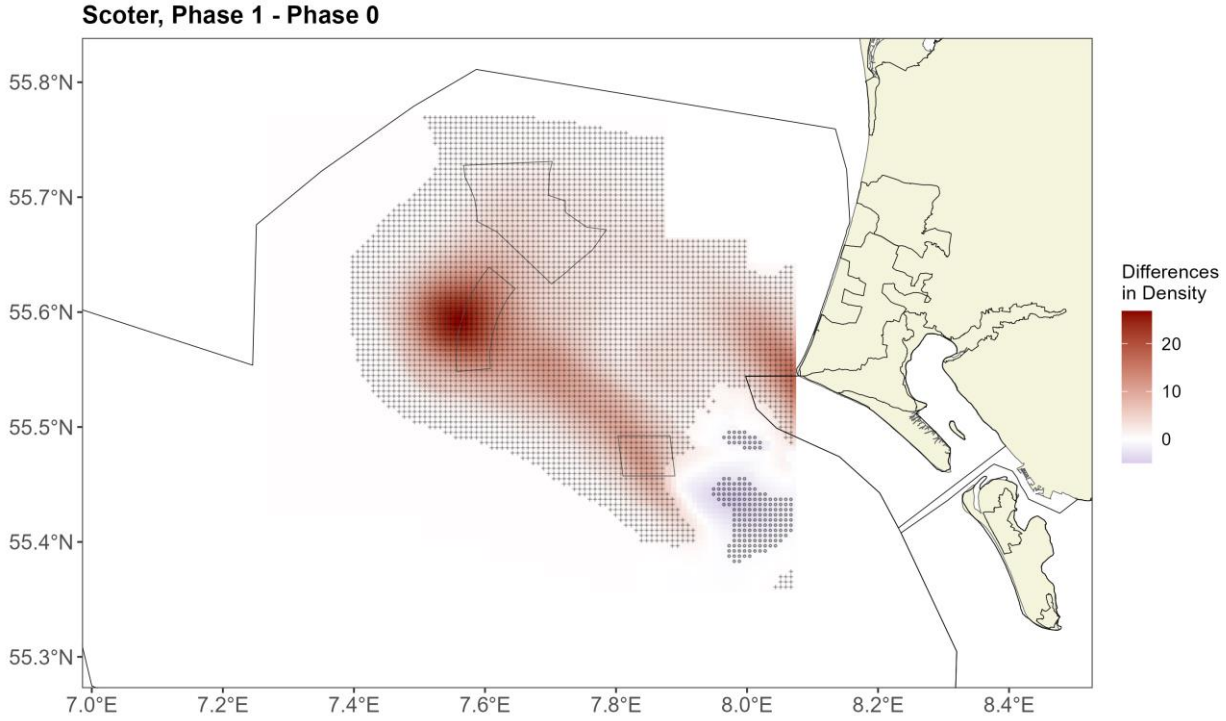

Figure 3.18. Figure showing the estimated differences in distribution between Phase 1 and Phase 0. Positive differences indicate more birds in Phase 1. A "+" sign in the bluish background colours indicates a significant positive difference and a "o" in reddish background colours a significant negative difference.

The statistically significant, and substantial, decreases in density in and around the HR II footprint subsequent to its construction (Phase 1 to Phase 2) is clear in Figure 3.19. This evidence-based shift away from the HR II footprint has delivered higher densities into the northeast and further north (in particular) of the HR II footprint, subsequent to its construction. The shift from Phase 1 to Phase 2 is also characterised by a concentration of common scoter numbers into the area south of the HR I footprint. The diminution in the previously relative abundant eastern edge of the survey area, is also signalled by the significant and relatively substantial decreases in this area (also Figure 3.19).

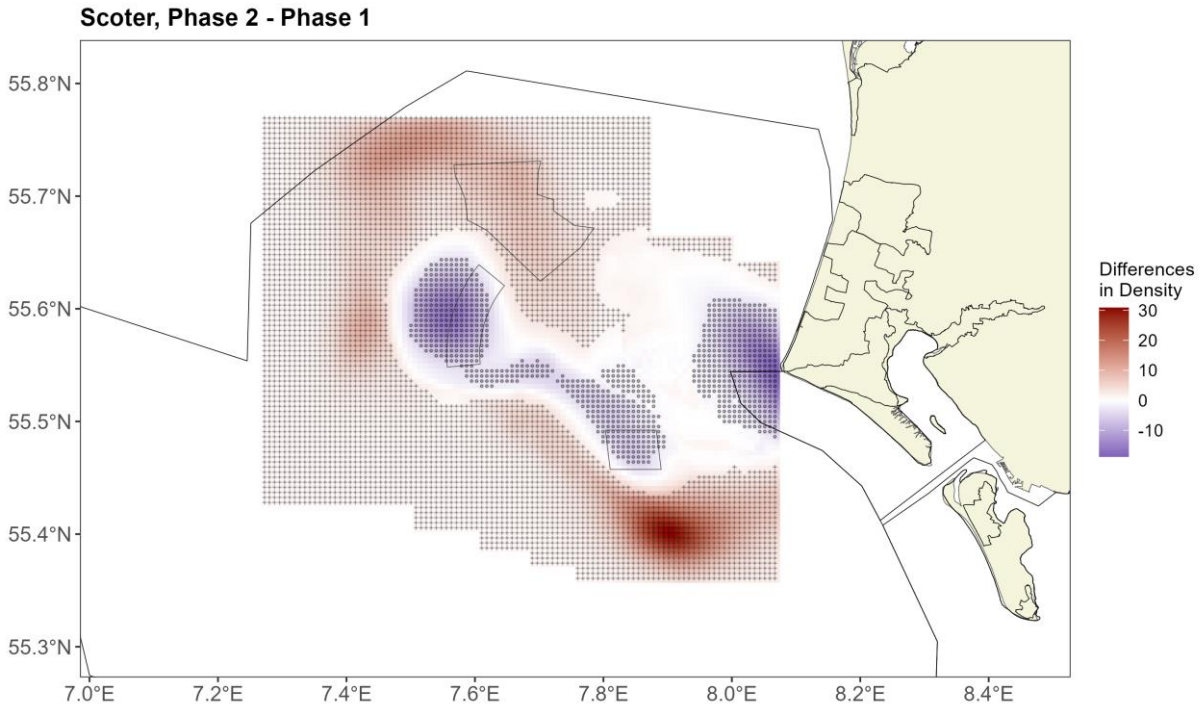

Figure 3.19. Figure showing the estimated differences in distribution between Phase 2 and Phase 1. Positive differences indicate more birds in Phase 2. A "+" sign in the bluish background colours indicates a significant positive difference and a "o" in reddish background colours a significant negative difference.

The relatively intense concentration in density in the centre of the survey area in Phase 3, compared to Phase 2, is clear from Figure 3.20. The large increases, evidenced by the red grid locations, do include the HR II footprint to some extent but with a more intense increase to the east of this footprint. While Phase 3 does demonstrate a density increase in the footprint of the HR III footprint (relative to Phase 2), these increases are largely not statistically significant and so these patterns show no evidence of an increase or decrease in numbers in the relatively recently built footprint. Of note here also is the significant decrease in numbers to the south of the HR I footprint and some additional decreases in the northwestern parts of the survey area.

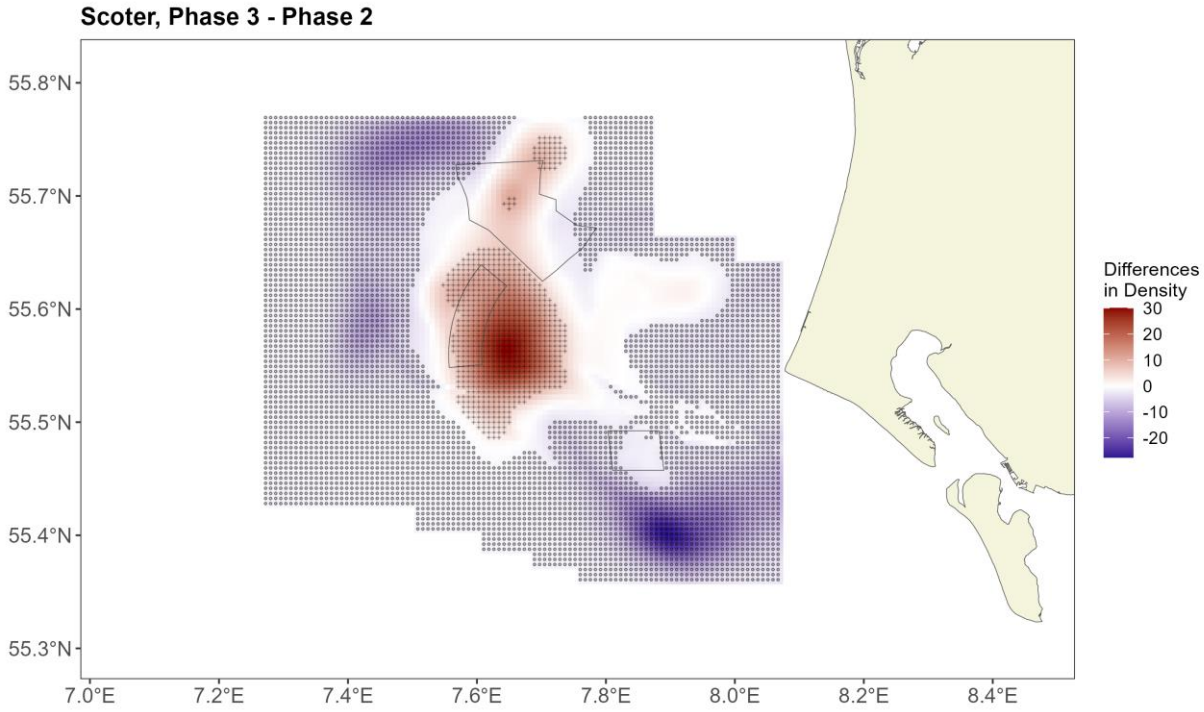

Figure 3.20. Figure showing the estimated differences in distribution between Phase 3 and Phase 2. Positive differences indicate more birds in Phase 3. A "+" sign in the bluish background colours indicates a significant positive difference and a "o" in reddish background colours a significant negative difference.

In Phase 3, common scoter show evidence of shifting into the east of the HR II footprint and to a lesser extent into the HR III footprint with some minor increases in the south-eastern edge, compared with Phase 1 (Figure 3.21).The significant and notable decreases are limited to the far-eastern edge of the survey area and to the west of the HR II wind farm, since there are statistically significant decreases in a larger number of locations, the estimated decreases in these locations are typically very small.

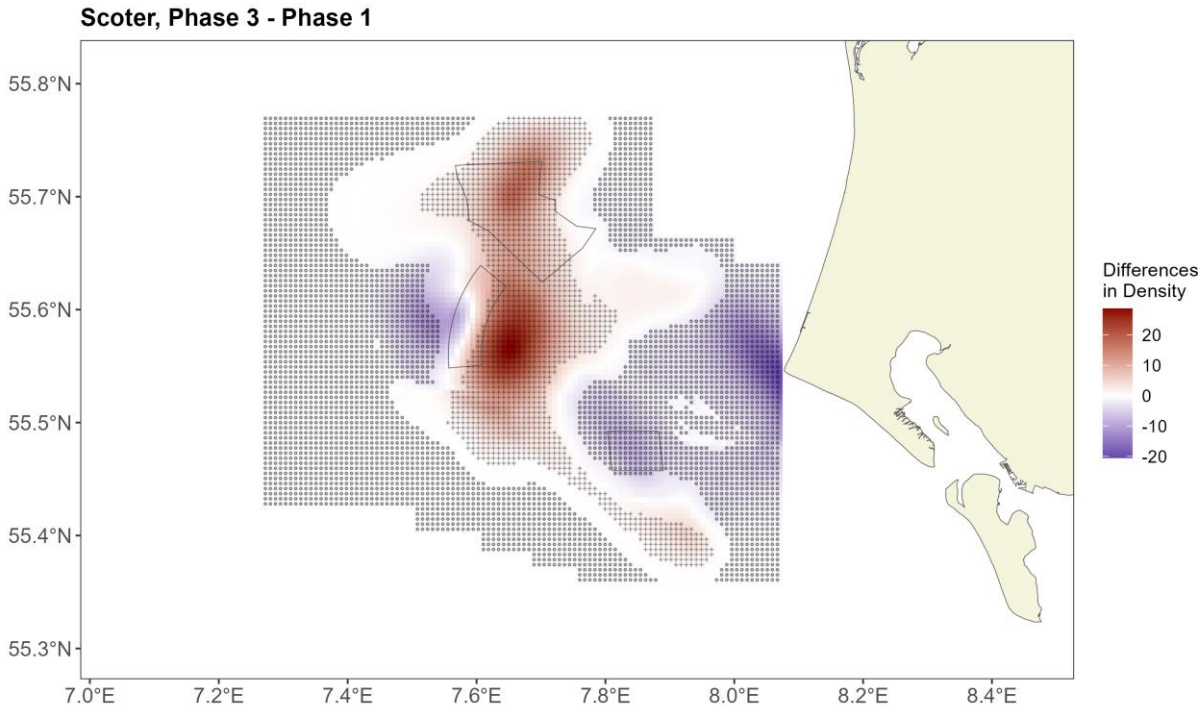

Figure 3.21. Figure showing the estimated differences in distribution between Phase 3 and Phase 1. Positive differences indicate more birds in Phase 3. A "+" sign in the bluish background colours indicates a significant positive difference and a "o" in reddish background colours a significant negative difference.

In general, these difference maps show that the area in and around HR I supported few birds pre-construction but showed an increase to relatively stable densities thereafter. It is hard to know if the birds showed low levels of displacement response to this wind farm and have always been present at low density in the area, or if the construction has kept numbers low within and around HR I. The common scoter densities around HR II increased prior to construction (from Phase 0 to 1), reflecting the expansion of their distribution westward at this time, particularly increasing on and to the west of HR II. After the construction of HR II (Phase 2) there was a significant decline in the footprint (approximately 50%, Table 3-3). Much later after construction of HRII, during Phase 3, numbers within the footprint returned to pre–construction levels. At the same time the common scoters expanded westwards at Horns Rev, with increasing densities around the HR II OWF.

From these results, it is possible to speculate that there was little/no effect of the installation of HR III on bird density and to potentially further conclude that this reduced impact may be due to the wider spacing of the turbines in the footprint for this farm in particular. While this is compelling speculation, there would need to be additional examples of windfarms with different/larger spacings in different locations to deliver this conclusion.

3.4 Common scoter Horns Rev II (HR II) specific results

The co-incidence of the expansion west and the lack of birds seen in the HR I footprint does not lend it to a finer scale investigation of displacement. The HR II wind farm is ideal with plenty of pre- and post-construction data available and notable changes in density. The change in survey coverage and the expansion west during Phase 1 do however have the potential to lead to misleading results. Figure 3.22 shows that while early surveys captured the footprint of HR II, there was limited coverage of HR III and the west of the study area. Figure 3.23 shows the mean density in early Phase 1 surveys (pre November 2005) compared with late surveys and all surveys combined. Including all surveys in Phase 1 conflates the longer-term change across the five-

year period, with any construction related changes we are hoping to detect. This leads to a dilution effect on the density surface, particularly around HR II, when including the early surveys in Phase 1. As there has been a clear distributional shift alongside a change in survey coverage, we have chosen to assess the HR II farm using only November 2005 data onwards, which is also in line with the analysis in the 2014 report (Petersen et al. 2014).

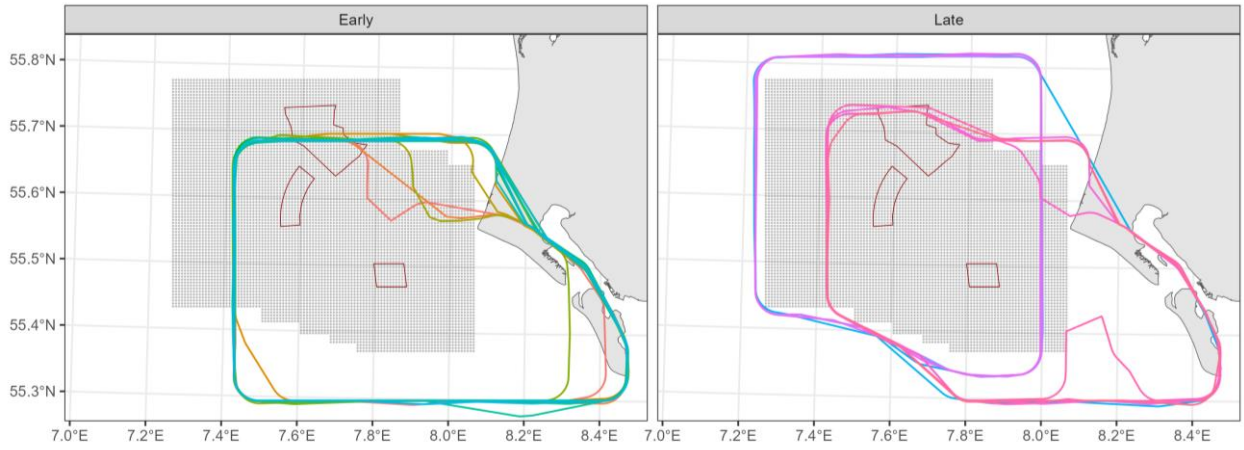

Figure 3.22. Figure showing the survey coverage within Phase 1 for "Early" surveys (pre November 2005) and "Late" surveys (post November 2005). The grey dots show the prediction grid coverage.

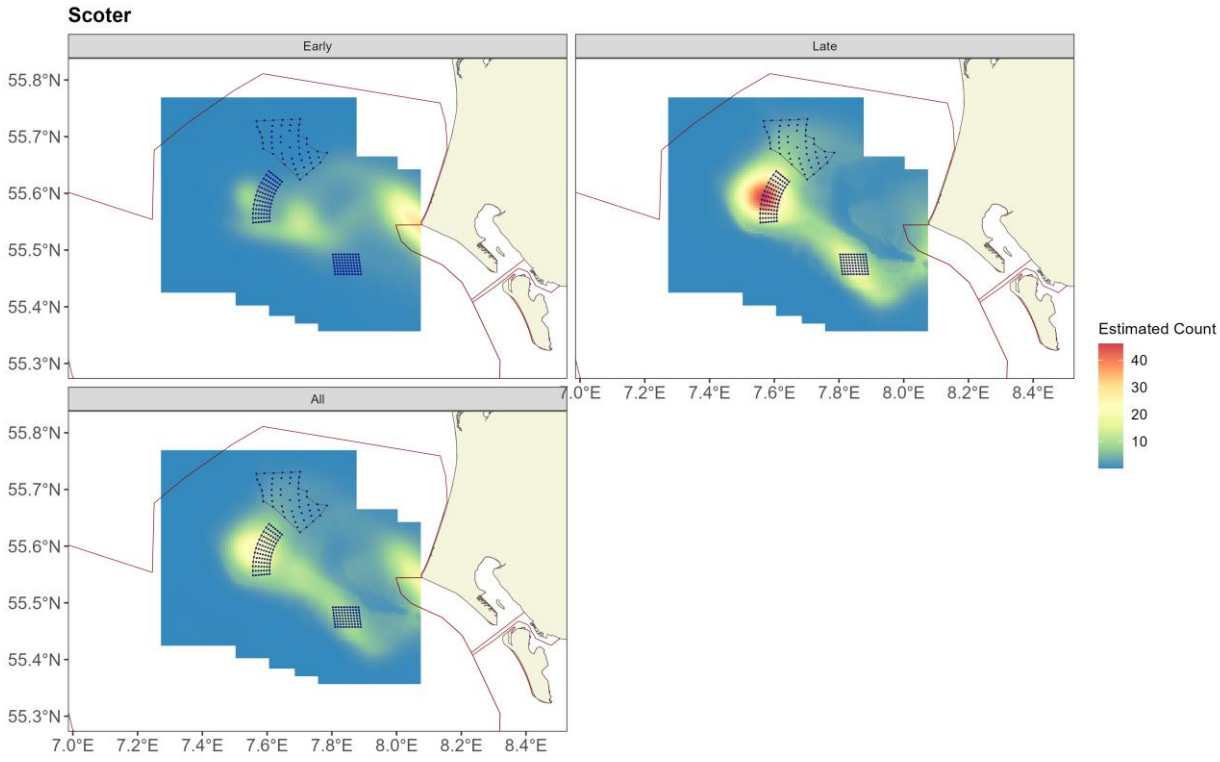

Figure 3.23. Figure showing the estimated common scoter abundance across the study site within Phase 1 for "Early" surveys (pre November 2005), "Late" surveys (post November 2005) and for all combined. The estimated counts are per 500 m x 500 m grid cell. The coloured graphics represent the predicted counts in each location.

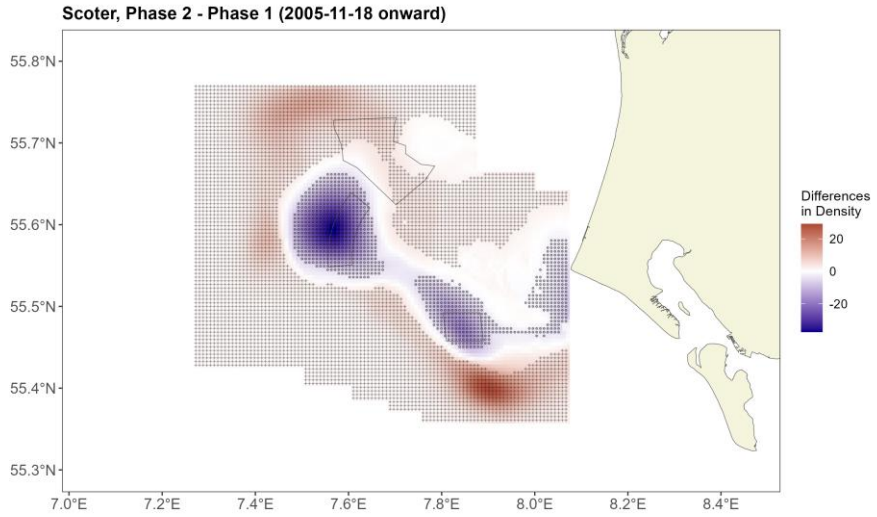

Figure 3.24. Figure showing the estimated differences in distribution between Phase 2 and the shortened Phase 1. Positive differences indicate more birds in Phase 2. A "+" sign indicates a significant positive difference and a "o" a significant negative difference.

Compared with Figure 3.19 (Phase 1-2), the use of the shortened Phase 1 (Figure 3.24) strengthens the decrease in density over the HR II footprint post-construction. Table 3-4 shows 100% of the cells in the HR II are estimated to have significantly decreased density post-construction.

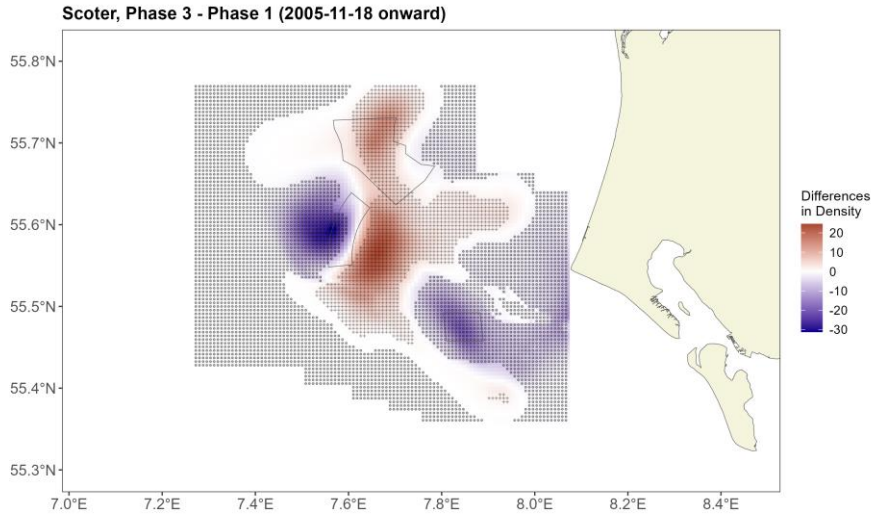

Figure 3.25. Figure showing the estimated differences in distribution between Phase 3 and the shortened Phase 1. Positive differences indicate more birds in Phase 3. A "+" sign indicates a significant positive difference and a "o" a significant negative difference.

Compared with Figure 3.21 (Phase 3-1), the use of the shortened Phase 1(Figure 3.25) strengthens both the decrease in density to the west of the HR II footprint post-construction and the increase to the east. Table 3-4 shows 34.4% of the cells in the HR II are estimated to have significantly decreased density post-construction and 13.9% significantly increased.

*Table 3-4. Table showing the percentage of cells in the Horns Rev II wind farm footprint that estimate an increase or a decrease in abundance and also the percentage of cells that significantly increase or decrease (calculated from the bootstrap predictions). The * for Phase 1 indicates the shortened Phase 1.*

Horns Rev II	**Pre-con. to 2-3 yrs post-con.**	**2-3yrs post-con. to 11-12 yrs post-con.**	**Pre-con. to 11-12 yrs post con.**
Phase	1*-2	Phase 2-3	Phase 1*-3
% Cells in footprint increasing	0	100	13.9
% Cells significantly increasing	0	94.3	0
% Cells in footprint decreasing	100	0	86.1
% Cells significantly decreasing	100	0	34.4

3.4.1 HR II related changes across phases in all directions

We can also collapse the spatial patterns down into one dimension using concentric rings of increasing distance from the footprint and assess how the density changes between phases varies with distance. Figure 3.26 illustrates a displacement effect (reduction in density) post-construction (Phase 2 - 1) out to approximately 5 km from the footprint (where the change rises to zero (no difference)).

Comparing Phase 3 to Phase 1 however, we see no compelling evidence for a difference in mean density in the HR II footprint, or up to 15 km from this footprint, after HR II and III are both constructed – a sort of recovery. This comment considers both the proximity of the difference in density estimates at each distance from the HR II footprint and the associated uncertainty of each estimate (indicated by the grey envelope in Figure 3.26).

In contrast to the earlier phase-based comparisons, the Phase 3-2 comparison shows an increase in density in Phase 3 compared to Phase 2 within 5 km of the HR II footprint, which declines to 'no change' thereafter. This shows that between two and three years post-construction and 11-12 years post-construction the mean density in the footprint and surrounding areas has returned to pre-construction levels.

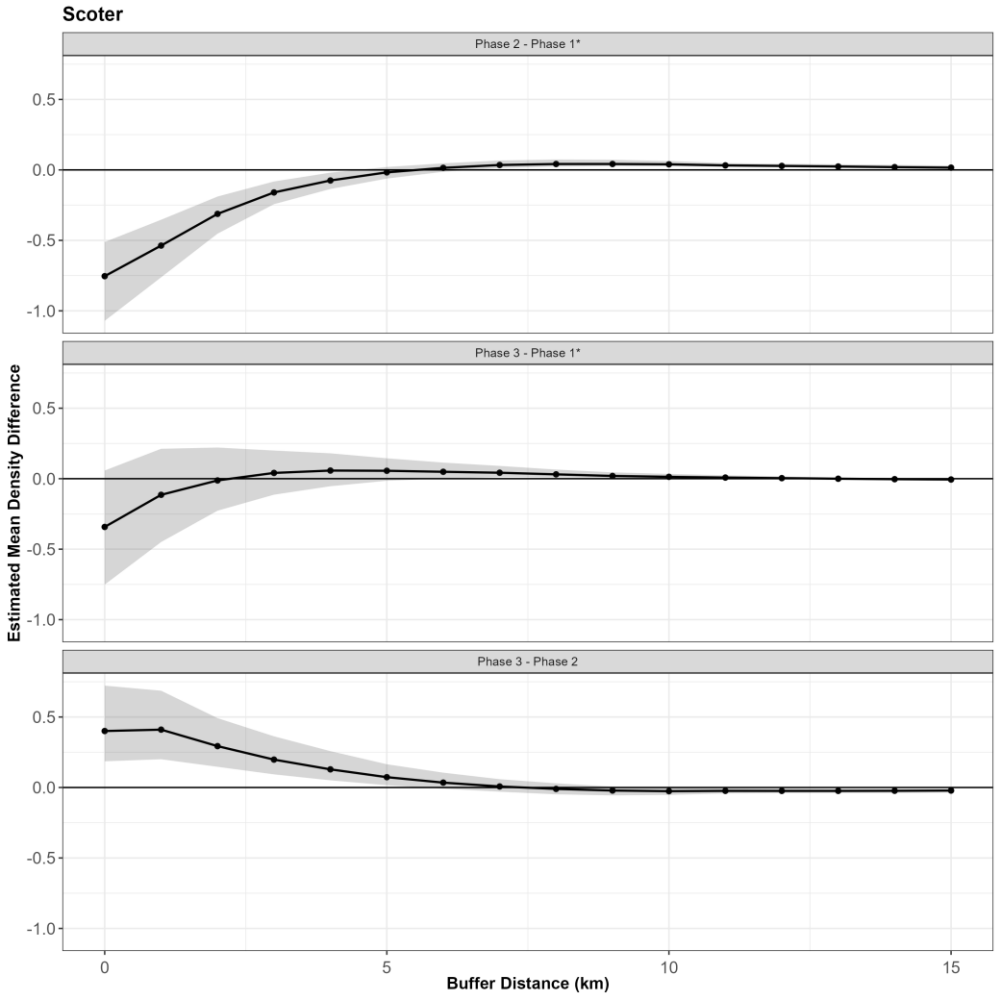

Figure 3.26. Figure showing the differences with distance to footprint by phase change.

3.4.2 HR II related changes across phases, direction specific

In contrast to Figure 3.26 which aggregates any distance related changes in and around the HR II footprint, across North-East (NE), South-East (SE) and West (W) sectors, the results were also examined by directional 'sector'.

The spatial differences in Figure 3.25 highlight the possibility that significant decreases in density to the west may be cancelled out or masked by increases in density to the east and make displacement distances appear to be less significant than they might otherwise be. For this reason, we selected three sectors: North-East (NE), South-East (SE) and West (W) to assess displacement in. The NE sector contains HR III and the first turbine is approximately 3km from the edge of HR II. The SE sector can be considered the inshore side of HR II and showed evidence of consistent increases in abundance post-construction. The W sector, on the offshore side of HR II, shows evidence of consistent decreases in density post construction. Rather than just assessing the displacement distance in concentric rings around the footprint of HR II we have assessed displacement separately in the three sectors.

Figure 3.27 illustrates that NE from the HR II footprint, which starts to encompass HR III after approximately 3 km, we see the displacement evident to 2 km of the footprint (seen in Figure 3 26) when HR II was constructed. Over the longer time span (Phase 3-1) in this sector, there is no evidence of a decrease or increase in density regardless of distance from HR II.

In the SE, we see evidence of a post-construction displacement effect to approximately 3 km from the footprint and over the longer time span (Phase 3-1) there is no evidence of displacement 1-1.5 km from the footprint and evidence of an increase 1.5 – 8 km away.
The Western sector shows a different set of effects. Post construction shows a displacement effect to approximately 5.5 km and, despite some increases in density in Phase 2 close to HR II, a longer-term displacement effect of 8-9 km.

This shows that, in this case, it matters in which direction from the footprint you look when investigating displacement effects. When assessed in concentric rings, the displacement distance was 2 km but when assessed by sectors, the displacement distances varied between 2 km (in the NE sector) to 5.5 km or 8-9 km (in the W sector).

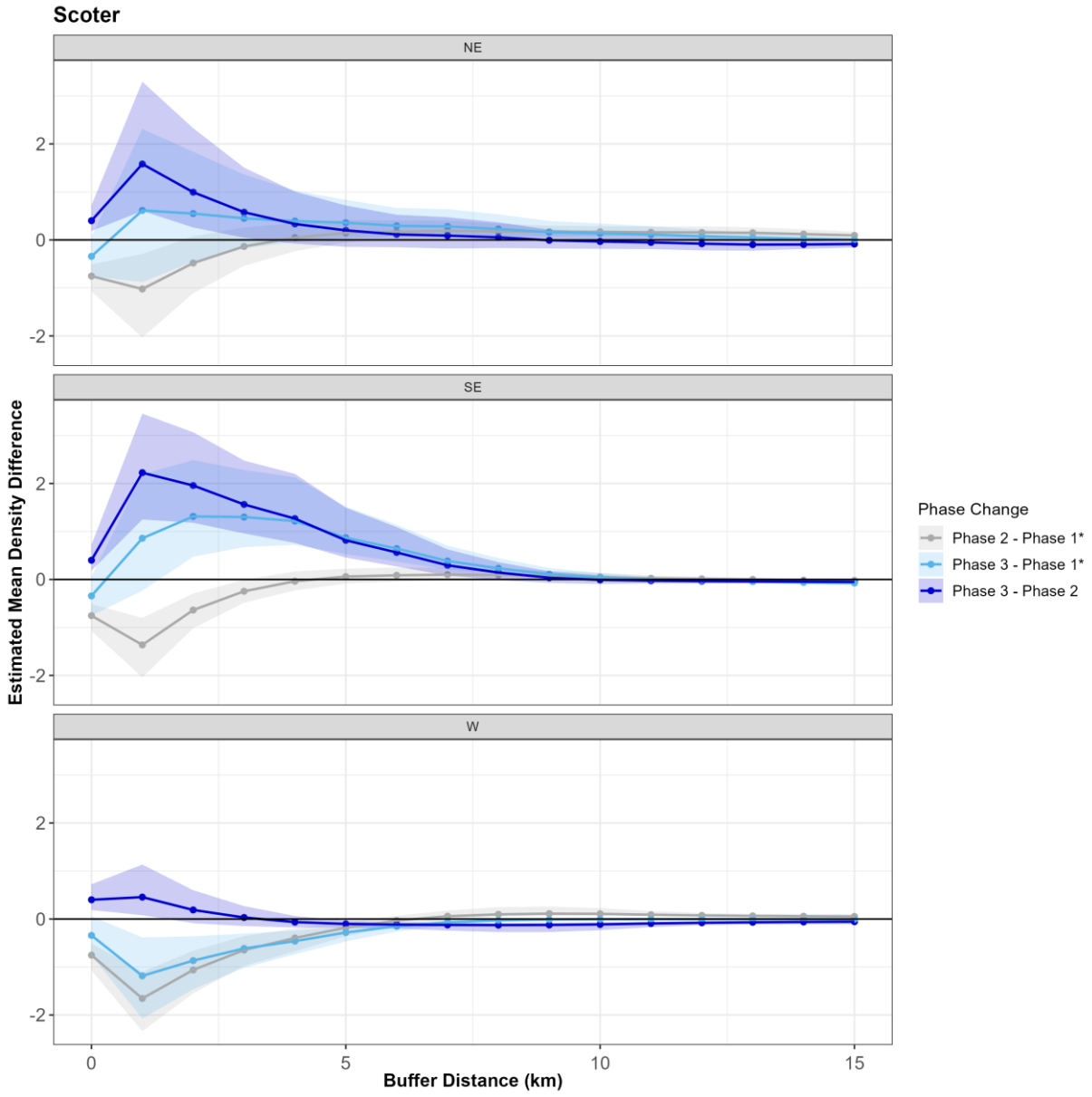

Figure 3.27. Figure showing the differences with distance to footprint by phase change and by sector. Any differences in underlying mean densities related to the HR II footprint would be indicated by a change near to the footprint with a decay thereafter.

3.5 Diver Distance Analysis

The average probability of sighting diver species was estimated to be 0.21 (CoV=0.02). This probability was estimated using a hazard rate detection function and observer and behaviour as covariates (Figure 3.28 and

Figure 3.29). The results show, as might be expected, a higher detection probability of flying compared with sitting birds.

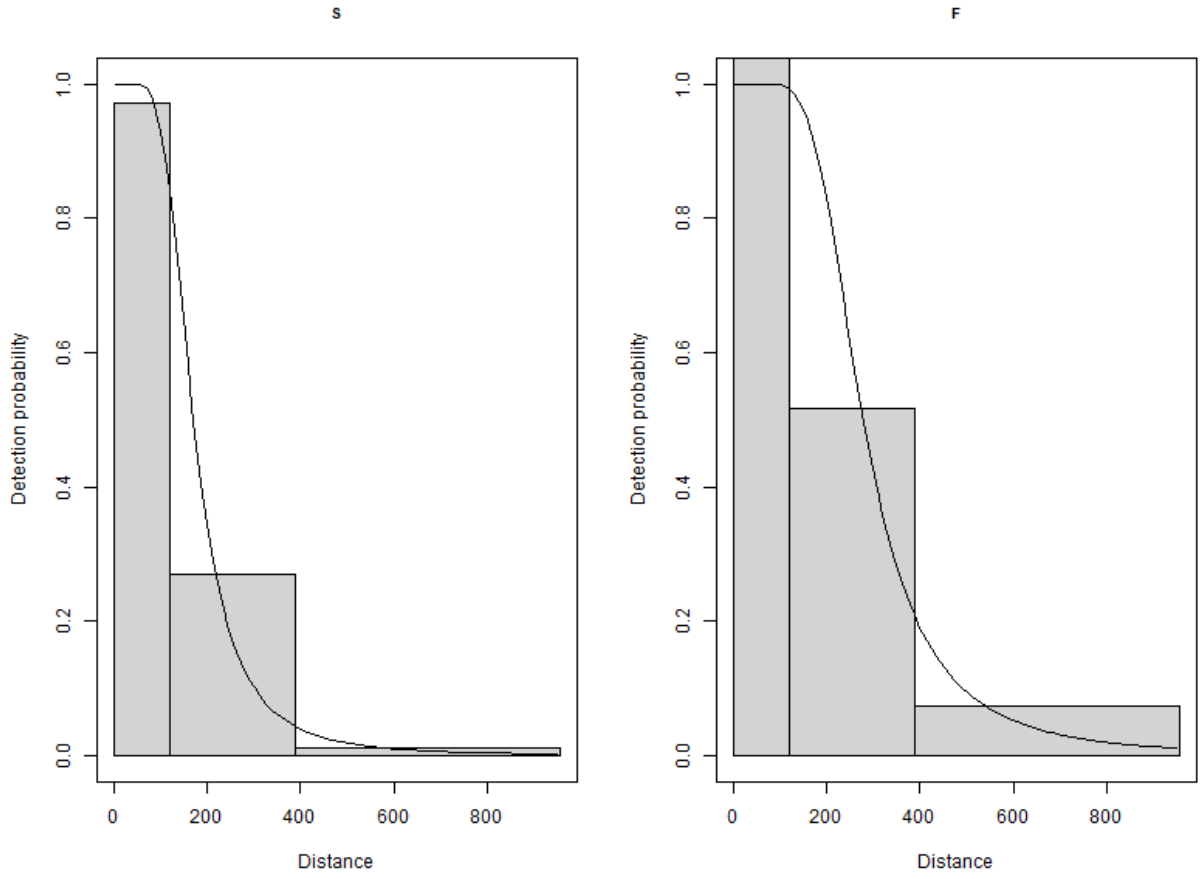

Figure 3.28. Figure showing the estimated detection function. The histograms represent the distances of the observed sightings across behaviour types: sitting (S) and flying (F).

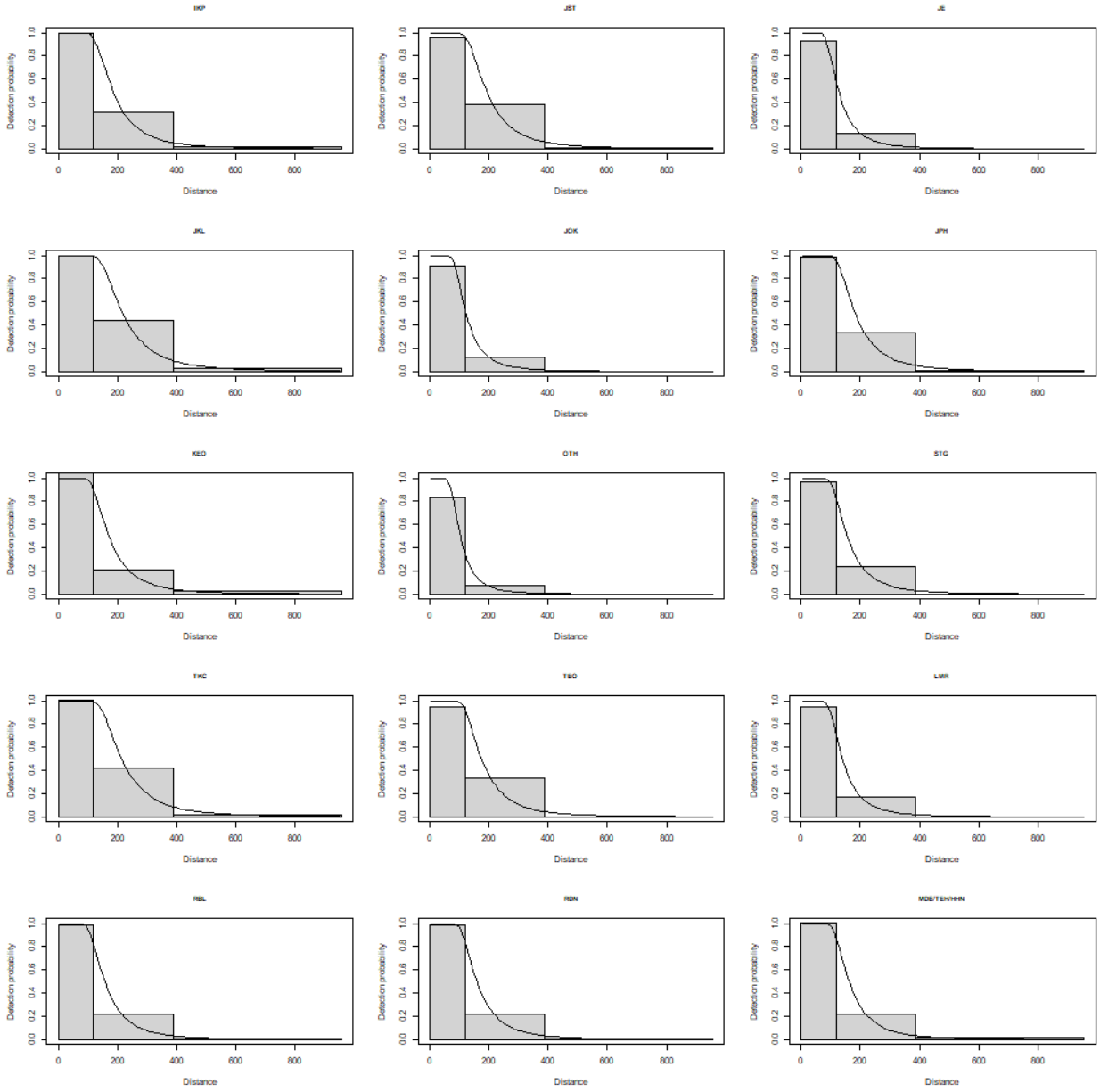

Figure 3.29. Figure showing the estimated detection function. The histograms represent the distances of the observed sightings across different observers.

3.6 Diver Spatial Results by Survey

Figure 3.30 shows the distribution of the distance corrected counts for each of the 56 surveys.

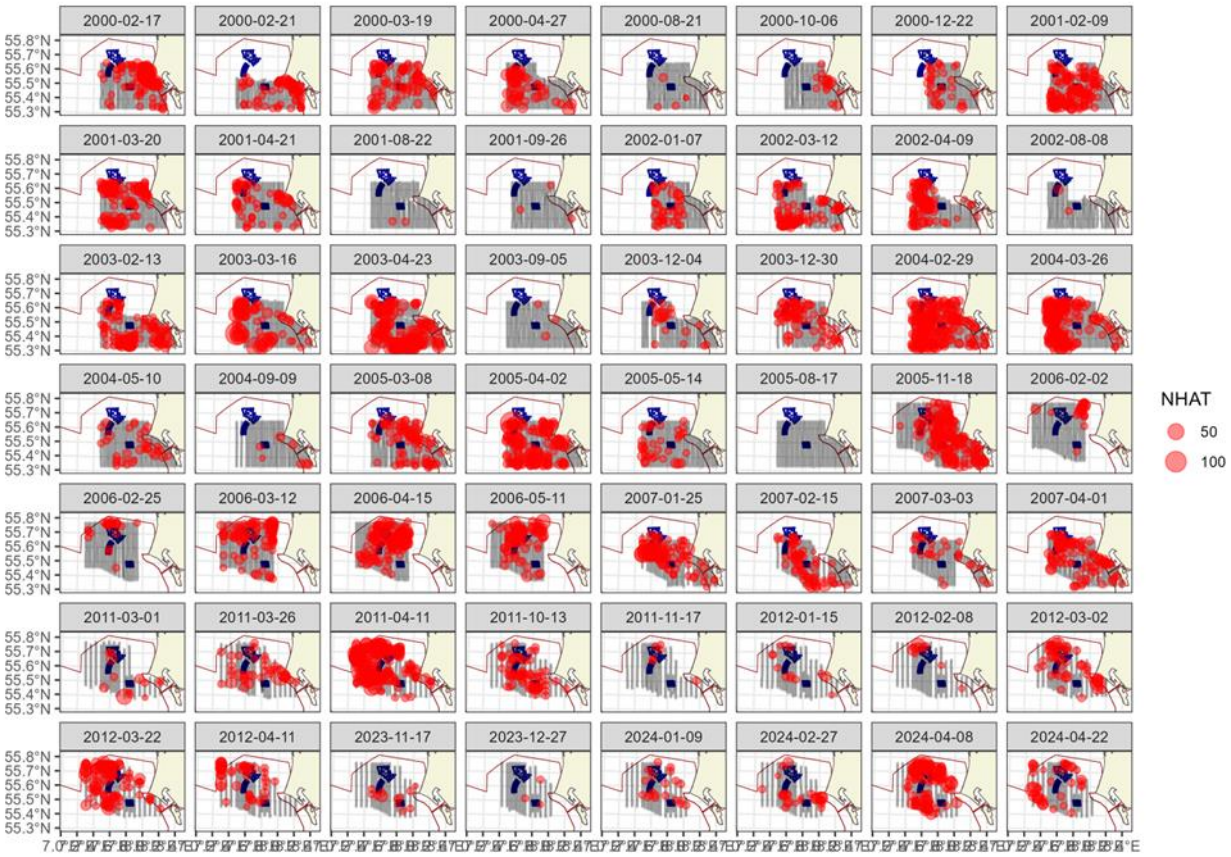

Figure 3.30. Distance-corrected counts for the diver species across the 56 surveys. The red circles indicate the distance-corrected counts along the transect lines. The pale grey dots are segments with a count of zero.

3.6.1 Model Selection

For seven of the 56 surveys, there were not enough observations of divers to fit any model and 26 models were selected as intercept only. This means a uniform distribution was estimated across the study region. However, for 23 of the 56 surveys, the models selected included a spatial term (of varying complexity) while the depth covariate (as a nonlinear term) was selected for four of the surveys – in all of these models however, the spatial term was also included. The distance to coast covariate was selected as a non-linear term in one model and a linear term in one model, both of which also included a spatial term. The spatial surfaces selected ranged from two to four parameters for the spatial term (Table 3-5). The estimated abundances and associated 95 percentile confidence intervals for each survey are given in Table 3-6 and Figure 3.31.

Table 3-5. Model selection results for Diver species for each survey. The model column represents the terms in the model.

Survey	Model	Distribution	Variable 1D	Variable 2D	Number of parameters	Dispersion parameter	Tweedie parameter
2000-02-17	2D Only	Tweedie	NA	s(x,y, df=2)	3	26.6	1.38
2000-02-21	Best 1D2D	Tweedie	distcoast, df=1	s(x,y, df=2)	4	9.3	1.21
2000-03-19	Intercept only	Tweedie	NA	NA	1	36.0	1.30
2000-04-27	Intercept only	Tweedie	NA	NA	1	137.5	1.35
2000-08-21	No Model	NA	NA	NA	NA	NA	NA
2000-10-06	Intercept only	quasipoisson	NA	NA	1	10.4	NA
2000-12-22	Intercept only	quasipoisson	NA	NA	1	6.4	NA
2001-02-09	2D Only	Tweedie	NA	s(x,y, df=2)	3	8.0	1.13
2001-03-20	2D Only	Tweedie	NA	s(x,y, df=4)	5	66.1	1.13
2001-04-21	Intercept only	Tweedie	NA	NA	1	14.5	1.21
2001-08-22	No Model	NA	NA	NA	NA	NA	NA
2001-09-26	No Model	NA	NA	NA	NA	NA	NA
2002-01-07	2D Only	Tweedie	NA	s(x,y, df=2)	3	10.4	1.19
2002-03-12	2D Only	Tweedie	NA	s(x,y, df=2)	3	18.1	1.21
2002-04-09	2D Only	Tweedie	NA	s(x,y, df=2)	3	28.4	1.24
2002-08-08	No Model	NA	NA	NA	NA	NA	NA
2003-02-13	Intercept only	quasipoisson	NA	NA	1	8.6	NA
2003-03-16	Intercept only	Tweedie	NA	NA	1	102.7	1.45
2003-04-23	Best 1D2D	Tweedie	s(distcoast, df=2)	s(x,y, df=2)	5	115.3	1.46
2003-09-05	No Model	NA	NA	NA	NA	NA	NA
2003-12-04	2D Only	Tweedie	NA	s(x,y, df=2)	3	18.9	1.28
2003-12-30	Intercept only	quasipoisson	NA	NA	1	28.7	NA
2004-02-29	2D Only	Tweedie	NA	s(x,y, df=2)	3	22.7	1.25
2004-03-26	2D Only	Tweedie	NA	s(x,y, df=3)	4	112.1	1.28
2004-05-10	Intercept only	quasipoisson	NA	NA	1	7.8	NA
2004-09-09	Intercept only	quasipoisson	NA	NA	1	9.2	NA
2005-03-08	Best 1D2D	Tweedie	s(depth, df=2)	s(x,y, df=2)	5	16.1	1.21
2005-04-02	Intercept only	Tweedie	NA	NA	1	79.6	1.34
2005-05-14	Intercept only	quasipoisson	NA	NA	1	7.3	NA
2005-08-17	No Model	NA	NA	NA	NA	NA	NA
2005-11-18	2D Only	Tweedie	NA	s(x,y, df=2)	3	15.3	1.24
2006-02-02	2D Only	Tweedie	NA	s(x,y, df=2)	3	15.2	1.19
2006-02-25	Intercept only	quasipoisson	NA	NA	1	13.5	NA
2006-03-12	Best 1D2D	Tweedie	s(depth, df=2)	s(x,y, df=2)	5	14.3	1.18
2006-04-15	2D Only	Tweedie	NA	s(x,y, df=3)	4	12.6	1.23

Survey	Model	Distribution	Variable 1D	Variable 2D	Number of parameters	Dispersion parameter	Tweedie parameter
2006-05-11	Best 1D2D	Tweedie	s(depth, df=2)	s(x,y, df=2)	5	28.5	1.25
2007-01-25	Best 1D2D	Tweedie	s(depth, df=2)	s(x,y, df=2)	5	13.1	1.18
2007-02-15	2D Only	Tweedie	NA	s(x,y, df=2)	3	9.6	1.18
2007-03-03	Intercept only	quasipoisson	NA	NA	1	4.6	NA
2007-04-01	2D Only	Tweedie	NA	s(x,y, df=2)	3	13.1	1.22
2011-03-01	Intercept only	Tweedie	NA	NA	1	164.4	1.41
2011-03-26	Intercept only	Tweedie	NA	NA	1	46.6	1.25
2011-04-11	2D Only	Tweedie	NA	s(x,y, df=2)	3	29.5	1.32
2011-10-13	Intercept only	quasipoisson	NA	NA	1	11.4	NA
2011-11-17	Intercept only	quasipoisson	NA	NA	1	5.1	NA
2012-01-15	Intercept only	quasipoisson	NA	NA	1	5.6	NA
2012-02-08	Intercept only	Tweedie	NA	NA	1	212.1	1.41
2012-03-02	Intercept only	Tweedie	NA	NA	1	25.6	1.22
2012-03-22	2D Only	Tweedie	NA	s(x,y, df=2)	3	44.8	1.28
2012-04-11	Intercept only	Tweedie	NA	NA	1	18.6	1.19
2023-11-17	Intercept only	quasipoisson	NA	NA	1	8.5	NA
2023-12-27	No Model	NA	NA	NA	NA	NA	NA
2024-01-09	Intercept only	quasipoisson	NA	NA	1	5.0	NA
2024-02-27	Intercept only	Tweedie	NA	NA	1	31.2	1.27
2024-04-08	2D Only	Tweedie	NA	s(x,y, df=4)	5	15.0	1.28
2024-04-22	Intercept only	Tweedie	NA	NA	1	22.7	1.18

The estimated abundances, densities and associated 95 percentile confidence intervals for each month are given in Table 3-6, and illustrated in Figure 3-32 for all surveys combined and in Figure 3-33 combined for each of the phases.

Table 3-6. Estimated abundance and density of diver species for each survey. The 95% CI are percentile-based confidence intervals.

Month	Area (km^2)	Estimated count	95% CI count	Estimated density	95% CI density
2000-02-17	2019	447	(227, 915)	0.2	(0.1, 0.5)
2000-02-21	2019	75	(38, 155)	0.0	(0, 0.1)
2000-03-19	2019	216	(115, 379)	0.1	(0.1, 0.2)
2000-04-27	2019	281	(122, 660)	0.1	(0.1, 0.3)

Month	Area (km^2)	Estimated count	95% CI count	Estimated density	95% CI density
2000-08-21	2019	8	(7, 9)	0.0	(0, 0)
2000-10-06	2019	35	(16, 77)	0.0	(0, 0)
2000-12-22	2019	65	(36, 118)	0.0	(0, 0.1)
2001-02-09	2019	286	(162, 501)	0.1	(0.1, 0.2)
2001-03-20	2019	339	(181, 669)	0.2	(0.1, 0.3)
2001-04-21	2019	138	(77, 254)	0.1	(0, 0.1)
2001-08-22	2019	4	(3, 5)	0.0	(0, 0)
2001-09-26	2019	5	(4, 6)	0.0	(0, 0)
2002-01-07	2019	105	(45, 229)	0.1	(0, 0.1)
2002-03-12	2019	107	(59, 190)	0.1	(0, 0.1)
2002-04-09	2019	313	(173, 572)	0.2	(0.1, 0.3)
2002-08-08	2019	5	(5, 5)	0.0	(0, 0)
2003-02-13	2019	275	(175, 427)	0.1	(0.1, 0.2)
2003-03-16	2019	421	(208, 925)	0.2	(0.1, 0.5)
2003-04-23	2019	656	(351, 1338)	0.3	(0.2, 0.7)
2003-09-05	2019	6	(5, 6)	0.0	(0, 0)
2003-12-04	2019	87	(37, 218)	0.0	(0, 0.1)
2003-12-30	2019	178	(102, 306)	0.1	(0.1, 0.2)
2004-02-29	2019	834	(533, 1313)	0.4	(0.3, 0.7)
2004-03-26	2019	706	(375, 1305)	0.3	(0.2, 0.6)
2004-05-10	2019	71	(46, 111)	0.0	(0, 0.1)
2004-09-09	2019	18	(9, 37)	0.0	(0, 0)
2005-03-08	2019	201	(96, 421)	0.1	(0, 0.2)
2005-04-02	2019	646	(380, 1098)	0.3	(0.2, 0.5)
2005-05-14	2019	72	(41, 127)	0.0	(0, 0.1)
2005-08-17	2019	0	(0, 0)	0.0	(0, 0)
2005-11-18	2019	578	(368, 904)	0.3	(0.2, 0.4)
2006-02-02	2019	17	(5, 57)	0.0	(0, 0)
2006-02-25	2019	50	(22, 114)	0.0	(0, 0.1)
2006-03-12	2019	230	(106, 527)	0.1	(0.1, 0.3)
2006-04-15	2019	512	(296, 887)	0.3	(0.1, 0.4)
2006-05-11	2019	410	(193, 895)	0.2	(0.1, 0.4)
2007-01-25	2019	457	(233, 925)	0.2	(0.1, 0.5)
2007-02-15	2019	169	(94, 302)	0.1	(0, 0.1)
2007-03-03	2019	43	(27, 70)	0.0	(0, 0)
2007-04-01	2019	313	(158, 726)	0.2	(0.1, 0.4)
2011-03-01	2019	51	(22, 114)	0.0	(0, 0.1)
2011-03-26	2019	123	(65, 225)	0.1	(0, 0.1)
2011-04-11	2019	1208	(728, 1986)	0.6	(0.4, 1)
2011-10-13	2019	164	(103, 263)	0.1	(0.1, 0.1)
2011-11-17	2019	11	(4, 29)	0.0	(0, 0)
2012-01-15	2019	24	(13, 46)	0.0	(0, 0)
2012-02-08	2019	44	(14, 141)	0.0	(0, 0.1)
2012-03-02	2019	162	(84, 360)	0.1	(0, 0.2)
2012-03-22	2019	506	(268, 1103)	0.3	(0.1, 0.5)
2012-04-11	2019	139	(54, 358)	0.1	(0, 0.2)
2023-11-17	2019	25	(11, 54)	0.0	(0, 0)

Month	Area (km^2)	Estimated count	95% CI count	Estimated density	95% CI density
2023-12-27	2019	5	(4, 5)	0.0	(0, 0)
2024-01-09	2019	38	(23, 65)	0.0	(0, 0)
2024-02-27	2019	77	(35, 174)	0.0	(0, 0.1)
2024-04-08	2019	565	(275, 1121)	0.3	(0.1, 0.6)
2024-04-22	2019	116	(49, 264)	0.1	(0, 0.1)

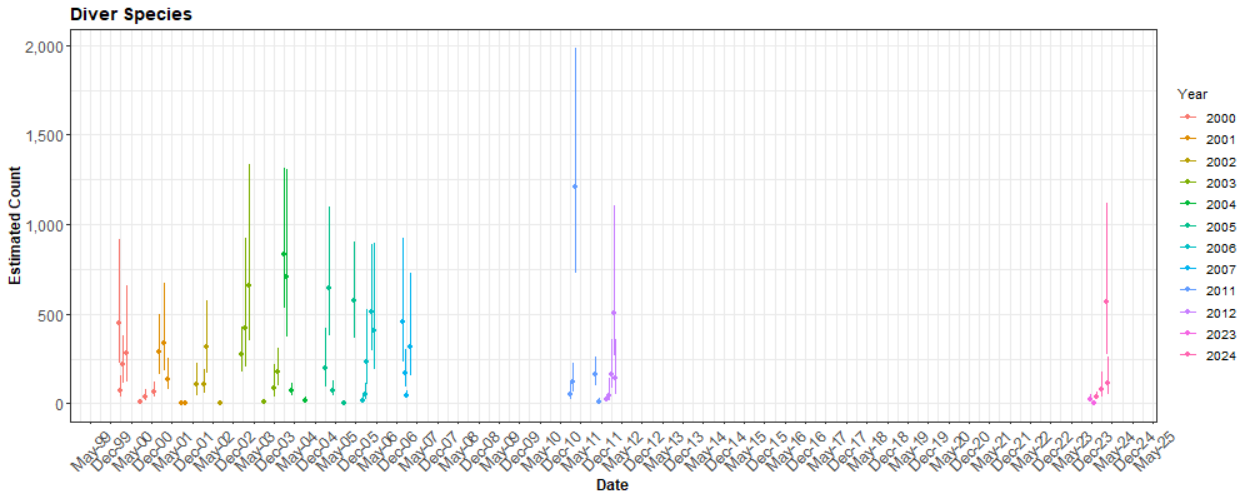

Figure 3.31. The estimated count of diver species for each survey. The 95% CI are percentile-based confidence intervals are from a parametric bootstrap with 500 replicates. As the analysis area had the same extension between surveys, the estimated abundances are comparable.

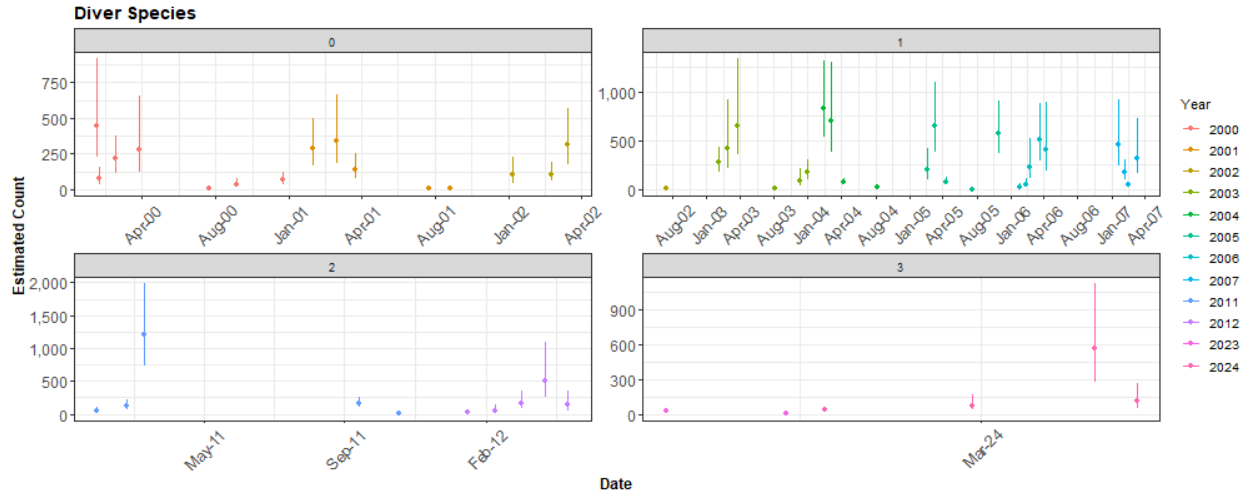

Figure 3.32. The estimated count of diver species for each survey by phase. The 95% CI are percentile-based confidence intervals are from a parametric bootstrap with 500 replicates. To show more detail the y-axis is different for each phase.

3.6.2 Density Distributions

Figure 3.33 to Figure 3.36 show the estimated counts of diver species in each 500 m^2 grid cells for each survey in the four phases. Generally, the estimated abundances fitted well to the raw data and there were no notable misalignments. In areas where the estimated counts were systematically higher, the abundances were also relatively high and there were no areas with large, estimated abundances unsupported by the data.

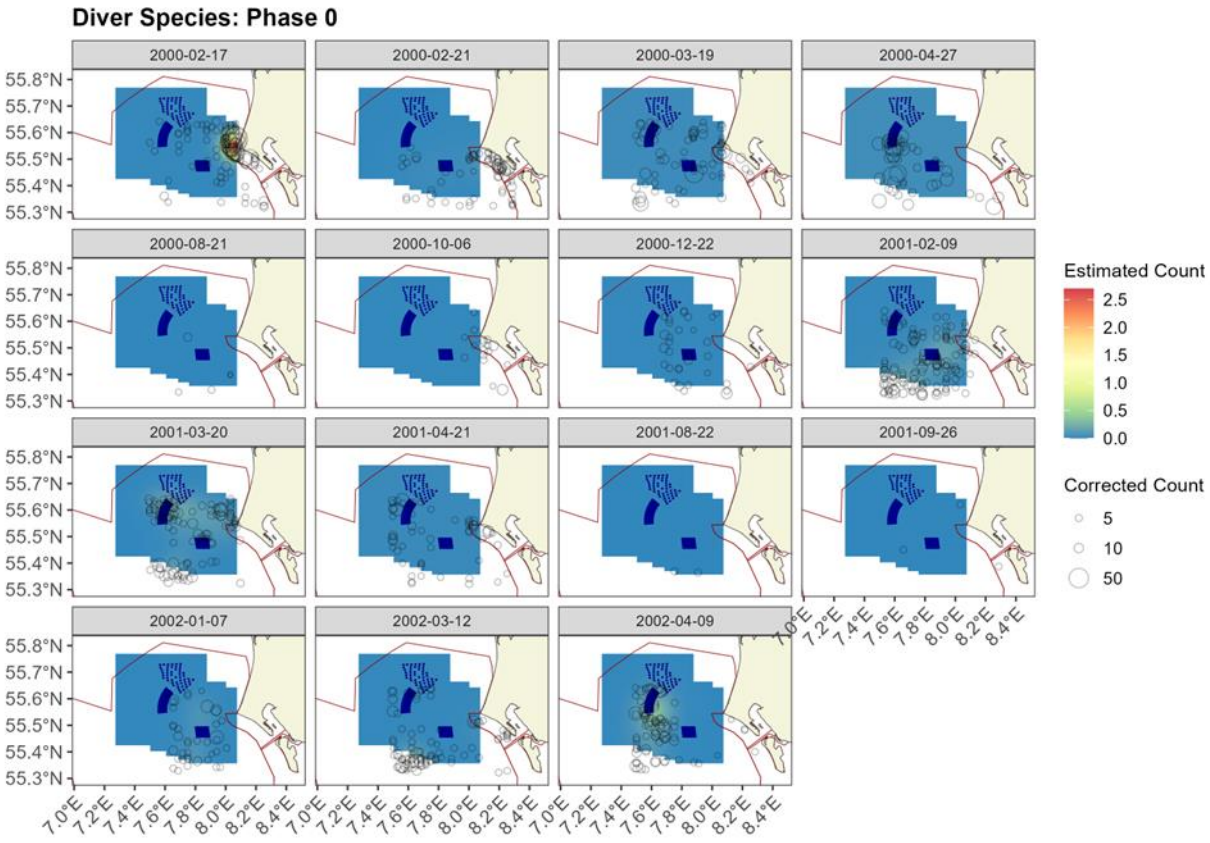

Figure 3.33. Figure showing the estimated diver abundance across the study site for each of the surveys in Phase 0. The estimated counts are per 500 m x 500 m grid cell. The open circles show the corrected counts. The coloured graphics represent the predicted counts in each location.

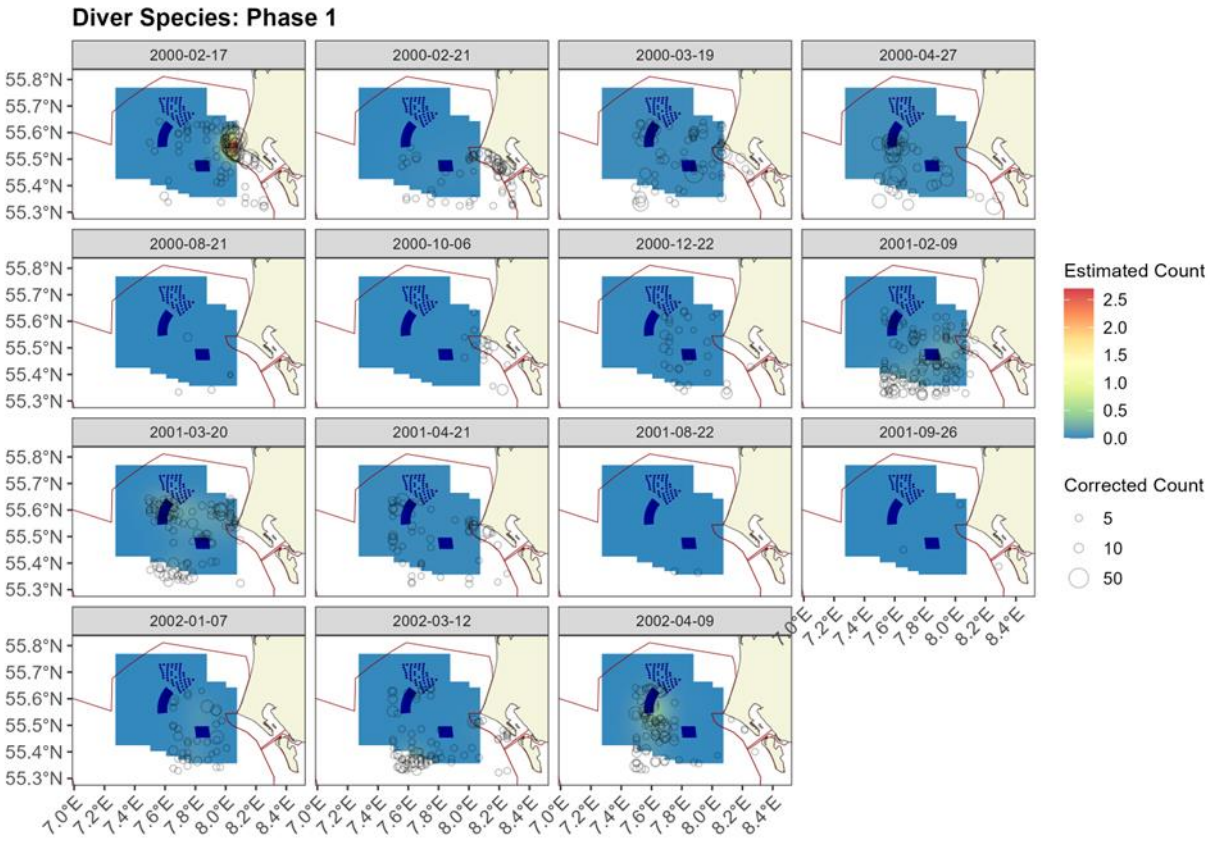

Figure 3.34. Figure showing the estimated diver abundance across the study site for each of the surveys in Phase 1. The estimated counts are per 500 m x 500 m grid cell. The open circles show the corrected counts. The coloured graphics represent the predicted counts in each location.

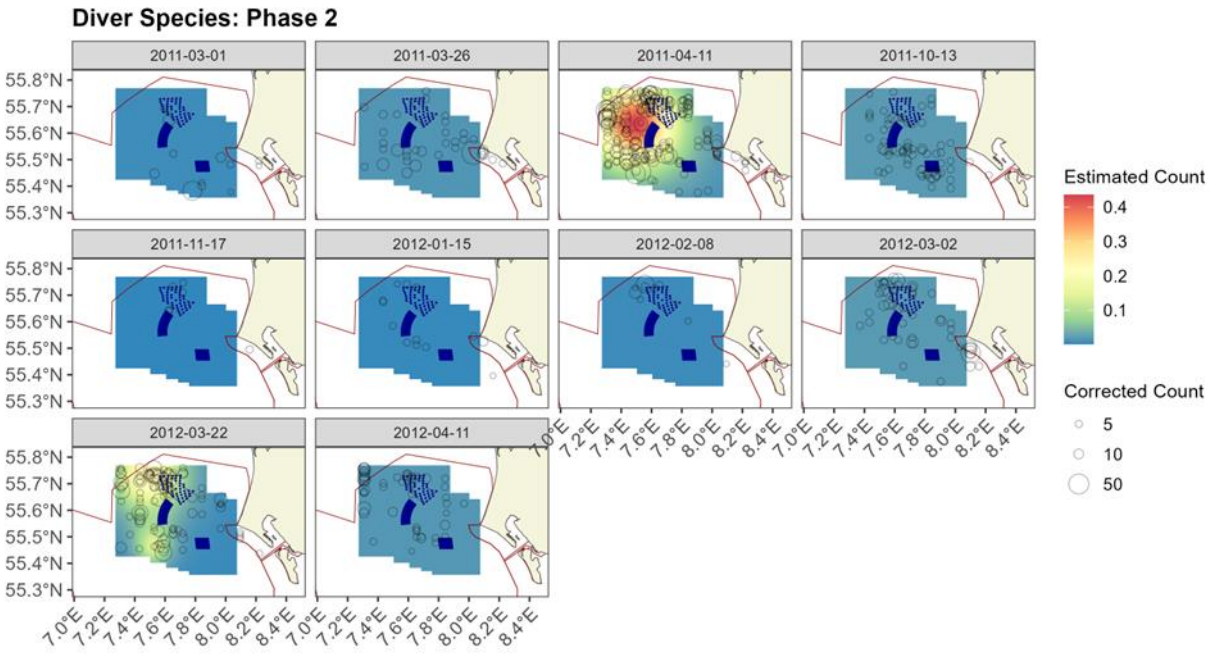

Figure 3.35. Figure showing the estimated diver abundance across the study site for each of the surveys in Phase 2. The estimated counts are per 500 m x 500 m grid cell. The open circles show the corrected counts. The coloured graphics represent the predicted counts in each location.

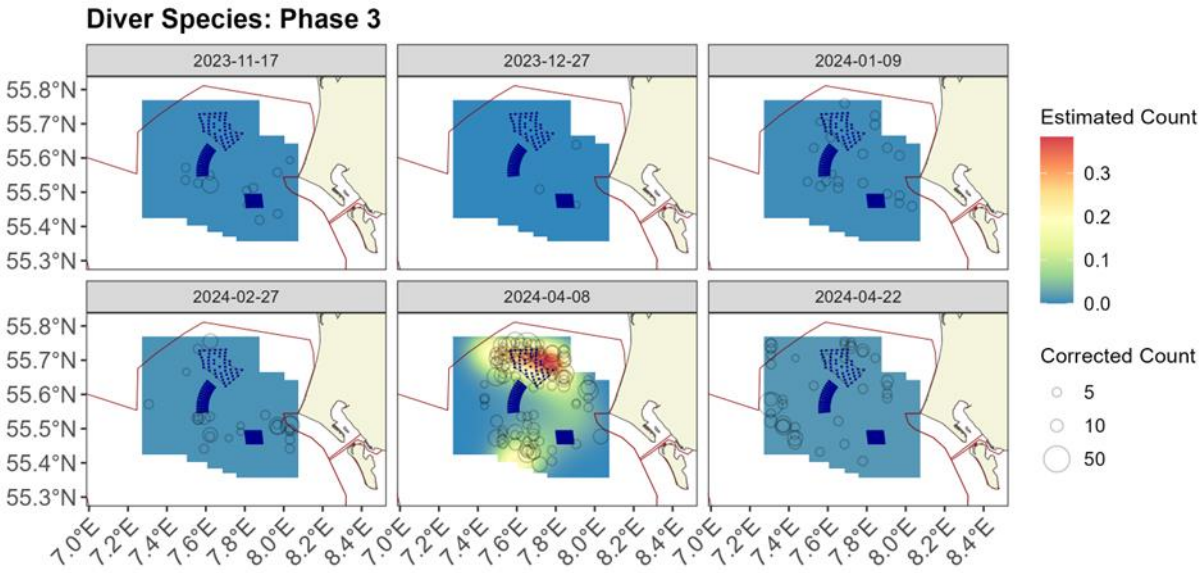

Figure 3.36. Figure showing the estimated diver abundance across the study site for each of the surveys in Phase 3. The estimated counts are per 500 m x 500 m grid cell. The open circles show the corrected counts. The coloured graphics represent the predicted counts in each location.

3.6.3 Uncertainty in spatial predictions

Broadly, the highest coefficient of variation (CoV) scores were associated with the `almost zero' predictions and it is known that the CoV metric is highly sensitive to any uncertainty for very small predictions. There was no material overlap between high values of the CoV metric and the transect lines/locations with non-zero counts and therefore results in no concerns in this case (Figure 3.37).

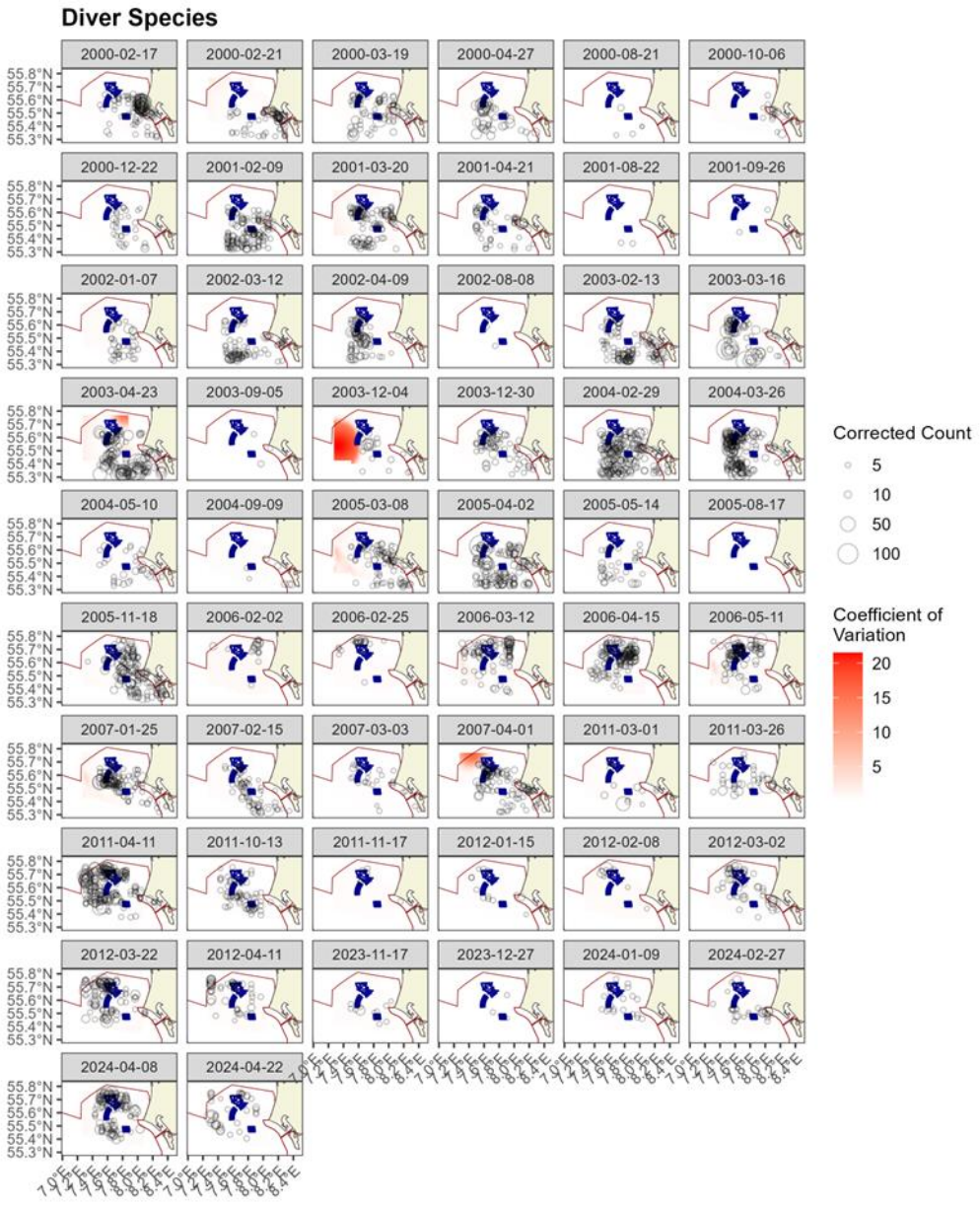

Figure 3.37. Figure showing the coefficient of variation across the study region for each of the surveys of divers. The open circles show the distance corrected counts. The presence of dark red CV scores in areas with virtually zero predictions are an artifact of the very small prediction rather than of any notable concern.

In the case, when the very small predicted values were excluded (Figure 3.38) there were a few remaining areas of moderately large CoV's. These tended to be in areas where there was little survey effort and so any wide confidence intervals resulting from this are not unwarranted.

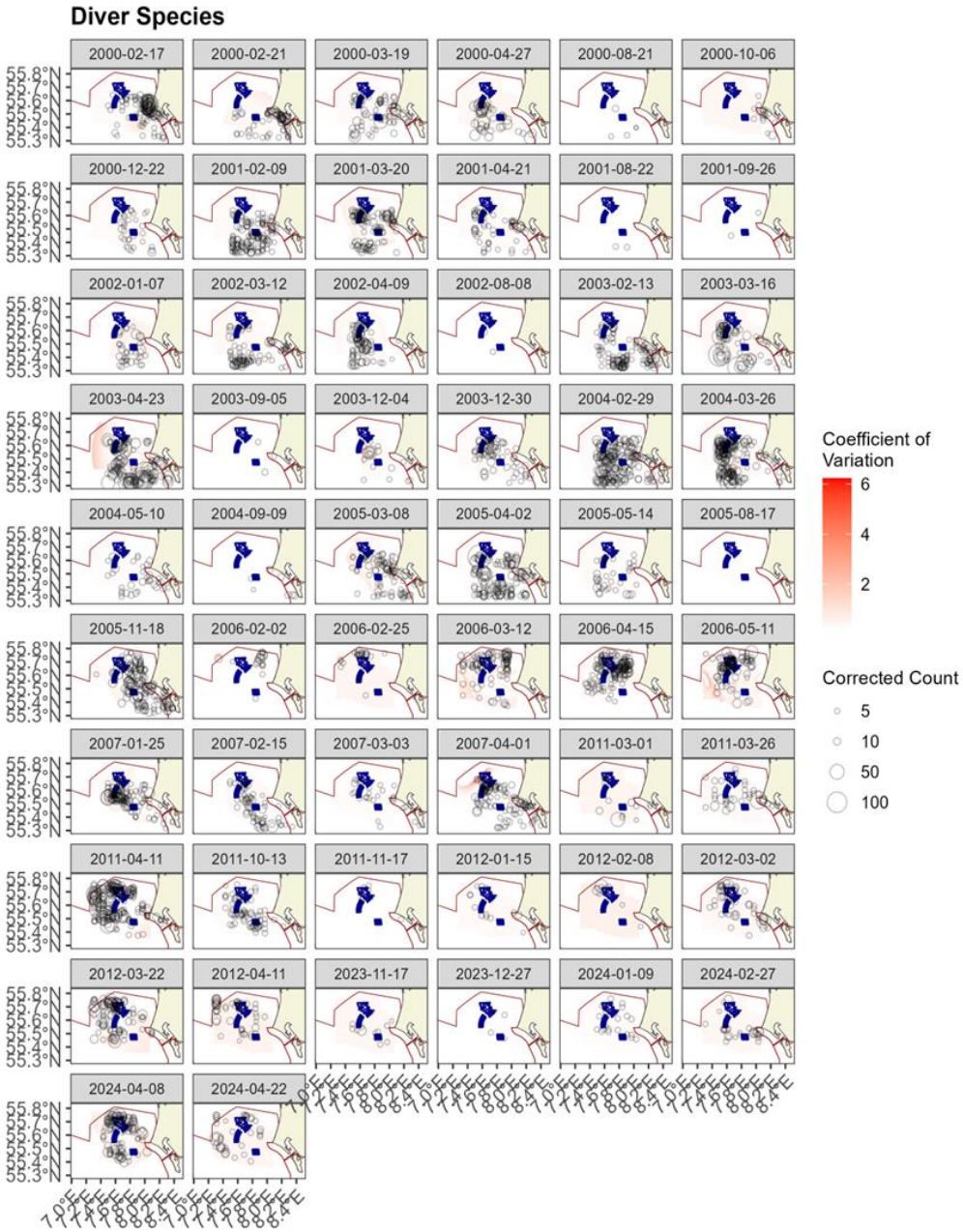

Figure 3.38. Figure showing the coefficient of variation across the study region for each of the surveys. The open circles show the distance corrected counts. The presence of dark red CV scores in areas with virtually zero predictions are an artifact of the very small prediction rather than of any notable concern.

3.7 Diver Spatial Results by Phase

3.7.1 Phase-specific spatial patterns

The distribution in Phase 0 (Figure 3.39) is concentrated to the east of the study region off the tip of Denmark's western most point with a lower density in the area of the future HR II. In Phase 1, the distribution is fairly widespread but the concentration shifts from the east to settle around the not-yet constructed HR II. After the construction of HR II there is a general decline in numbers particularly in the east and the birds are more broadly distributed. In Phase 3, there is a dramatic decrease in the central distribution with numbers mostly in the north around the constructed HR III farm.

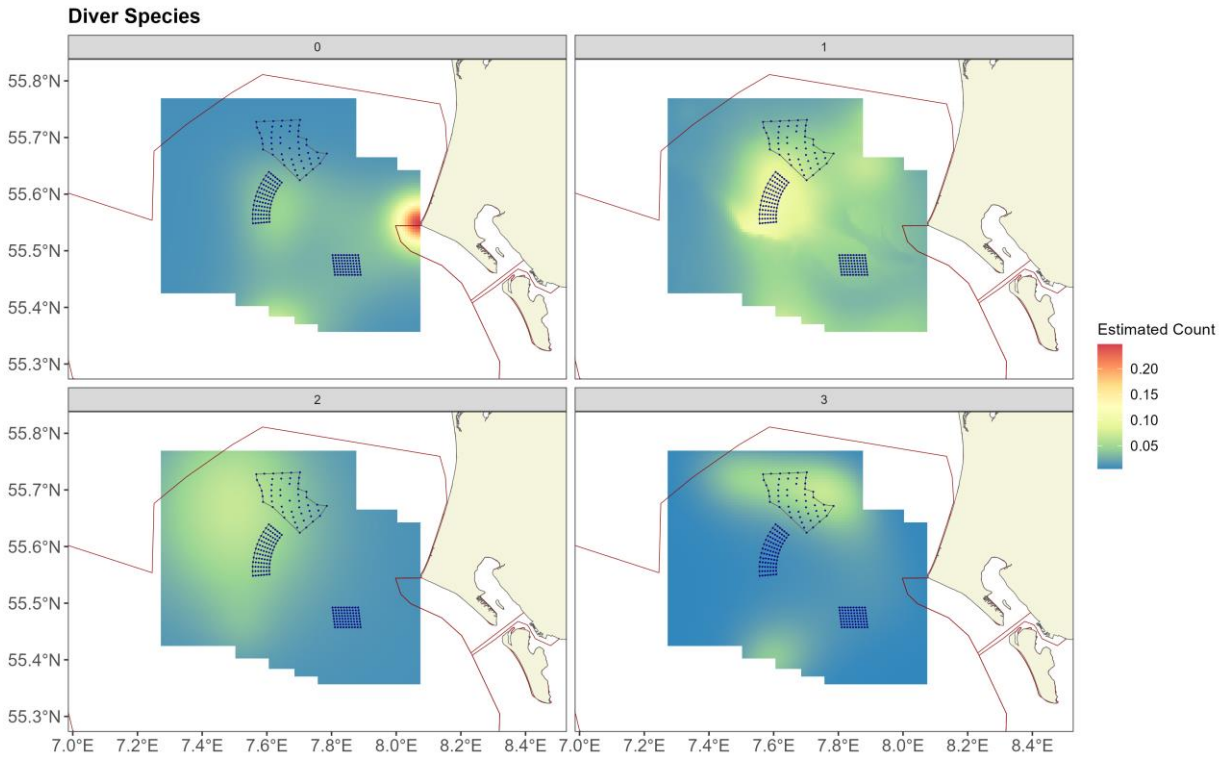

Figure 3.39. Figure showing the estimated diver species abundance across the study site for each of the surveys in Phase 0. The estimated counts are per 500 m x 500 m grid cell. The open circles show the corrected counts. The coloured graphics represent the predicted counts in each location.

3.7.2 Overall Persistance

As well as looking at the mean distribution of birds in each phase, which may be swayed by a few surveys with large numbers of birds, we can assess the persistence of birds in each grid cell overall and by phase. The persistence analysis describes, at a fine geographical scale, areas of higher or lower usage by the species, evaluated over many surveys.

Across the 56 surveys (spanning 24 years) there is moderate to low persistence across much of the predicted area (Figure 3.40). The highest persistence (~ 50%) occurs in the central parts of the study area, with some reduction in this metric towards the western edge of the area of interest.

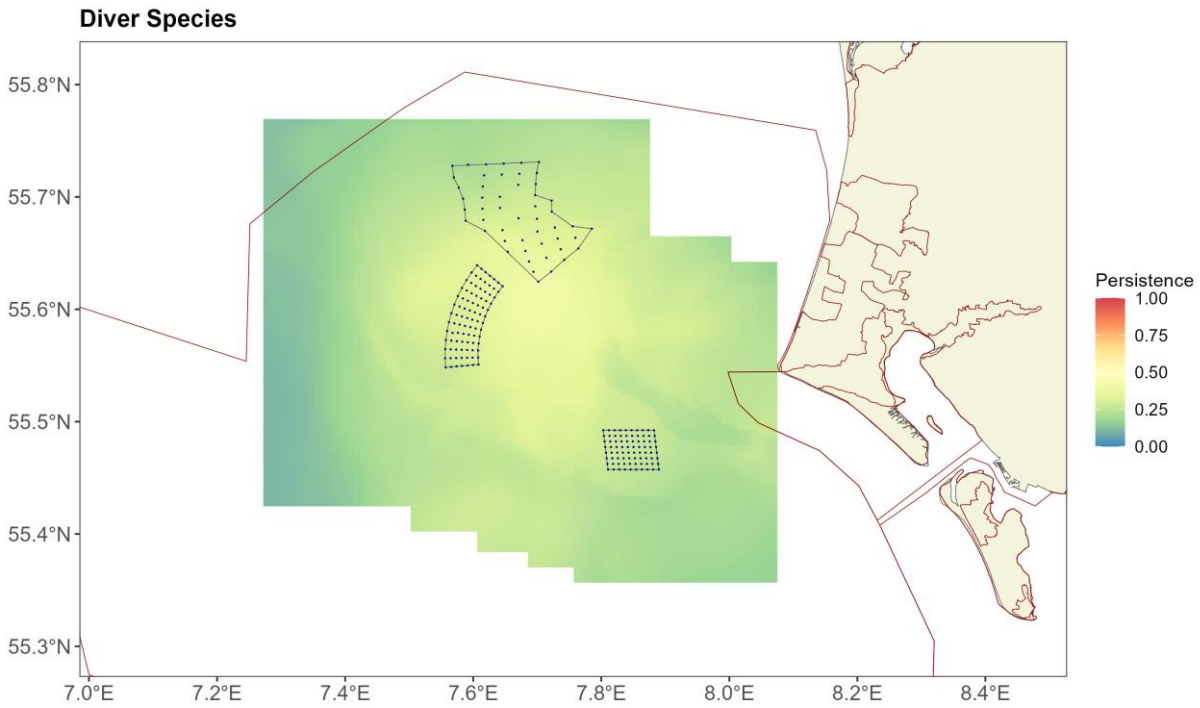

Figure 3.40. Persistence scores for divers across the 56 surveys. The polygons represent the windfarms Horns Rev I, II and III (black line) with turbine locations indicated by the black dots.

3.7.3 Phase-specific Persistence

Figure 3.41 to Figure 3.44 show the persistence of birds within each phase. In Phase 0, prior to any construction, the birds are widely distributed across the area with some concentrations to the southern and eastern edges, indicating that the birds, across multiple surveys, consistently preferred those areas to other parts of the area. Notably, there is moderate persistence in the footprint of soon-to-be constructed HR I, with less observed in the to-be footprints of HR II and III (Figure 3.41).

In Phase 1 however, there is a notable shift into the centre of the area from the outer edges and closer to the areas where HR II and HR III will ultimately be constructed. Though, its clear persistence is concentrated largely outside of these soon-to-be footprints (Figure 3.42).

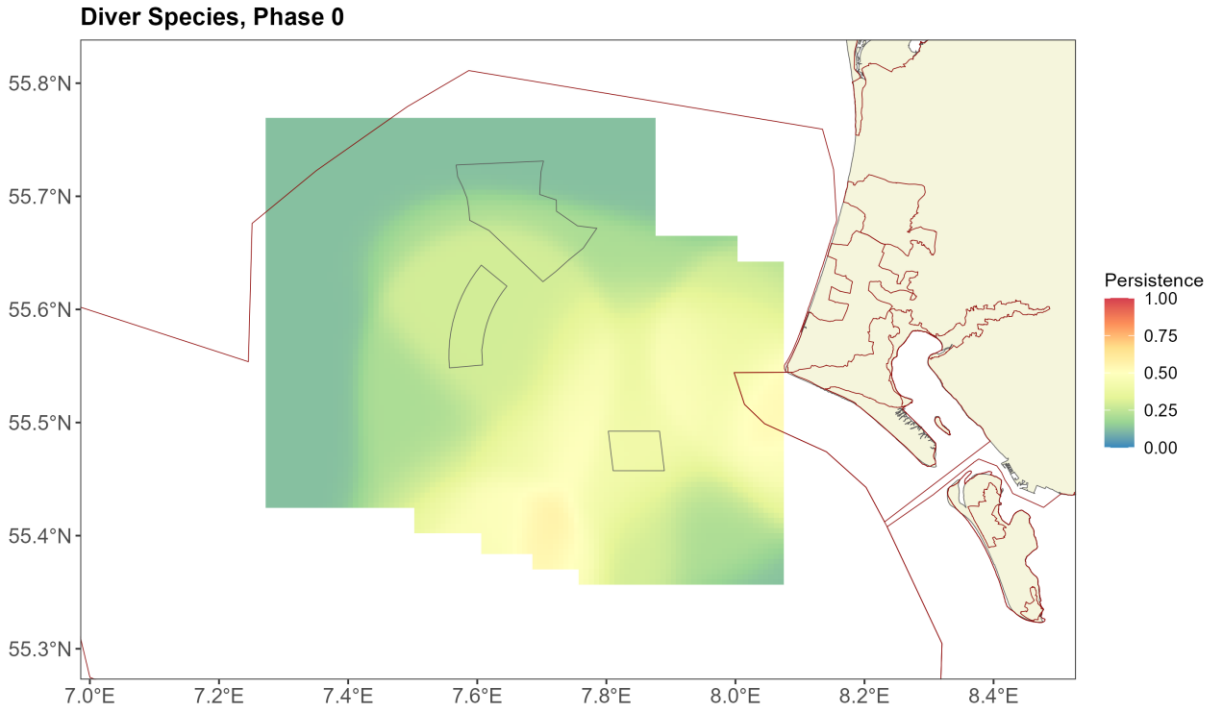

Figure 3.41. Persistence scores across the 15 surveys in Phase 0. The polygons represent the windfarms Horns Rev I, II and III (black line) with turbine locations indicated by the black dots.

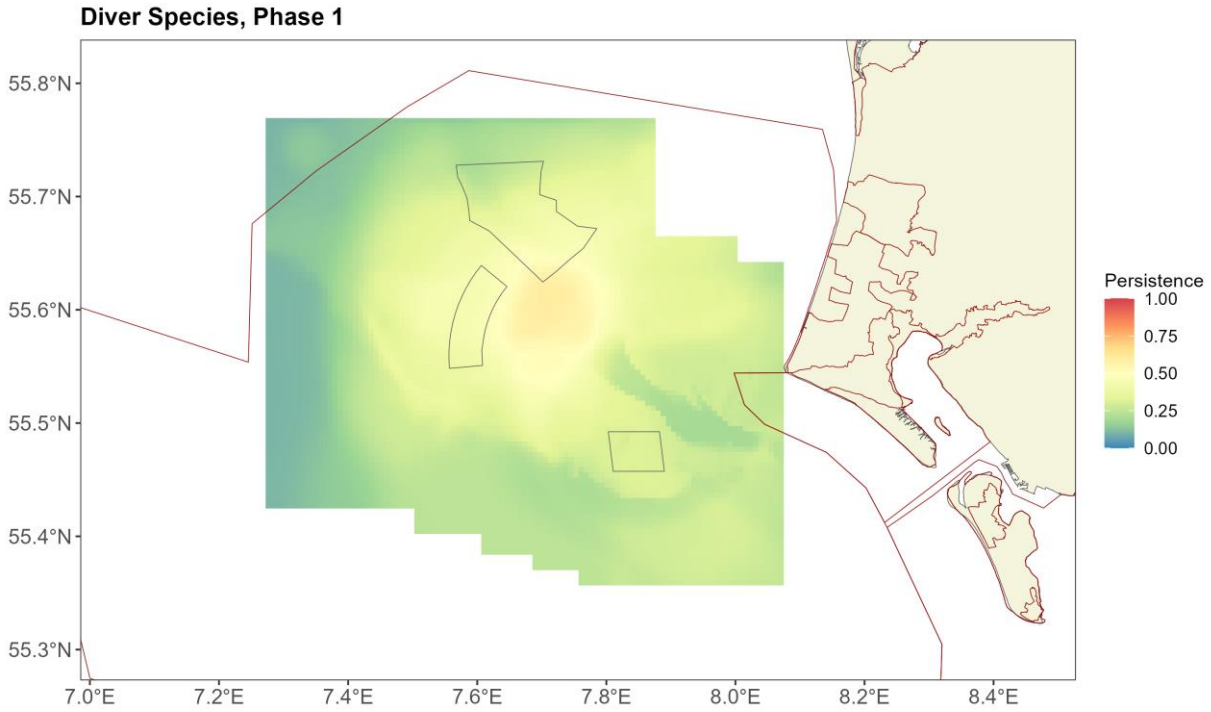

Figure 3.42. Persistence scores across the 25 surveys in Phase 1. The polygons represent the windfarms Horns Rev I, II and III (black line) with turbine locations indicated by the black dots.

Phase 2 is 2-5 years post-construction HR II and 9-10 years post-construction HR I. In this phase, the divers have a much more broadly distributed pattern and are largely evenly spread, except where persistence is lower

in the south-eastern edge of the area (Figure 3.43). Persistence in the HR I footprint is relatively low and lower than in Phases 0 and 1.

The most recent surveys, Phase 3, are 5-6 years post-construction of HR III, 11-12 years post-construction HR II and 21-22 years post-construction of HR I. During these surveys, the birds were still relatively widely distributed (and showed relatively low persistence overall) with extremely low persistence at the south-eastern edge and the western edge (Figure 3.44).

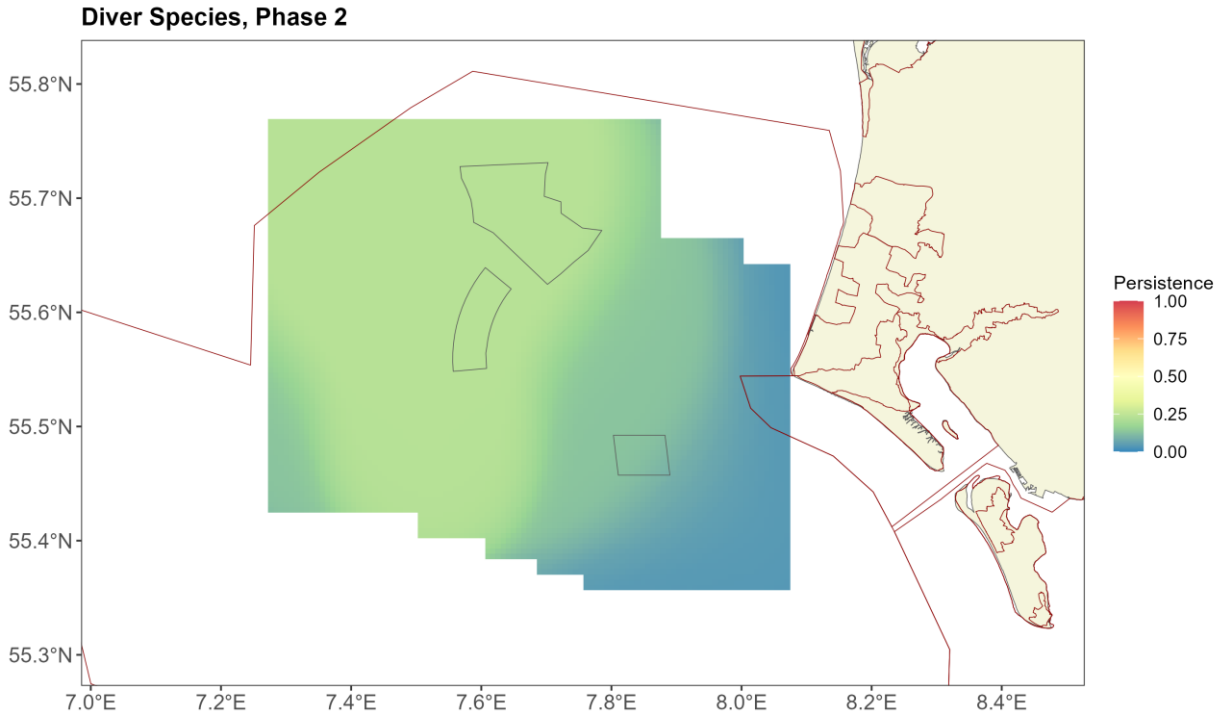

Figure 3.43. Persistence scores across the 10 surveys in Phase 2. The polygons represent the windfarms Horns Rev I, II and III (black line) with turbine locations indicated by the black dots.

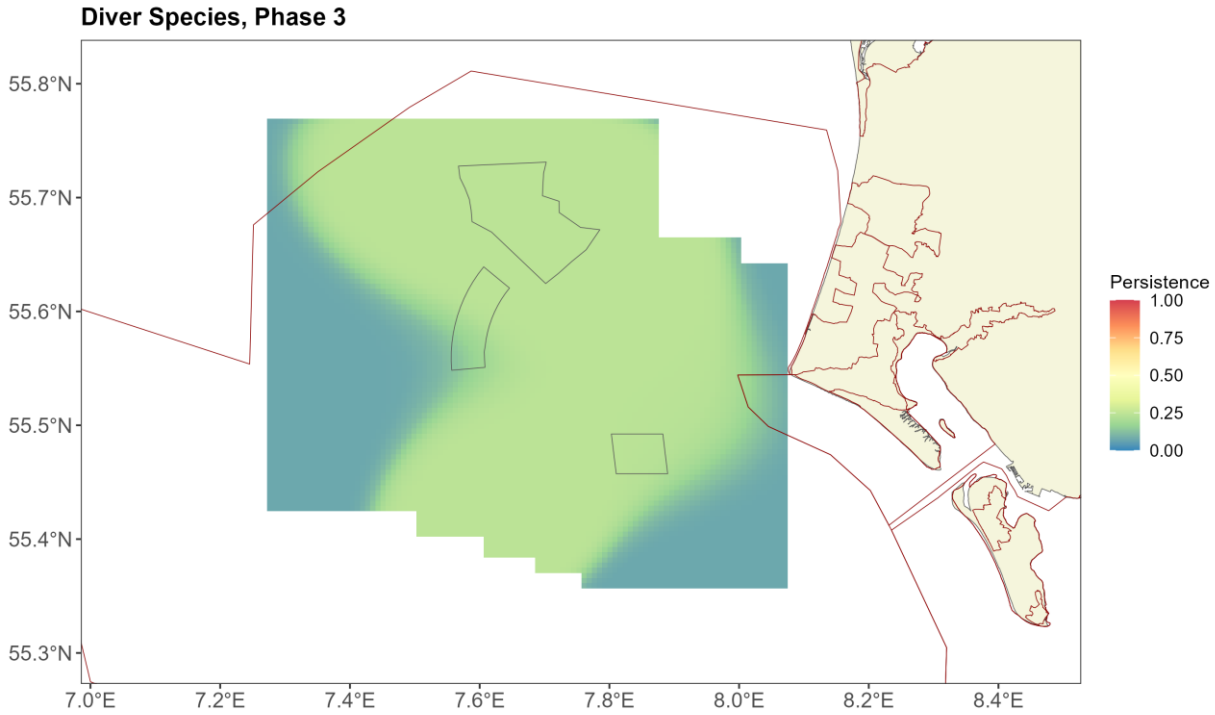

Figure 3.44. Persistence scores across the six surveys in Phase 3. The polygons represent the windfarms Horns Rev I, II and III (black line) with turbine locations indicated by the black dots.

3.7.4 Phase-specific windfarm footprint densities

Closer inspection of the estimated density of birds within windfarm-based footprints at various spatial scales was carried out to better understand any windfarm related changes (Figure 3.45 and **Error! Reference source not found.**).
For instance, if there were no changes in diver species density across the 24 years in this figure: either inside the footprint or up to one or two kilometers from the footprint then we would expect to see horizontal lines for all four colours in Figure 3.45. However, the likelihood of changes in bird density across this time frame is incredibly high, regardless of windfarm construction, and so any changes must be examined from several perspectives.
There has been a general increase in diver density from Phase 0 to 1 followed by a general decline from Phase 1 to 3, returning to similar levels as Phase 0 (indicated by the black lines in Figure 3.45), providing a backdrop of variable densities during the 24 years across the survey area.

Inside the footprint of each of the three windfarms (HR I, HR II and HR III) we see different patterns as each windfarm is constructed. Post-construction of HR I (Phase 1) we see an increased density within the footprint compared with Phase 0. After Phase 1, the density in HR I declines in line with what is seen in the general study region.

For HR II we see a much sharper increase in density from Phase 0 to 1 followed by a steep decline in Phase 2, post-construction of HR II, which continues into Phase 3 and ends at a density significantly lower than that seen in Phase 0.

For HR III, we see increasing density from Phases 0 to 1, which is in line with the study wide increase in density. From Phase 1 to 3 (pre- to post-construction of HR III) there is no significant change in footprint densities.

Within one and two kilometers of each windfarm footprint we also saw very similar patterns to those observed inside the footprint in each case.

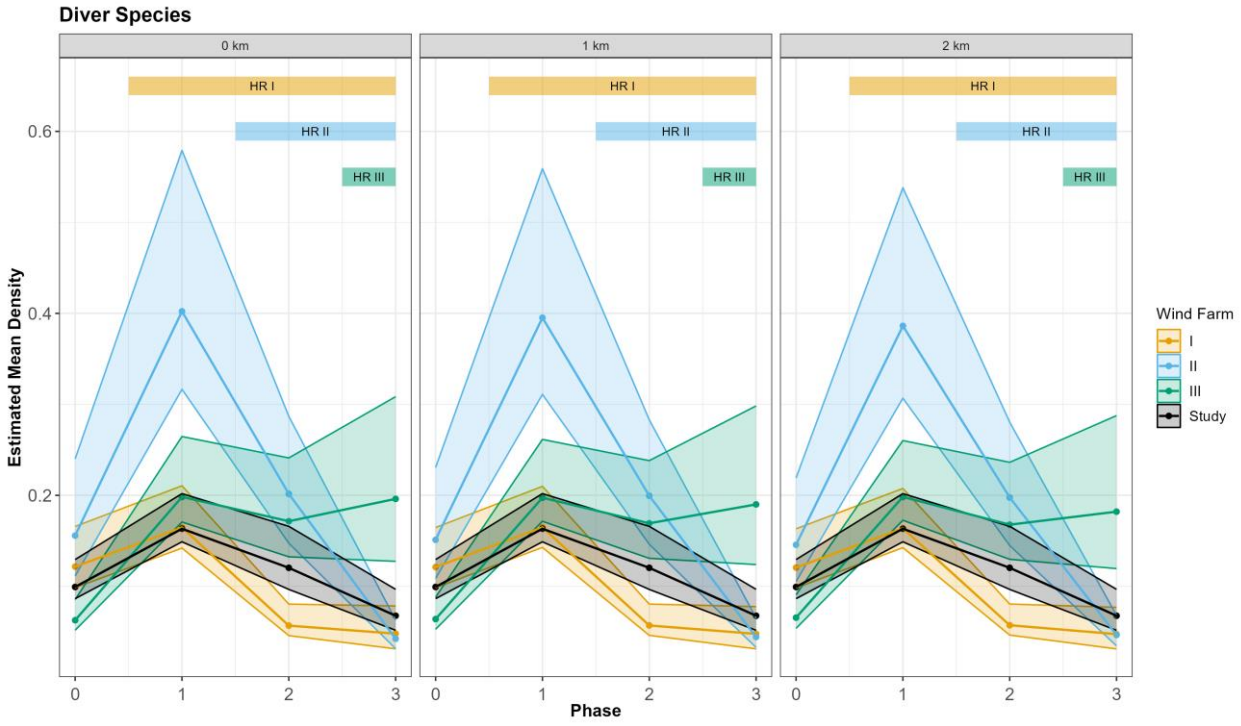

Figure 3.45. Figure showing the estimated mean density in the footprint, footprint + 1 km buffer and footprint + 2 km buffer of each windfarm for all phases. The bars at the top show the post-construction periods for each wind farm. Note that survey coverage in HR III during Phase 0 was limited.

Table 3-7. Table of abundance estimates and 95 percentile-based confidence intervals for each wind farm footprint and phase.

Phase	HR I	HR II	HR III
0	2.47 (2, 3.36)	4.75 (3.4, 7.33)	5.37 (4.43, 7.31)
1	3.34 (2.88, 4.27)	12.3 (9.66, 17.7)	17 (14.6, 22.6)
2	1.15 (0.929, 1.63)	6.15 (4.5, 8.76)	14.7 (11.3, 20.6)
3	0.973 (0.635, 1.59)	1.29 (0.964, 1.92)	16.8 (10.9, 26.4)

3.7.5 Phase-specific differences

Between Phases 0 and 1 there was a widespread significant increase in numbers with the largest appearing centrally around the future HR II footprint (Figure 3.46). In the HR II area there was a 50% decrease in diver density between Phase 1 and Phase 2, followed by a further decrease of 80% between Phase 2 and Phase 3, summarizing in a 90% decline between Phase 1 and Phase 3 (Table 3-7). There was also a large significant decrease off Blåvandshuk. Notably, there is little significant change in the HR I footprint.

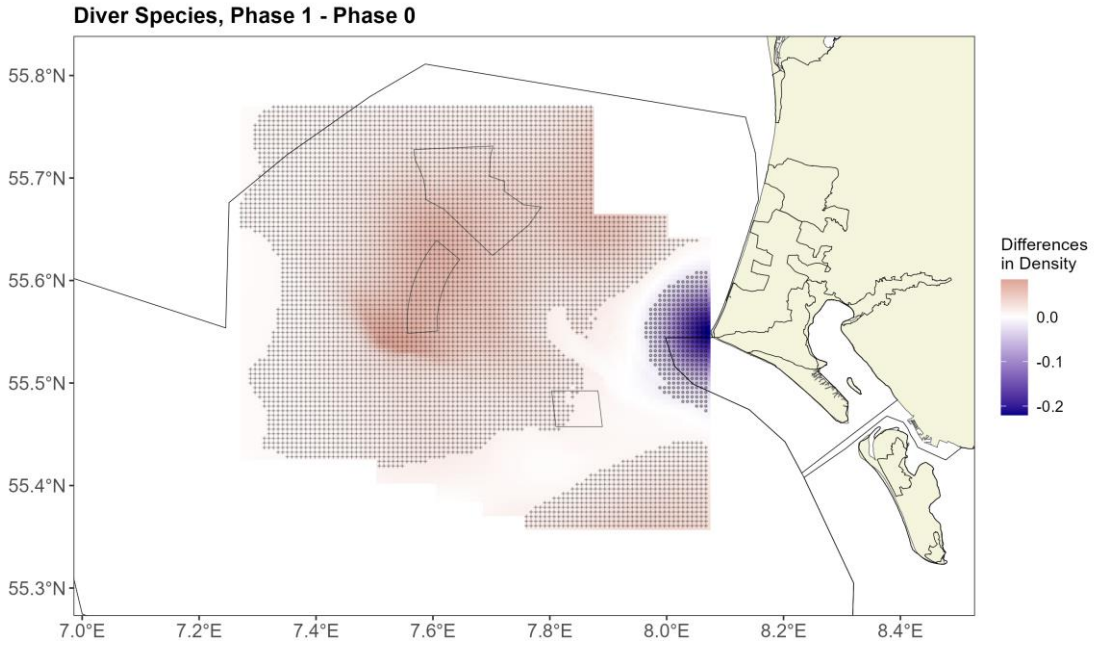

Figure 3.46. Figure showing the estimated differences in distribution between Phase 1 and Phase 0. Positive differences indicate more birds in Phase 1. A "+" sign in the bluish background colours indicates a significant positive difference and a "o" in reddish background colours a significant negative difference.

The statistically significant, and substantial, decreases in density in and around the HR II footprint subsequent to its construction is clear in Figure 3.47. This evidence-based shift away from the HR II footprint and the coastal region in general has delivered significantly higher densities into the northwest.

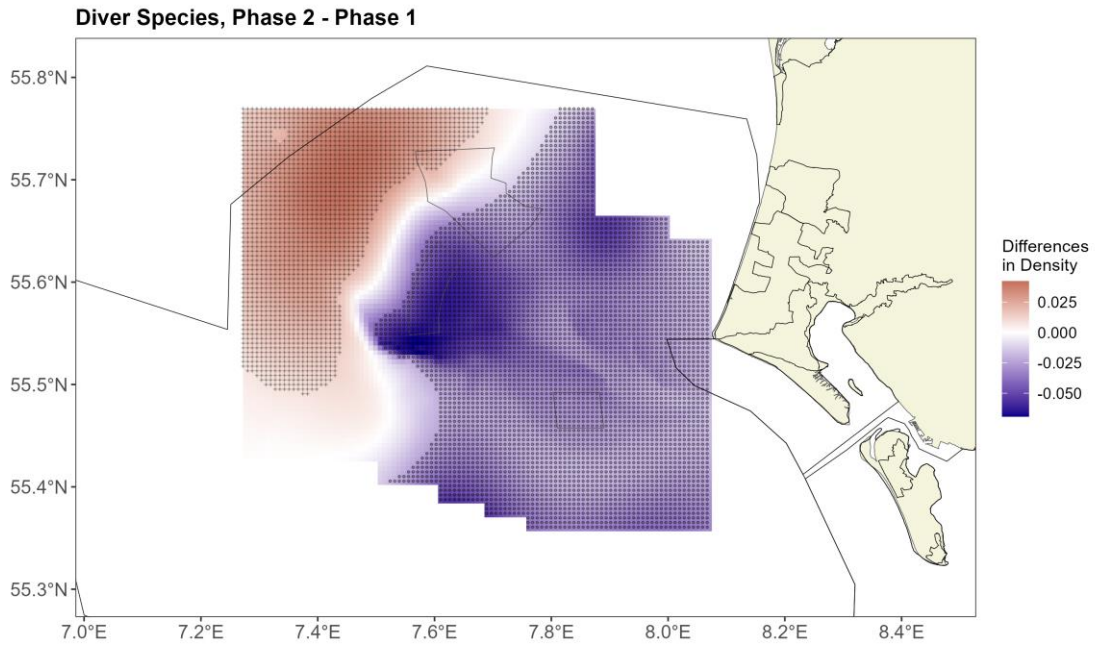

Figure 3.47. Figure showing the estimated differences in distribution between Phase 2 and Phase 1. Positive differences indicate more birds in Phase 2. A "+" sign in the bluish background colours indicates a significant positive difference and a "o" in reddish background colours a significant negative difference.

Eleven to twelve years post-construction of HR II there were significant decreases in the centre and west compared with two to three years post-construction, particularly focused in the region to the west of the HR II footprint (Figure 3.48). The concentration of divers has shifted from the west in Phase 2 to increase, in Phase 3, inshore from the now constructed HR III windfarm. There was also a small but significant increase in numbers in the far south.

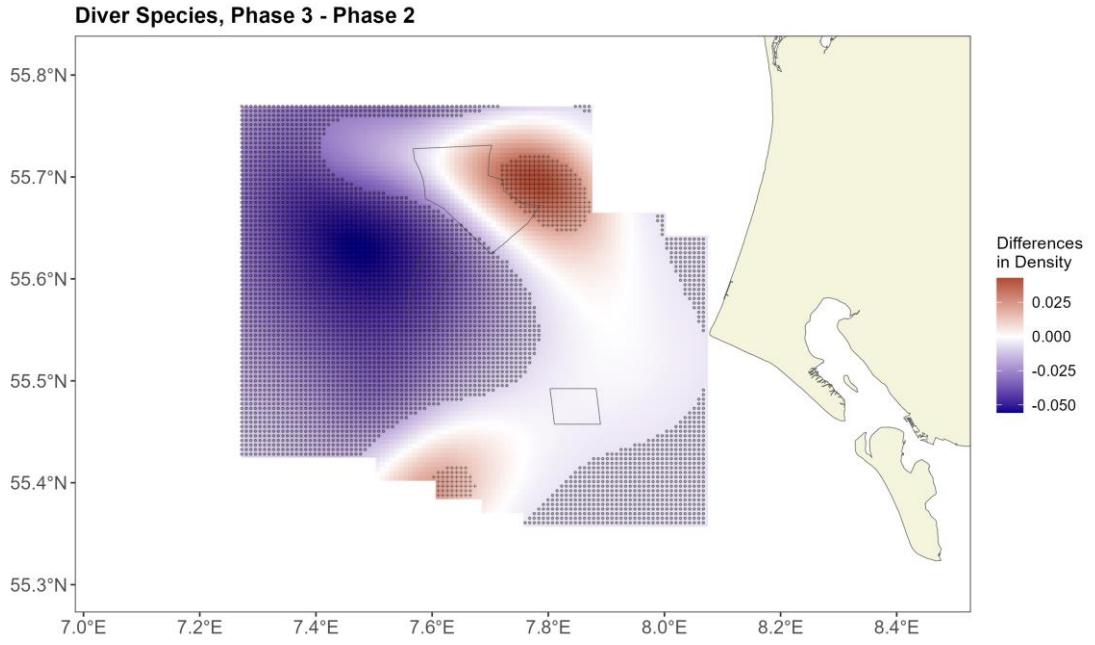

Figure 3.48. Figure showing the estimated differences in distribution between Phase 3 and Phase 2. Positive differences indicate more birds in Phase 3. A "+" sign in the bluish background colours indicates a significant positive difference and a "o" in reddish background colours a significant negative difference.

Although overall there were significant decreases almost everywhere (Phase 3 to 1), the largest significant decreases are centred completely over the footprint of HR II (Figure 3.49). There was evidence of some decline

in density in the HR III footprint in the area closest to HR II but otherwise there is no evidence of a change in density owing to the construction of HR III.

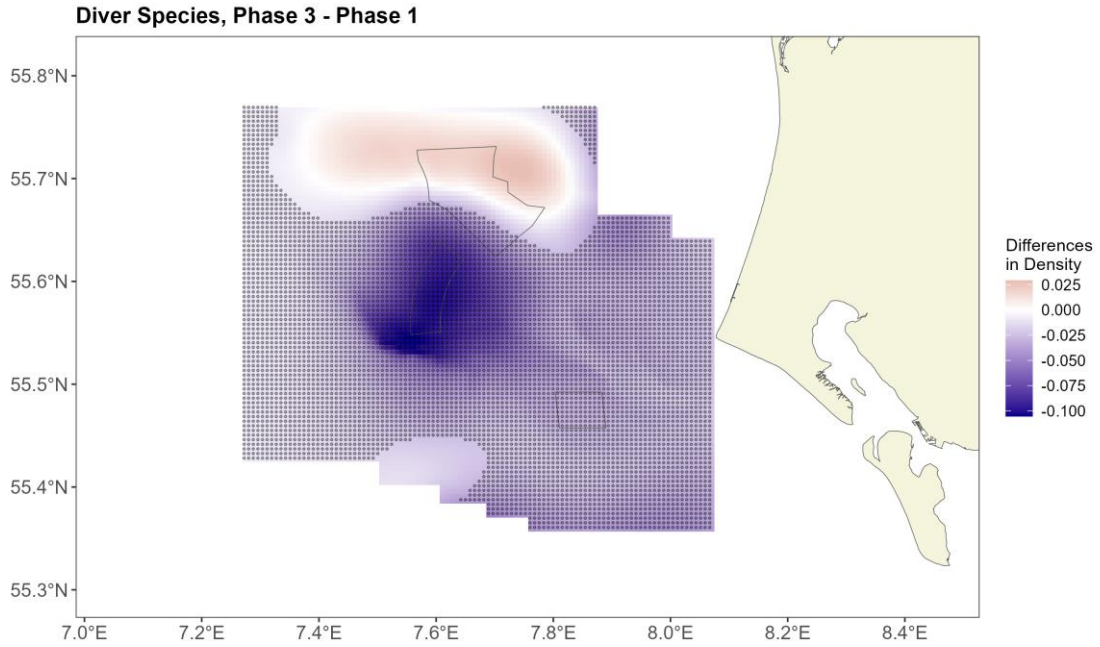

Figure 3.49. Figure showing the estimated differences in distribution between Phase 3 and Phase 1. Positive differences indicate more birds in Phase 3. A "+" sign in the bluish background colours indicates a significant positive difference and a "o" in reddish background colours a significant negative difference.

In general, these difference plots show that there is no clear pattern of displacement around the HR I or III windfarms but that despite widespread decreases there is compelling evidence of a larger decline in and around the footprint of HR II. From these results it is possible to speculate that, just like scoters, there was little/no effect of the installation of HR III on bird density.

3.8 Diver Horns Rev II (HR II) specific results

Divers do not show the expansion of range that common scoters did in the early 2000's but owing to the changing survey coverage for this widespread species and in keeping with the scoter analysis and 2014 report (Petersen et al. 2014) we chose to use data from November 2005 for a more detailed assessment of HR II. Furthermore, Figure 3.50 shows the mean density distribution in late Phase 1 surveys (post November 2005) is quite different compared with early surveys and all surveys combined.

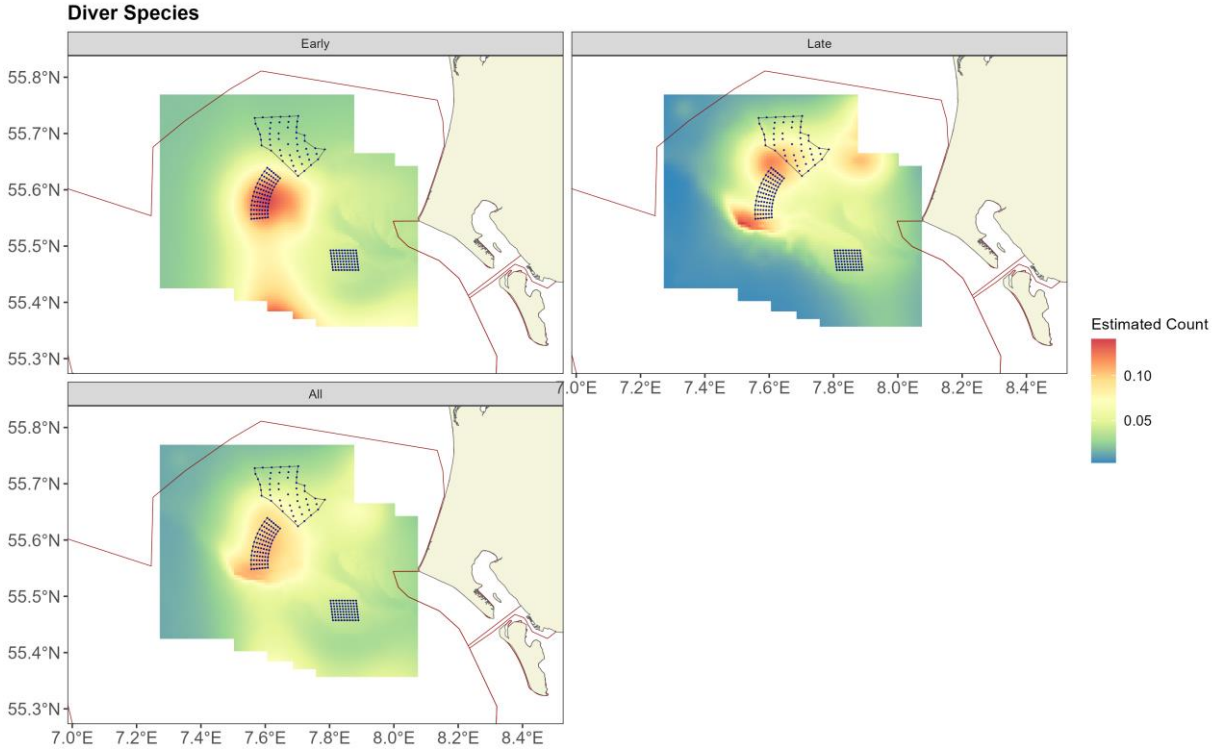

Figure 3.50. Figure showing the estimated diver abundance across the study site within Phase 1 for "Early" surveys (pre November 2005), "Late" surveys (post November 2005) and for all combined. The estimated counts are per 500 m x 500 m grid cell. The coloured graphics represent the predicted counts in each location.

Compared with Figure 3.47 (Phase 1-2), the use of the shortened Phase 1 (Figure 3.51) shifts some of the decrease in density in the central part of the HR II footprint post-construction. Figure 3.51 shows 60% of the cells in the HR II are estimated to have significantly decreased density post-construction.

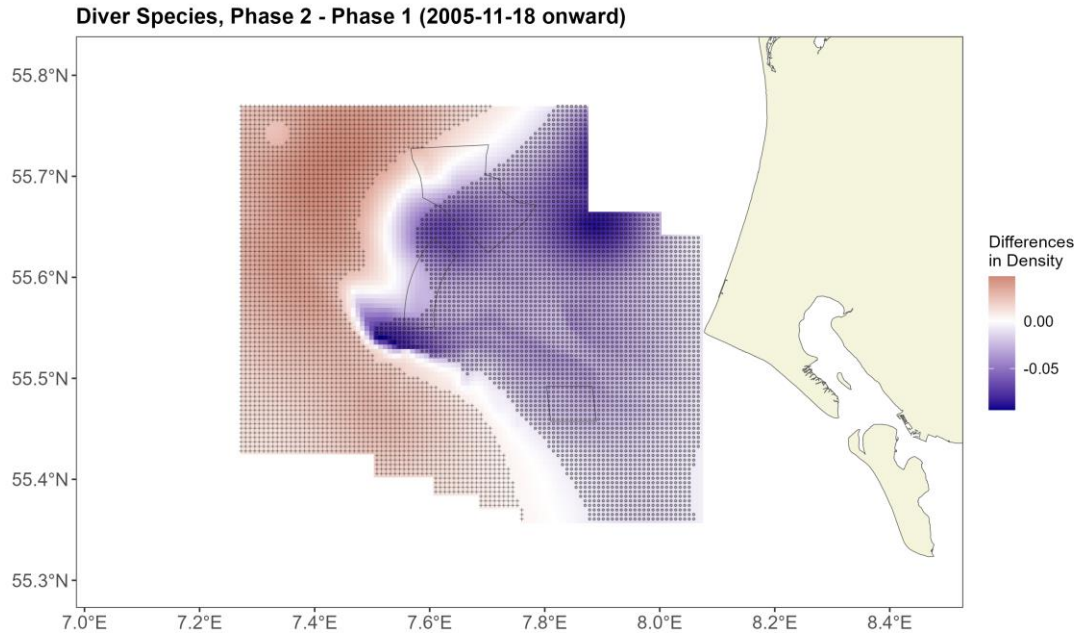

Figure 3.51. Figure showing the estimated differences in distribution between Phase 2 and Phase 1 with the shortened time frame. Positive differences indicate more birds in Phase 2. A "+" sign indicates a significant positive difference and a "o" a significant negative difference.

Compared with Figure 3.49 (Phase 1-3), the use of the shortened Phase 1 (Figure 3.52) splits the concentrated decrease in density in the HR II footprint into two concentrations slightly to the north and south of the footprint. There is also evidence of a significant increase in the south of the study area and in the north-west.

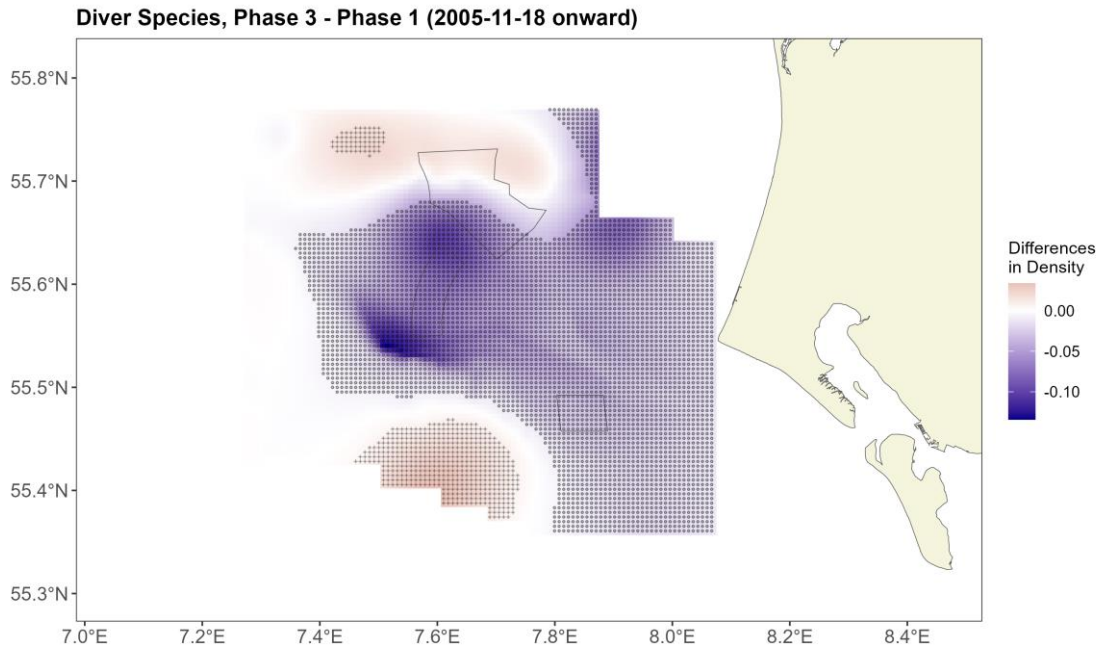

Figure 3.52. Figure showing the estimated differences in distribution between Phase 3 and the shortened Phase 1. Positive differences indicate more birds in Phase 3. A "+" sign indicates a significant positive difference and a "o" a significant negative difference.

*Table 3-8. Table showing the percentage of cells in the Horns Rev II wind farm footprint that estimate an increase or a decrease in abundance and also the percentage of cells that significantly increase or decrease (calculated from the bootstrap predictions). The * for Phase 1 indicates the shortened Phase 1.*

Horns Rev II	Pre-con. to 2-3 yrs post-con.	2-3yrs post-con. to 11-12 yrs post-con.	Pre-con. to 11-12 yrs post con.
Phase	1*-2	2-3	1*-3
% Cells in footprint increasing	0	0	0
% Cells significantly increasing	0	0	0
% Cells in footprint decreasing	100	100	100
% Cells significantly decreasing	59.0	100	100

3.8.1 HR II related changes across phases in all directions

We can also collapse the spatial patterns down into one dimension using concentric rings of increasing distance from the footprint and assess how the density changes between phases varies with distance. Figure 3.53 illustrates a displacement effect (reduction in density) post-construction (Phase 2 - 1) out to approximately 4 km from the footprint (where the upper 95% confidence interval rises to zero (no difference)).

The Phase 2-3 comparison shows a similar pattern but there was evidence of an increase in displacement distance from 4 km two to three years post-construction out to 10 km 11-12 years post-construction.

Comparing Phase 3 to Phase 1, 11-12 years post-construction, we see the combination of these effect giving compelling evidence for a displacement effect out to about 9.5 km from the HR II footprint (Figure 3.53). Beyond this, the densities return to pre-construction levels.

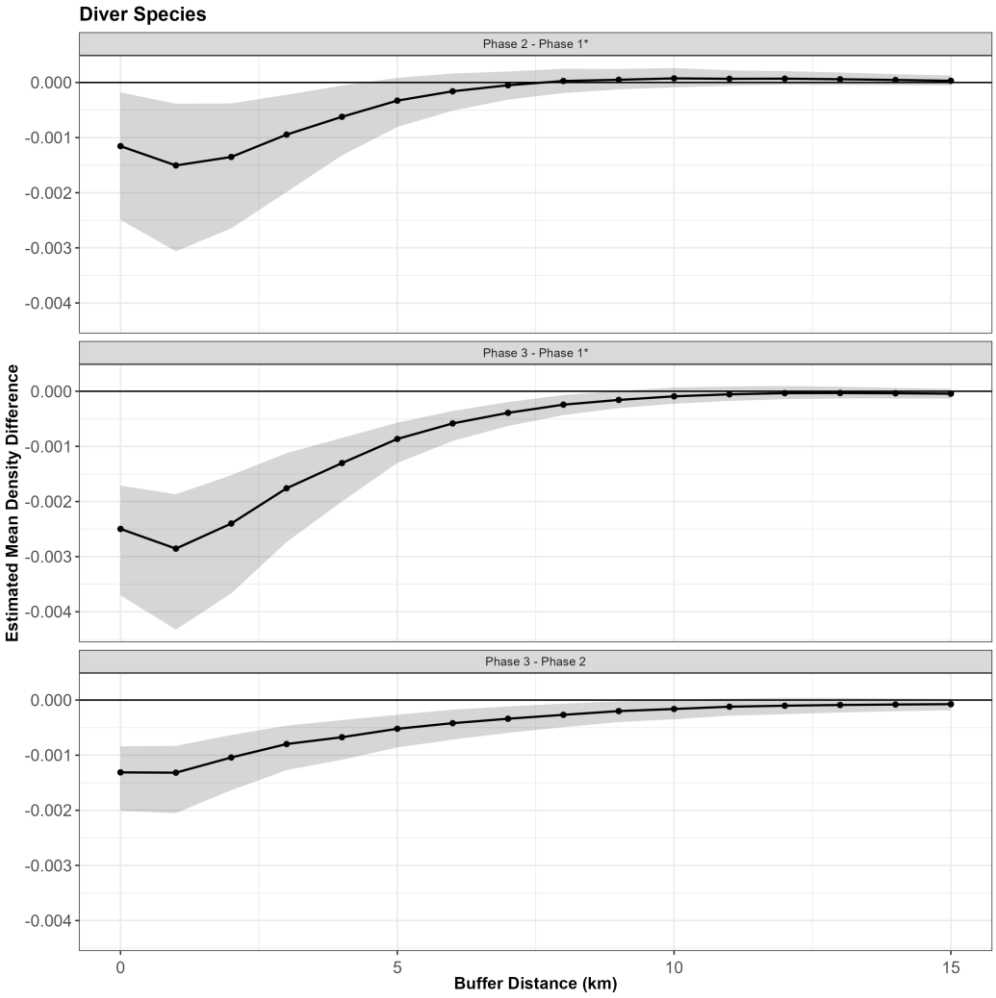

Figure 3.53. Figure showing the change in the estimated mean density difference between Phases 2-1, 3-1 and 3-2, with increasing distance to the HR II footprint.

3.8.2 HR II related changes across phases, direction specific

In contrast to Figure 3.53 which aggregates any distance related changes in and around the HR II footprint the results were also examined by 'sector'. In keeping with the common scoter outputs, we selected the same three sectors: North-East (NE) which includes the HR III footprint, South-East (SE), and West (W).

Figure 3.54 illustrates that NE of the HR II footprint, which starts to encompass HR III after approximately 3 km, we see the displacement evident to 6-7 km of the footprint (seen in Figure 3.53) 2-3 years and 11-12 years post-construction of HR II. After the construction of HR III (Phase 3-2 difference) the displacement is much less, out to 4 km.

Given the widespread displacement seen in earlier outputs it is not surprising to see that the patterns for the SE and W sectors are very similar to the NE. In the SE, displacements were consistently estimated to be about 9 km, regardless of phase. The pattern is less clear for the west sector with no discernible displacement effect early post-construction (Phase 2-1), displacement as far as 15 km (the maximum assessed) between Phases 2 and 3 and overall from Phase 1 to 3 a displacement of approximately 8 km.

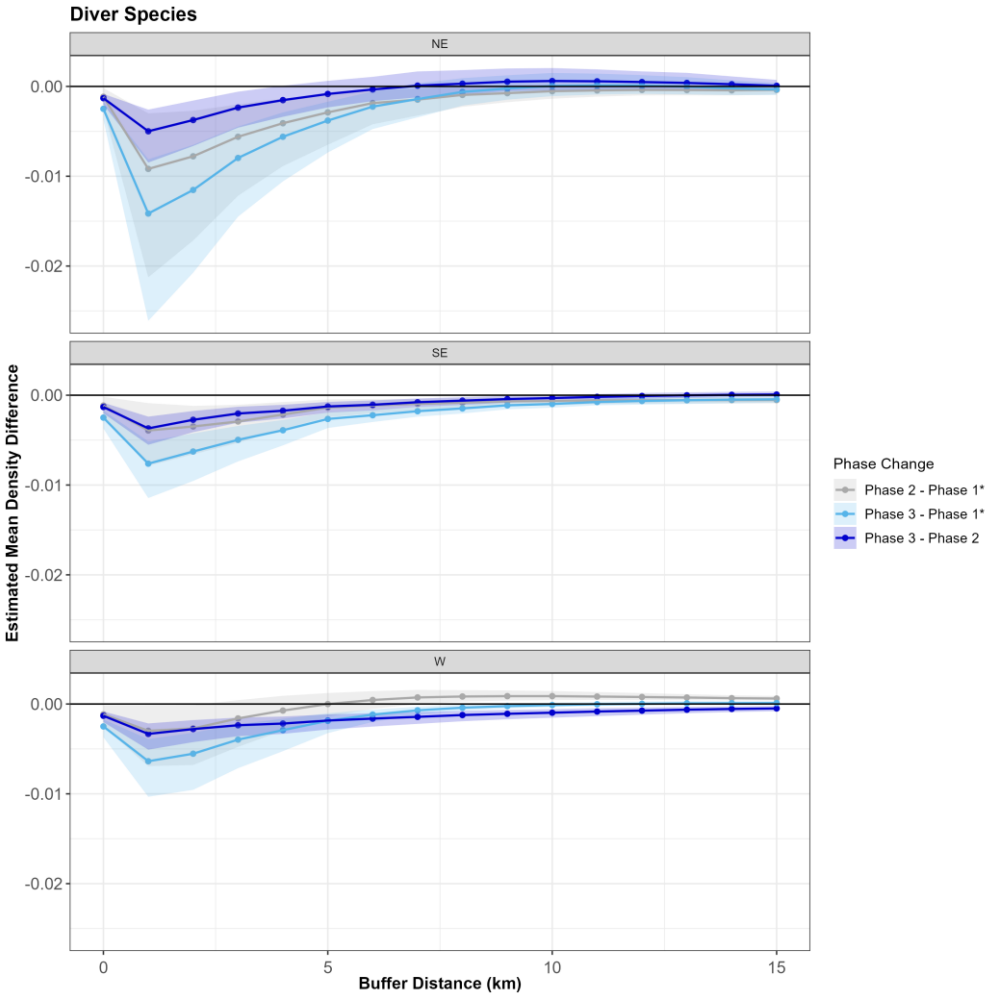

Figure 3.54. Figure showing the differences with distance to footprint by phase change and by sector.

4 Discussion

These unique results from 56 aerial surveys across 24 years covering the construction of three major OWF's in the Horns Rev area showed that common scoters dramatically changed their distribution in the study area during the period from 2000 onwards for reasons other than the presence of the turbines. There was a general increase in common scoter density throughout the entire area from Phase 0 to Phase 2, levelling off in Phase 3 during which time common scoter increasingly spread offshore. This makes interpretation of these results slightly more difficult than if densities had remained constant and even throughout the study area and study period. Nevertheless, post-construction of HR I (Phase 1) common scoter increased within its footprint compared to Phase 0, which was difficult to associate with the construction due the dramatic increase and expansion in the range of the species that occurred throughout this area during Phase 1. There was a significant decline in density within the HR I footprint in Phase 2 relative to Phase 1 and densities in Phase 3 were significantly lower than in Phase 1. HR I was either constructed in an area less attractive to common scoters or the area was utilized less by common scoters because of the presence of the wind farm, which makes the results difficult to interpret. The distributional data suggest some displacement within the footprint in phases 2 and 3, but this may simply have been an area less attractive to the species anyway. In contrast, there were very significant reductions in density in HR II after construction compared to previous periods, with some recovery in Phase 3 compared to Phase 1 (i.e. pre-construction levels), suggesting major effects of its construction, which were detectable out to 5 km from the windfarm. Common scoter densities were increasing in the footprint of HR III throughout Phase 0 to Phase 2 but showed no significant change between phases 2 and 3, suggesting no detectable effect of its construction of HR III.

Despite the area's outstanding importance for the species, densities of divers (the vast majority red-throated divers) in the Horns Rev study area were very much lower compared to those of common scoters. This means that even small changes in very local abundance can have major effects on comparisons between years and that detecting statistically significant changes between very low densities of birds across years is a challenge in this species. Diver densities increased from Phase 0 to 1 followed by a general decline from Phase 1 to 3, returning to similar levels as in Phase 0, so the results here need to be viewed against a backdrop of variable densities during the 24 years across the survey area. Changes in densities of divers within each of the three windfarms showed different patterns post-construction. Densities increased post-construction of HR I (Phase 1) compared with Phase 0, but after this, densities in the HR I footprint declined in line with the rest of study area. In the HR II footprint, there was a great increase in density from Phase 0 to 1 followed by a steep decline in Phase 2 (i.e. post HR II construction), which continued into Phase 3 at densities significantly lower than those in Phase 0. Densities in the HR III footprint increased from Phases 0 to 1 in parallel with those throughout but showed no significant change from Phase 1 to 3 (pre- to post-construction of HR III), suggesting no significant detectable change post-construction.

Overall, these results show that while the construction of HR I and HR II may have had effects on diver densities, like the common scoter, there was no discernible effect of HR III on bird densities post-construction.

We can only speculate what the mechanisms behind these observed displacement effects are. It seems highly likely that above and beyond complicating factors such as the abundance and distribution of the food supply for both species, there are four likely major factors that could be the stimuli behind the displacement responses shown by common scoter and divers. These are displacement from (i) physical disruption caused by maintenance ship-traffic associated with the servicing of the wind turbines, (ii) visual disruption caused by the turning turbine blades or (iii) the lighting of the turbines at night or (iv) the noise caused by the turbines. We infer that the shipping traffic associated with the turbines is likely constant and more or less of equal intensity across all of the three HR windfarms and therefore this is unlikely to be a major explanation for the apparent lack of response to the construction of HR III. In the case of (ii), (iii) and (iv) above, the responses of birds to these visual and auditory stimuli are likely to mediated by distance and if both divers and common scoter avoid adverse stimuli by remaining at a certain distance from such stimuli, it might be expected that displacement is a distance related response to point-stimulus. If the birds prefer to keep a certain distance away from a turbine because of its visual (rotating blades or lighting at night) or auditory impact, and that that distance is less than half the distance between adjacent turbines, they will be reticent to swim between consecutive lines of turbines. If this is the case, we may hypothesise that the more irregular distribution of turbines and the far

greater inter-turbine distances associated with HR III could contribute to the lack of apparent displacement response of both species that was so evident following the construction of HR II.

It is difficult to interpret these changes in density distributions as "habituation" in the sense that whatever response was driving divers to avoid the turbines initially showed a clear and consistent reduction over time. The diminished response of common scoter to the construction of HR II does seem to show some reduction in displacement over the time after the creation of the wind farm which might be interpreted as habituation. However, the lack of any significant detectable response in either species to the construction of HR III is more remarkable, especially given the apparent avoidance responses to the construction of offshore windfarms by divers elsewhere in Europe.

In the eastern German North Sea a long-term data set on diver distributions was used to analyse the effect from OWF's on divers. The analysis covered a major part of the German North Sea and was based on 14 years of pre-construction data from March and April, collected from ship-based and aerial human observer-based surveys. The post-construction data covered ten surveys between late February and early May of 2015 till 2017, collected as digital aerial surveys (Mendel et al. 2019). The results showed marked displacements of divers, with decreasing effect out to ca. 16 km from the wind farms.

A study from the same German North Sea aera used a combined aerial digital survey data set on the distribution of Red-throated Diver and satellite telemetry data from the same species. Data was collected in April and May from 2015 to 2017 from two sources, namely four aerial digital surveys and Argos PPT satellite telemetry data from 33 birds. The results showed a 90% reduction in Red-throated Diver density within the footprint of the OWF's and out to a distance of 5 km from their periphery, and significant displacement could be shown out to a distance of 10-15 km (Heinänen et al. 2020).

5 Conclusions

Environmental impact assessments of OWF's evaluate the potential impact on birds, but very few studies have ever attempted to empirically study the actual effects of construction by comparing pre- and post-construction studies. We have been able to undertake such a unique study at Horns Rev to assess the displacement effects of two critical bird species following the construction of three OWF's during 2002 to 2019 based on 56 aerial surveys of birds conducted in that area up until 2024. We found equivocal evidence for displacement of divers and common scoter after the construction of the first windfarm HR I perhaps because of changes in distribution of both species in the study area and low densities of both species in and around HR I. There was strong evidence for divers being displaced out to 4 km (with no habituation since) and common scoters out to 5 km (with some signs of habituation since) after the construction of HR II in 2009. While there was little or no evidence for habituation by the divers to HR II, common scoter seemed to show reduced levels of displacement by the end of the study period. In contrast, there was little or no evidence for displacement effects of HR III on densities of either species post-construction.

6 Recommendations for future studies

The results of this report emphasize the importance of compiling long term data series on bird distributions within and around wind farm sites, both pre- and post-construction of OWF's. We recommend such studies to be conducted in and around existing and upcoming wind farm sites. The Rødsand II/Nysted OWF's offer an opportunity to investigate long-term changes in the distribution of long-tailed duck, which could potentially provide valuable information on the long-term effect from OWF's on this species. The German OWF's Wikinger and Arkona on Adler Grund in the Baltic Sea may provide additional options for investigating this. Similarly, the Anholt OWF in Kattegat offers an opportunity to compare pre- and post-construction effects on divers.

We urge immediate investigation into the effects of inter-turbine distances at other European offshore windfarm developments on the displacement effects on these two species, or similar species, to find support for the hypothesis that the density and size of turbines may affect the degree of displacement of certain bird species. Kriegers Flak and neighbouring wind farms in Swedish and German water have wind farms of varying turbine size and densities. Unfortunately, there are no available pre-construction bird distribution data from Kriegers Flak to support such analyses. Data from various OWF's in the German Bight, Germany, in the Thames Estuary and the Wash, UK could also potentially provide data for such comparisons.

The HR I wind farm has been in operation since 2002 and will be approaching time for repowering in coming years. This could potentially involve the redevelopment of that area with fewer and larger turbines, which could offer an opportunity to further find support for the hypothesis that avian displacement may be reduced in relation to greater inter-turbine distances, but the same extent of the footprint, as a feature of the new windfarm there.

7 References

Berman, Mark, and T. Rolf Turner. 1992. "Approximating Point Process Likelihoods with GLIM." *Journal of the Royal Statistical Society. Series C (Applied Statistics)* 41 (1): 31–38. http://www.jstor.org/stable/2347614.

Buckland, S. T., DR Anderson, KP Burnham, JL Laake, D. L. Borchers, and L. Thomas. 2001. *Introduction to Distance Sampling: Estimating Abundance of Biological Populations*. United Kingdom: Oxford University Press.

Buckland, S. T., Rexstad, E.A., Marques, T.A, & Oedekoven, C.S. 2015. Distance Sampling: Methods and Applications. – Springer, DOI 10.1007/978-3-319-19219-2.

Heinänen, S. Zydelis, R., Kleinschmidt, B., Dorsch, M., Burger, C., Markunas, J., Quillfeldt, P. & Nehls, G. 2020. Satellite telemetry and digital aerial surveys show strong displacement of red-throated divers (Gavia stellata) from offshore wind farms. - Marine Environmental Research 160, 104989.

Fliessbach, K.L., Borkenhagen, K., Guse, N., Markones, N, Schwemmer, P. & Garthe, S. 2019. A Ship Traffic Disturbance Vulnerability Index for Northwest European Seabirds as a Tool for Marine Spatial Planning. – Front.Mar.Sci. 6:192. https://doi.org/10.3389/fmars.2019.00192

Lamb, J., Gulka, J., Adams, E., Aonghais, C. & Williams, K. 2024. A synthetic analysis of post-construction displacement and attraction of marine birds at offshore wind energy installations. - Environmental Impact Assessment Review 108, 107611.

Leys, Christophe, Christophe Ley, Olivier Klein, Philippe Bernard, and Laurent Licata. 2013. "Detecting Outliers: Do Not Use Standard Deviation Around the Mean, Use Absolute Deviation Around the Median." *Journal of Experimental Social Psychology* 49 (4): 764–66.
https://doi.org/https://doi.org/10.1016/j.jesp.2013.03.013.

Marques, F. F. C., and S T Buckland. 2004. "Covariate Models for the Detection Function." In *Advanced Distance Sampling*, edited by ST Buckland, DR Anderson, KP Burnham, JL Laake, DL Borchers, and L Thomas, pp31–47. United Kingdom: Oxford University Press.

Marques, T. A., L. Thomas, S. G. Fancy, and S. T. Buckland. 2007. "Improving Estimates of Bird Density Using Multiple- Covariate Distance Sampling." *The Auk* 124 (4): 1229–43.
https://doi.org/10.1093/auk/124.4.1229.
R Core Team. 2022. *R: A Language and Environment for Statistical Computing*. Vienna, Austria: R Foundation for Statistical Computing. https://www.R-project.org/.

Petersen, I.K., Christensen, T.K, Kahlert, J., Desholm, M. & Fox, A.D 2006. Final results of bird studies at the offshore wind farms at Nysted and Horns Rev, Denmark. – Report request, Commissioned by DONG energy and Vattenfall A/S. NERI, National Environmental Research Institute, Ministry of the Environment, 161 pp.

Petersen, I.K. & Fox, A.D. 2007. Changes in bird habitat utilisation around the Horns Rev 1 offshore wind farm, with particular emphasis on Common Scoter. Report request, Commissioned by Vattenfall A/S. NERI, National Environmental Research Institute, Ministry of the Environment, 36 pp.

Petersen, I.K. & Nielsen, R.D. 2011. Number and distribution of birds in and around the Horns Rev 2 Offshore Wind Farm. Spring 2011. Report commissioned by DONG Energy A/S. Aarhus University, DCE - Danish Centre for Environment and Energy. 22 pp.

Petersen, I.K., Nielsen, R.D. & Mackenzie, M.L. 2014. Post-construction evaluation of bird abundances and distributions in the Horns Rev 2 offshore wind farm area, 2011 and 2012. Report commissioned by DONG Energy. Aarhus University, DCE – Danish Centre for Environment and Energy. 51 pp.

Petersen, I.K., Nielsen, R.D., Therkildsen, O.R. & Balsby, T.J.S. 2017. Fældende havdykænders antal og fordeling i Sejerøbugten i relation til menneskelige forstyrrelser. Aarhus Universitet, DCE – Nationalt Center for Miljø og Energi, 38 s. - Videnskabelig rapport fra DCE - Nationalt Center for Miljø og Energi nr. 239.

http://dce2.au.dk/pub/SR239.pdf

Petersen, I.K. & Sterup, J. 2019. Number and distribution of birds in and around two potential offshore wind farm areas in the Danish North Sea and Kattegat. Aarhus University, DCE – Danish Centre for Environment and Energy, 40 pp. Scientific Report. No. 327. http://dce2.au.dk/pub/SR327.pdf

Schwemmer, P., Mendel, B., Sonntag, N., Dierschke, V. & Garthe, S. 2011. Effects of ship traffic on seabirds in offshore waters: implications for marine conservation and spatial planning. - Ecological Applications, 21(5), 2011, pp. 1851-1860

Scott-Hayward, L. A. S., M. L. Mackenzie, C. R. Donovan, C. G. Walker, and E. Ashe. 2014. "Complex Region Spatial Smoother (CReSS)." *Journal of Computational and Graphical Statistics* 23 (2): 340–60.

Scott-Hayward, L. A. S., M. L. Mackenzie, and C. G. Walker. 2023. "MRSea R Package (V1.5.0): Spatially Adaptive Uni and Bi-Variate Regression Splines Using SALSA." University of St Andrews.

Scott-Hayward, L. A. S., M. L. Mackenzie, C. G. Walker, G. Shatumbu, W. Kilian, and P. du Preez. 2023. "Automated Surface Feature Selection Using SALSA2D: Assessing Distribution of Elephant Carcasses in Etosha National Park." https://arxiv.org/abs/2202.07977.

Scott-Hayward, L. A. S., C. S. Oedekoven, M. L. Mackenzie, and C. G. Walker. 2014. "MRSea R Package: Statistical Modelling of Bird and Cetacean Distributions in Offshore Renewables Development Areas. University of St. Andrews: Contract with Marine Scotland: SB9 (CR/2012/05)." University of St Andrews.

Walker, C. G., M. L. Mackenzie, C. R. Donovan, and M. J. O'Sullivan. 2010. "SALSA - a Spatially Adaptive Local Smoothing Algorithm." *Journal of Statistical Computation and Simulation* 81 (2): 179–91.

8 APPENDICES

Appendix 1

Survey overview with distribution maps for common scoter and divers by survey

8.1 Survey overview

The 56 aerial surveys of bird in the Horns Rev area were conducted between February 2000 and April 2024. The transect coverage in kilometers by survey was between 516 and 1.612 Km (Table 8-1).

Table 8-1. Table detailing the survey effort (number kilometer covered transect line by survey) for each of the 56 surveys conducted between 2000 and 2024. Note that survey numbers 27 and 31 (marked with asterisks) were conducted over two days.

Survey number	Survey date	Km of transect	Survey number	Survey date	Km of transect	Survey number	Survey date	Km of transect
1	2000-02-17	826.9	21	2003-12-04	698.4	39	2007-03-03	1368.8
2	2000-02-21	574.3	22	2003-12-30	634.9	40	2007-04-01	1612.1
3	2000-03-19	823.4	23	2004-02-29	870.8	41	2011-03-01	599.6
4	2000-04-27	738.0	24	2004-03-26	867.6	42	2011-03-26	645.0
5	2000-08-21	755.6	25	2004-05-10	865.5	43	2011-04-11	643.6
6	2000-10-06	724.0	26	2004-09-09	794.3	44	2011-10-13	642.3
7	2000-12-22	612.3	27*	2005-03-08	296.0	45	2011-11-17	619.5
8	2001-02-09	754.7	27*	2005-03-09	580.7	46	2012-01-15	658.8
9	2001-03-20	826.1	28	2005-04-02	868.3	47	2012-02-08	637.4
10	2001-04-21	826.2	29	2005-05-14	871.5	48	2012-03-02	604.1
11	2001-08-22	818.9	30	2005-08-17	868.2	49	2012-03-22	627.2
12	2001-09-26	761.7	31*	2005-11-18	634.4	50	2012-04-11	630.9
13	2002-01-07	685.1	31*	2005-11-19	577.4	51	2023-11-17	599.3
14	2002-03-12	728.3	32	2006-02-02	847.8	52	2023-12-27	531.8
15	2002-04-09	681.4	33	2006-02-25	848.3	53	2024-01-09	589.7
16	2002-08-08	685.2	34	2006-03-12	850.2	54	2024-02-27	587.4
17	2003-02-13	699.1	35	2006-04-15	845.4	55	2024-04-08	586.0
18	2003-03-16	850.8	36	2006-05-11	852.7	56	2024-04-22	592.0
19	2003-04-23	859.6	37	2007-01-25	1441.0			
20	2003-09-05	840.0	38	2007-02-15	1357.7			

The transect coverage and the distribution of the observed common scoters by survey is given in Figure 8.1 to Figure 8.10.

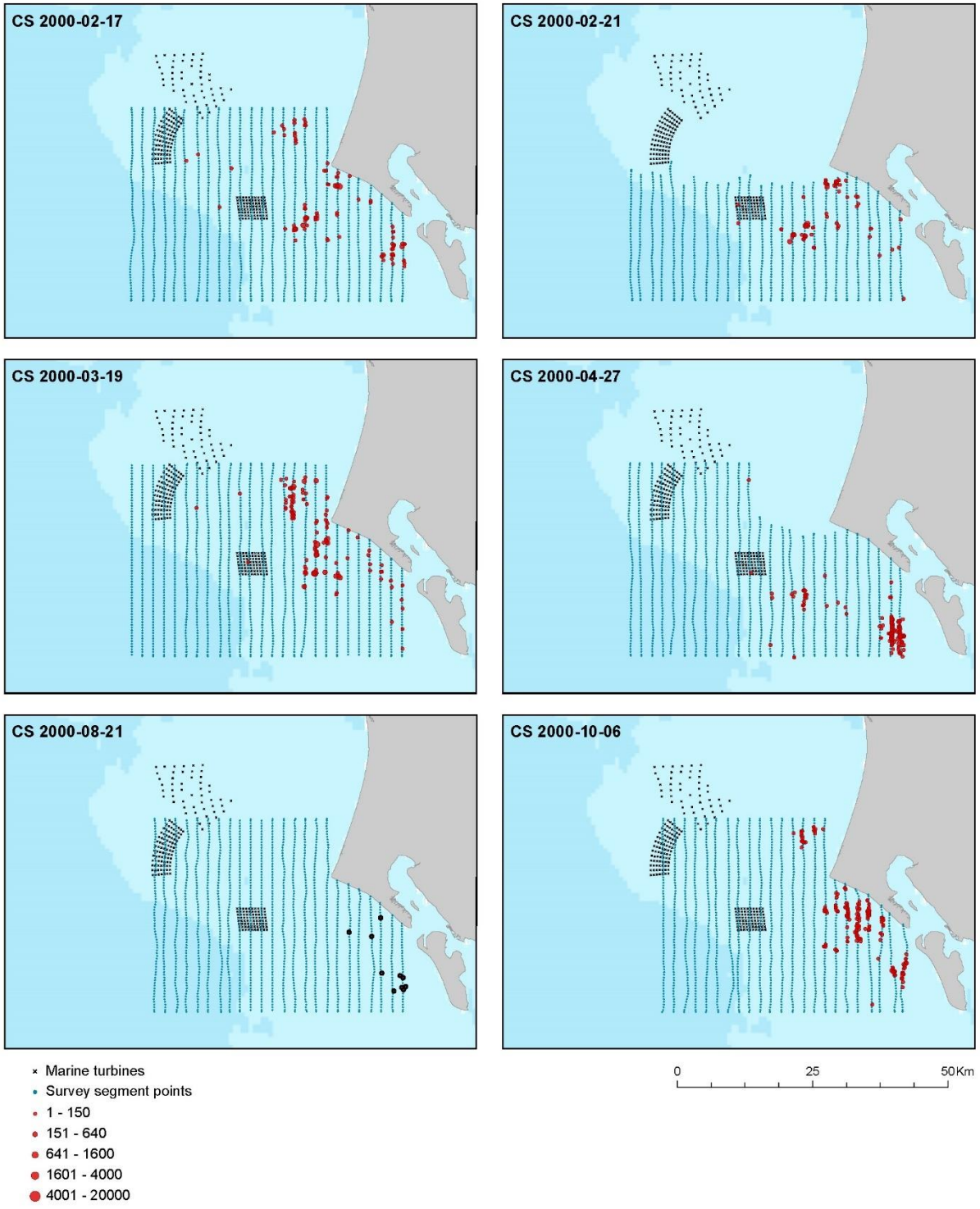

Figure 8.1. The distribution of observed common scoter during six surveys from February 2000 to October 2000.

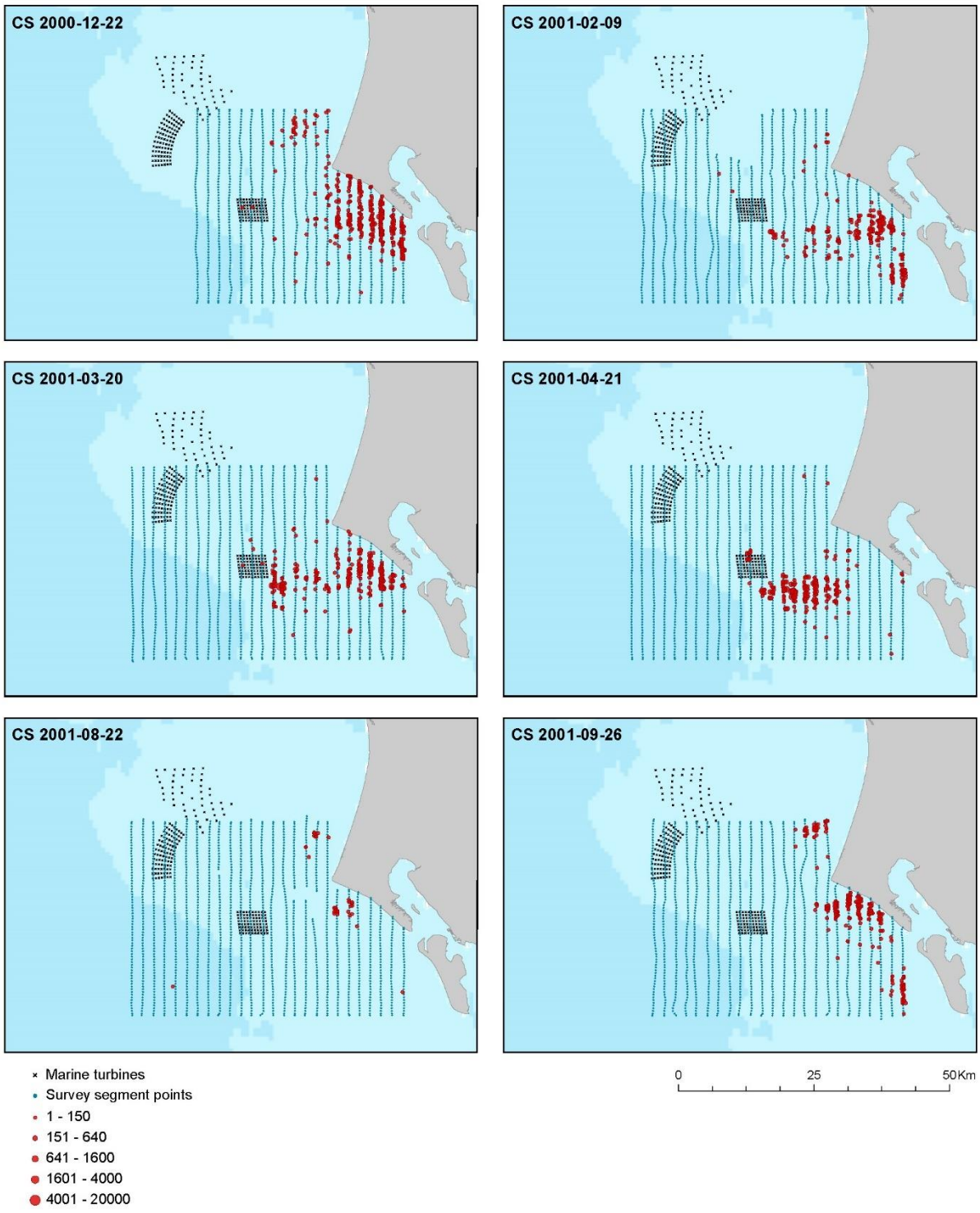

Figure 8.2. The distribution of observed common scoter during six surveys from December 2000 to September 2001.

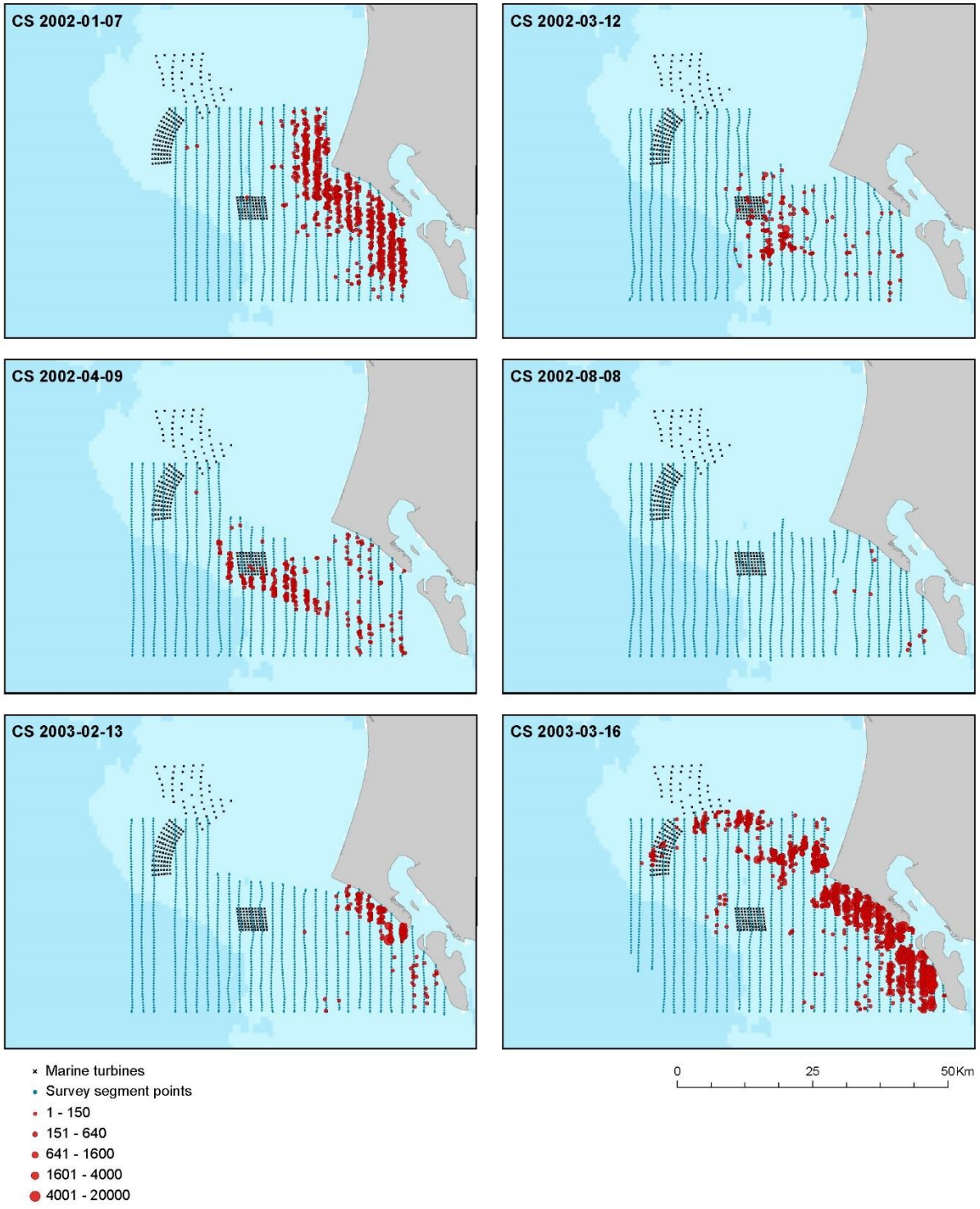

Figure 8.3. The distribution of observed common scoter during six surveys from January 2002 to March 2003.

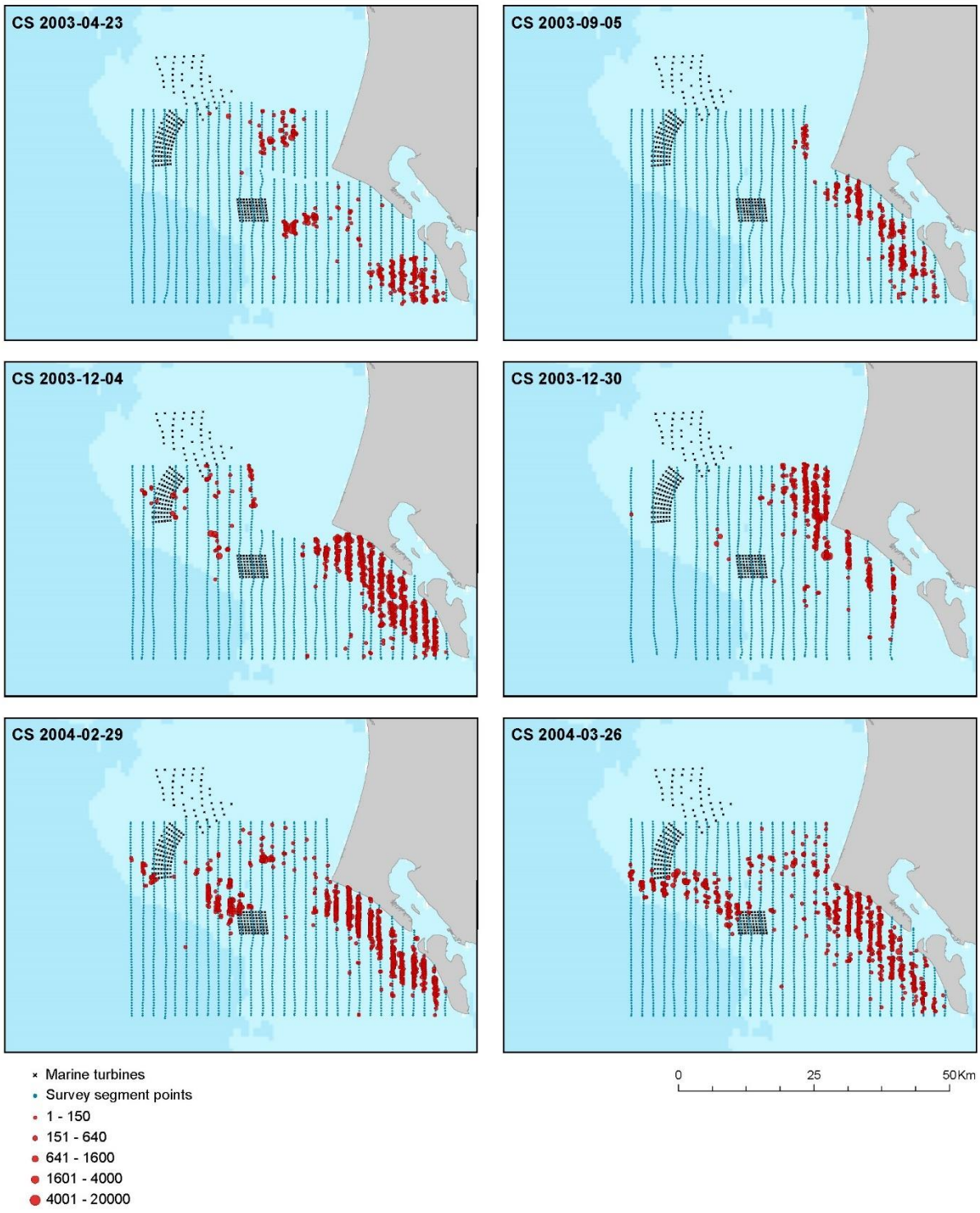

Figure 8.4. The distribution of observed common scoter during six surveys from April 2003 to March 2004.

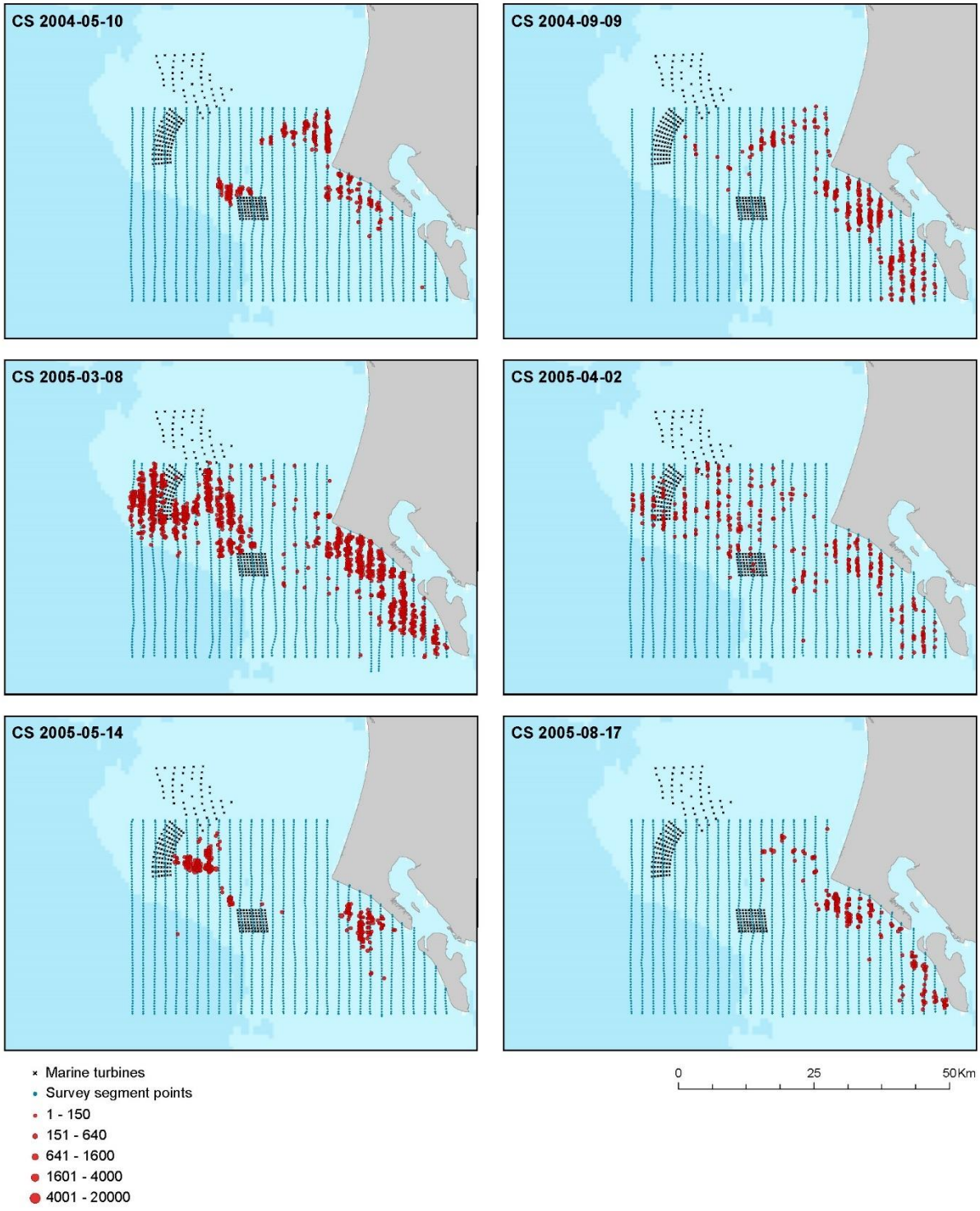

Figure 8.5. The distribution of observed common scoter during six surveys from May 2004 to August 2005.

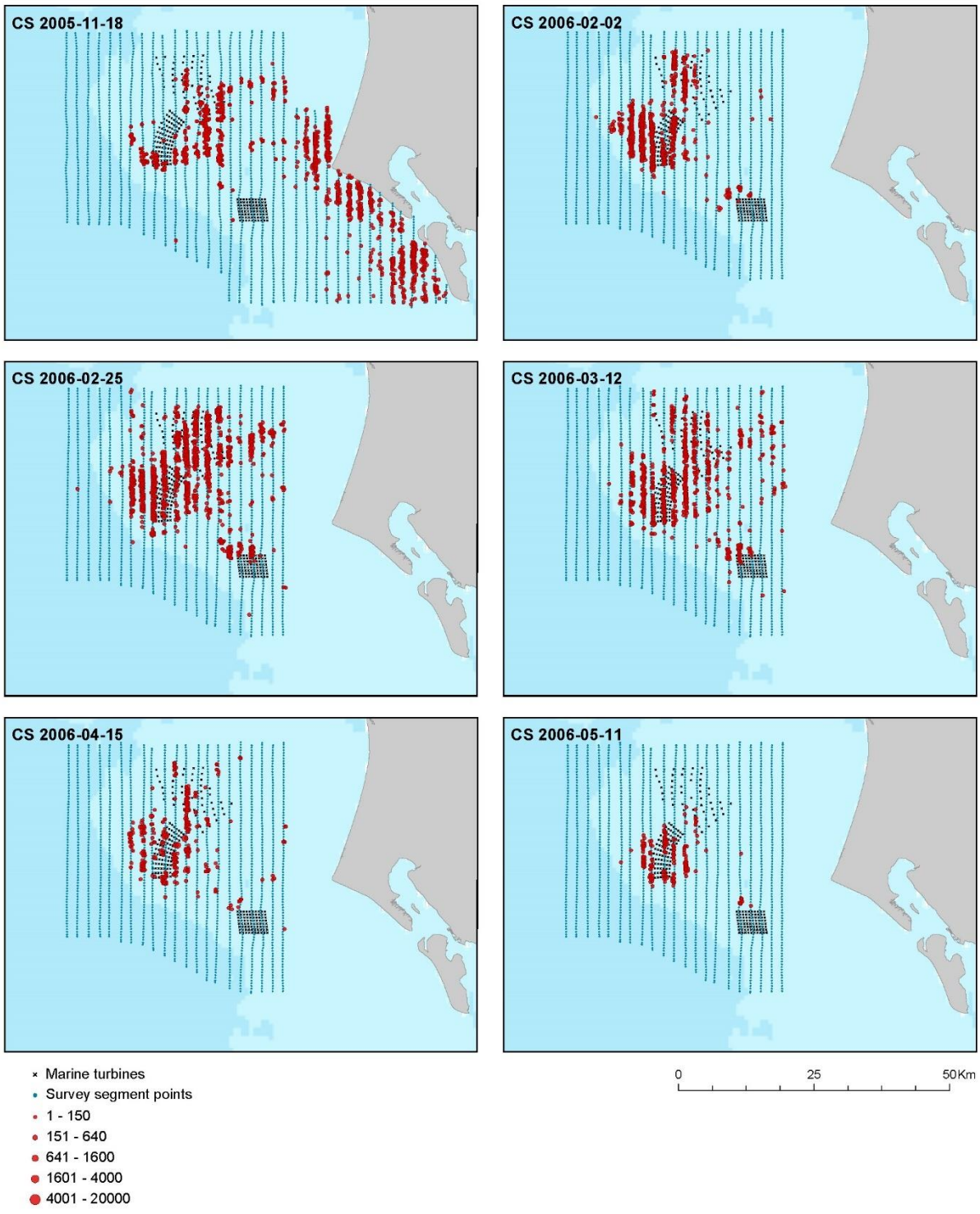

Figure 8.6. The distribution of observed common scoter during six surveys from November 2005 to May 2006.

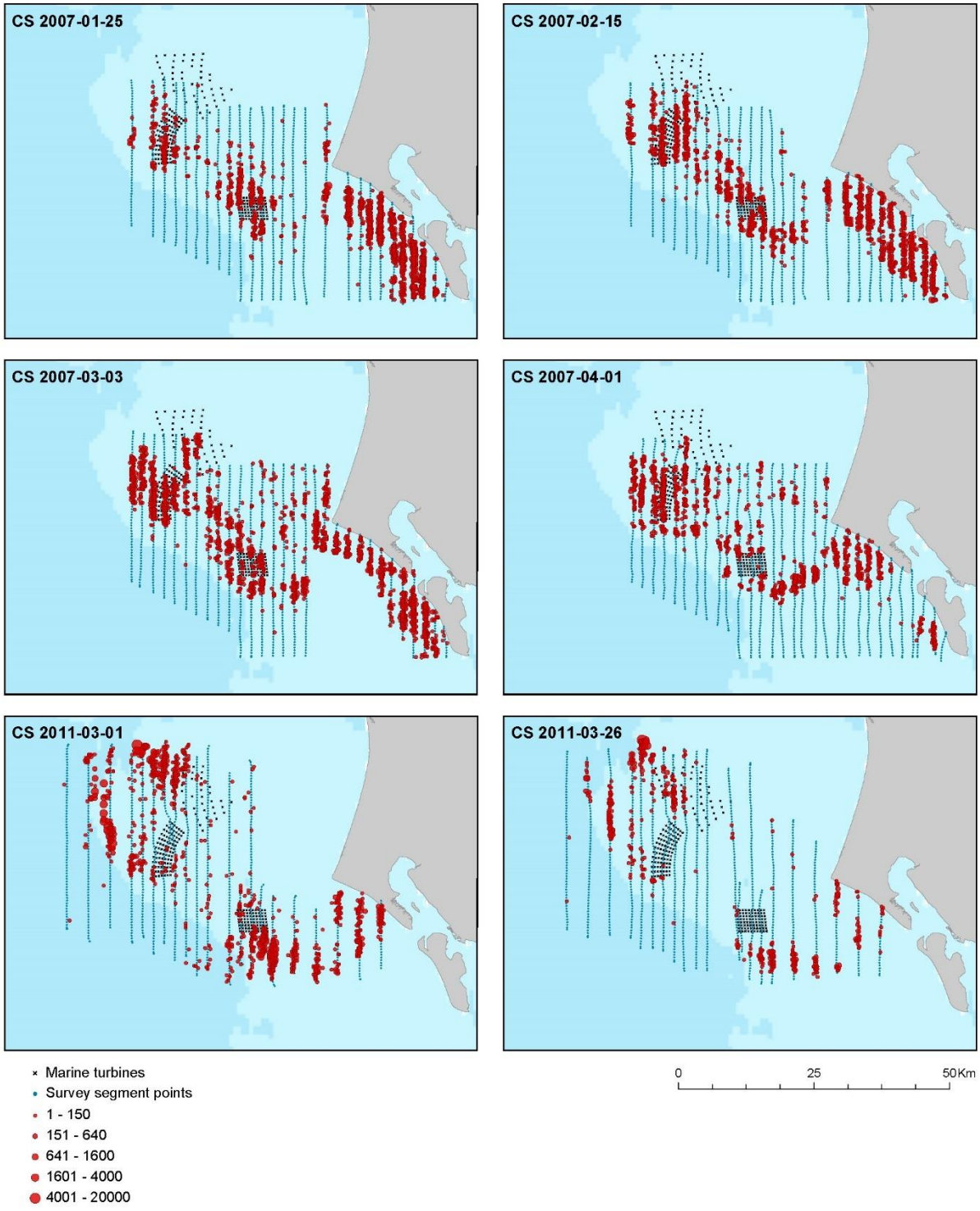

Figure 8.7. The distribution of observed common scoter during six surveys from January 2007 to March 2011.

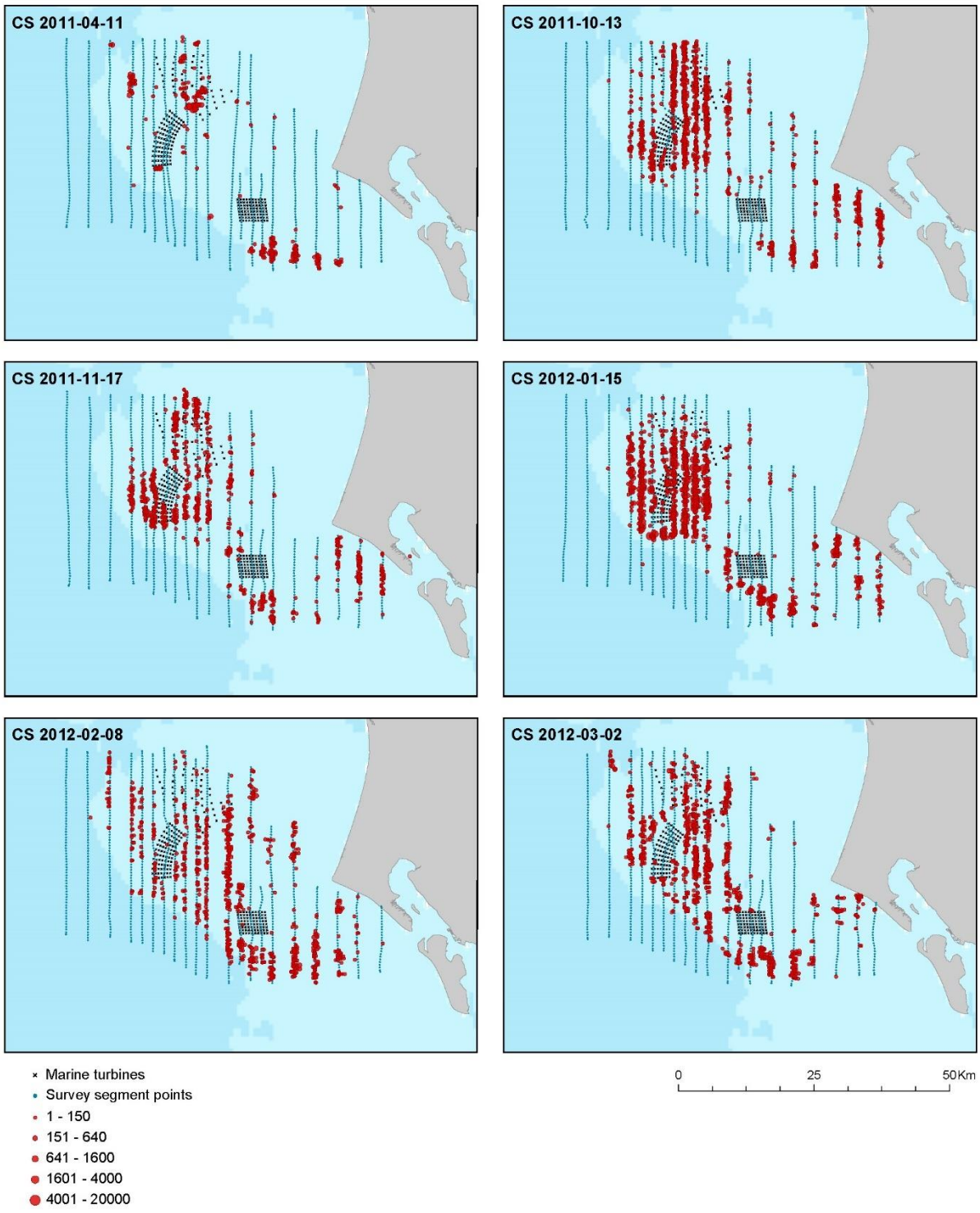

Figure 8.8. The distribution of observed common scoter during six surveys from April 2011 to March 2012.

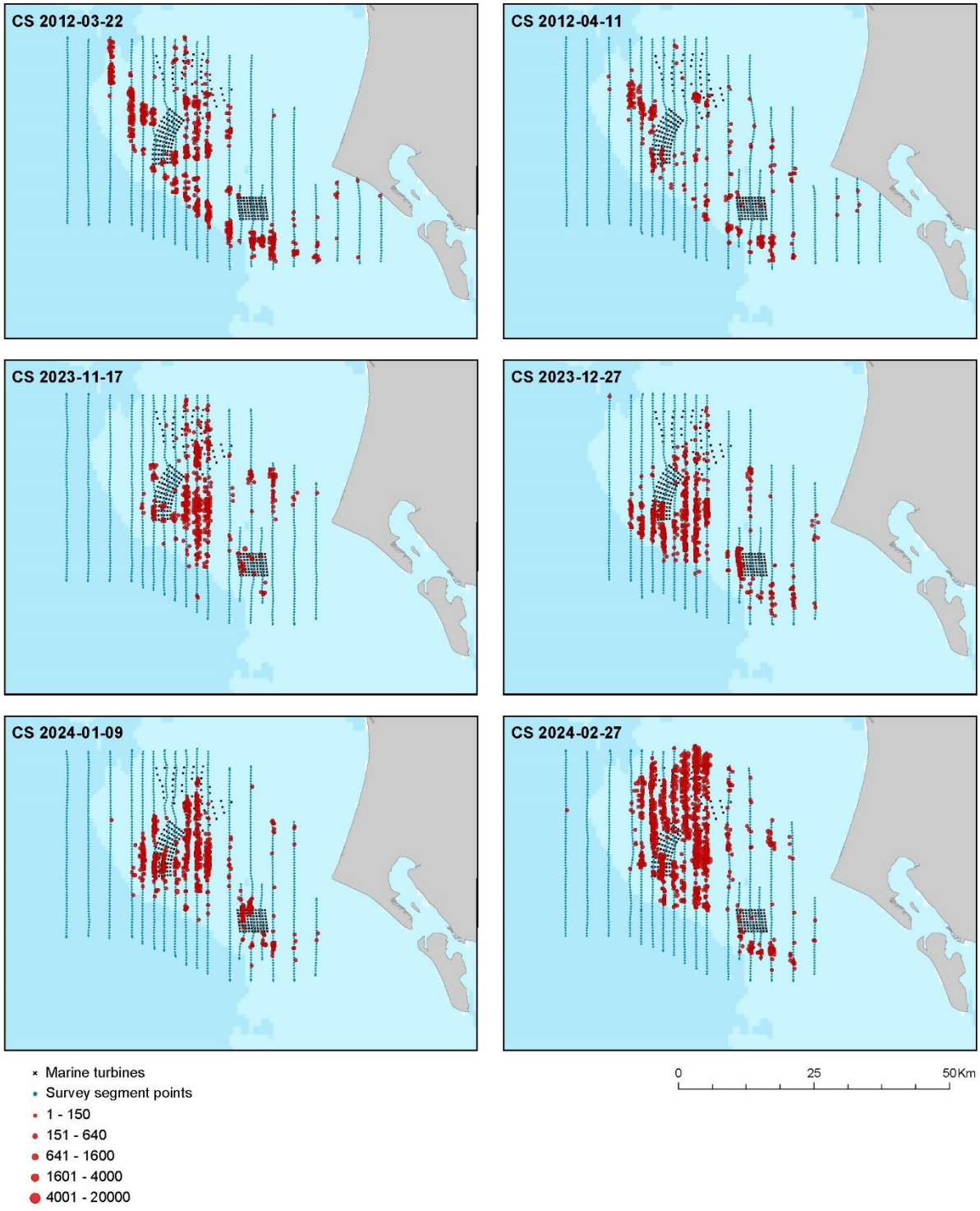

Figure 8.9. The distribution of observed common scoter during six surveys from March 2012 to February 2024.

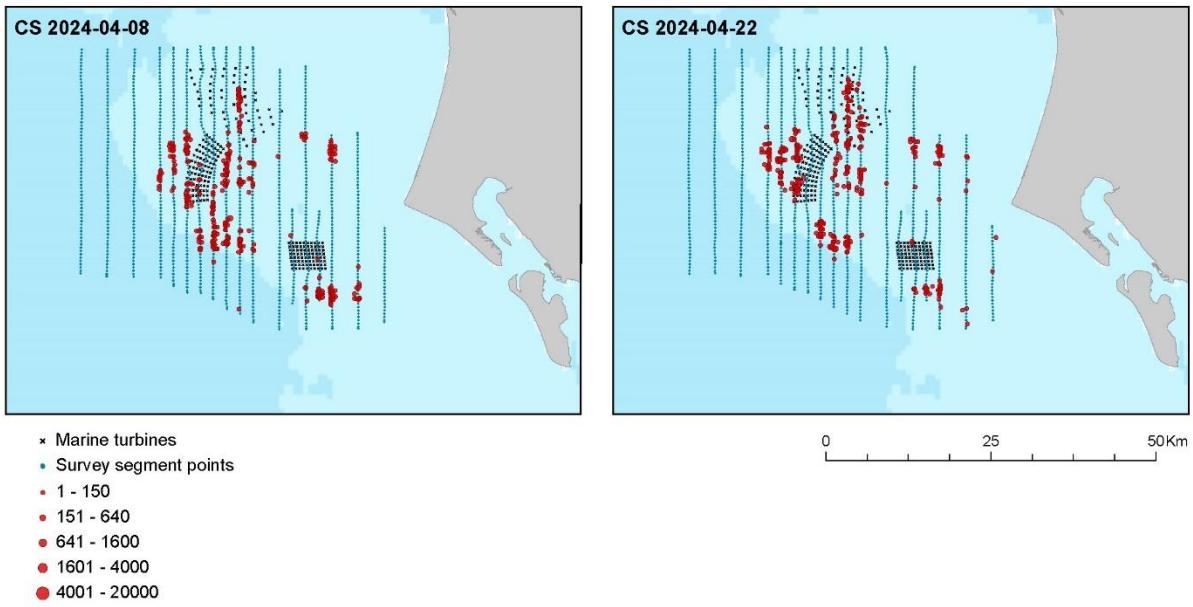

Figure 8.10. The distribution of observed common scoter during two surveys in April 2012.

The transect coverage and the distribution of the observed red-throated divers/black-throated divers by survey is given in Figure 8.11 to Figure 8.20.

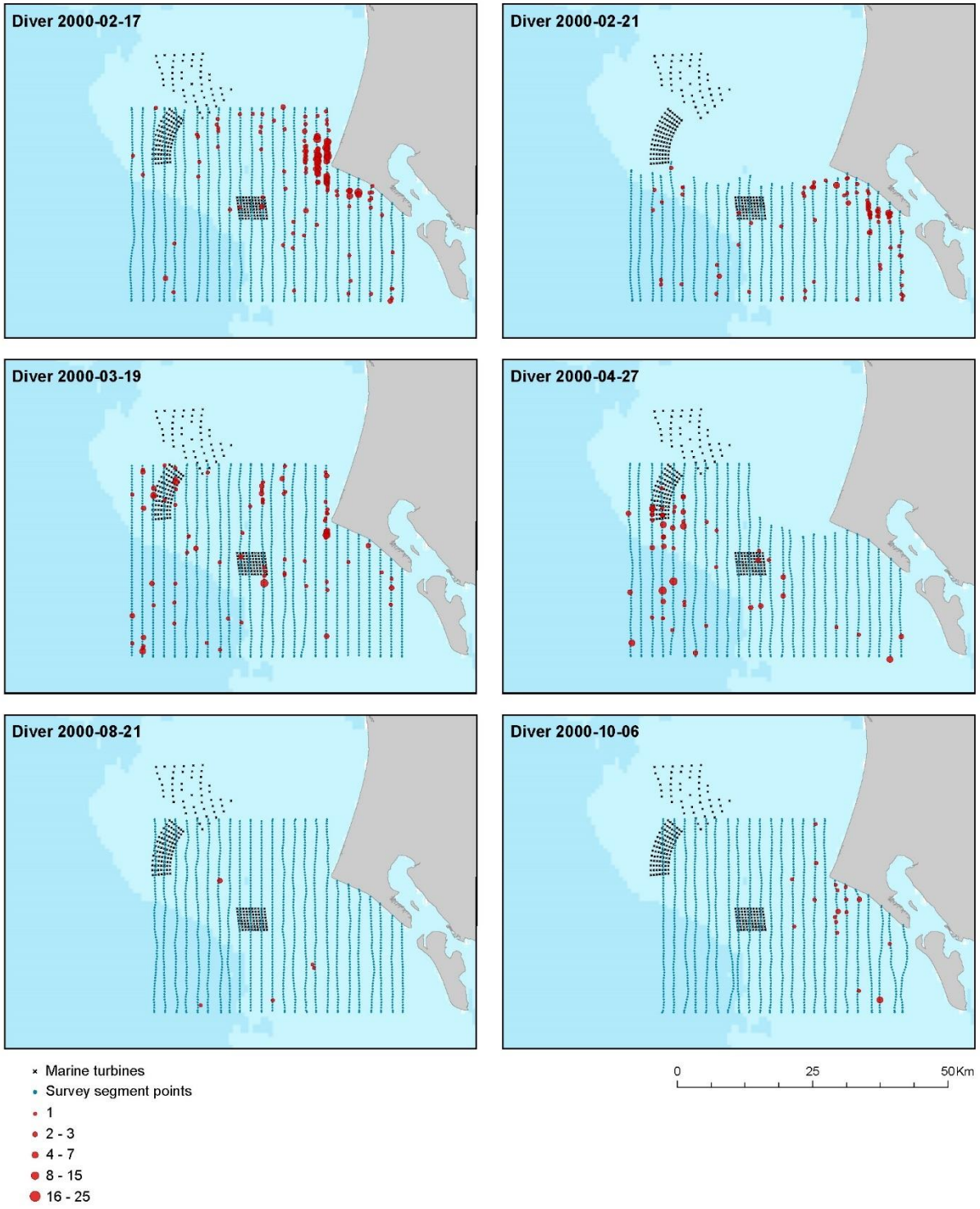

Figure 8.11. The distribution of observed red-throated diver/black-throated diver during six surveys from February 2000 to October 2000.

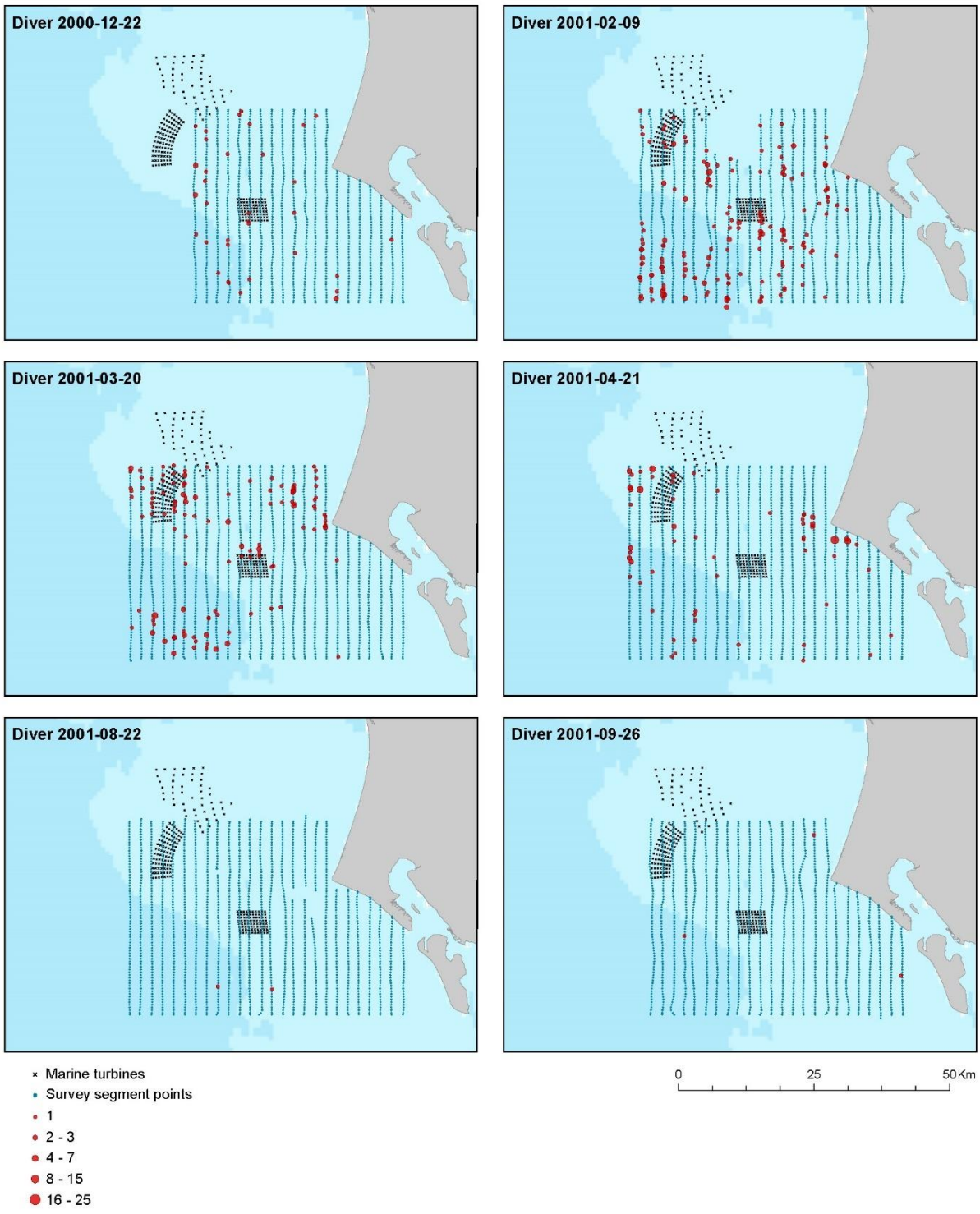

Figure 8.12. The distribution of observed red-throated diver/black-throated diver during six surveys from December 2000 to September 2001.

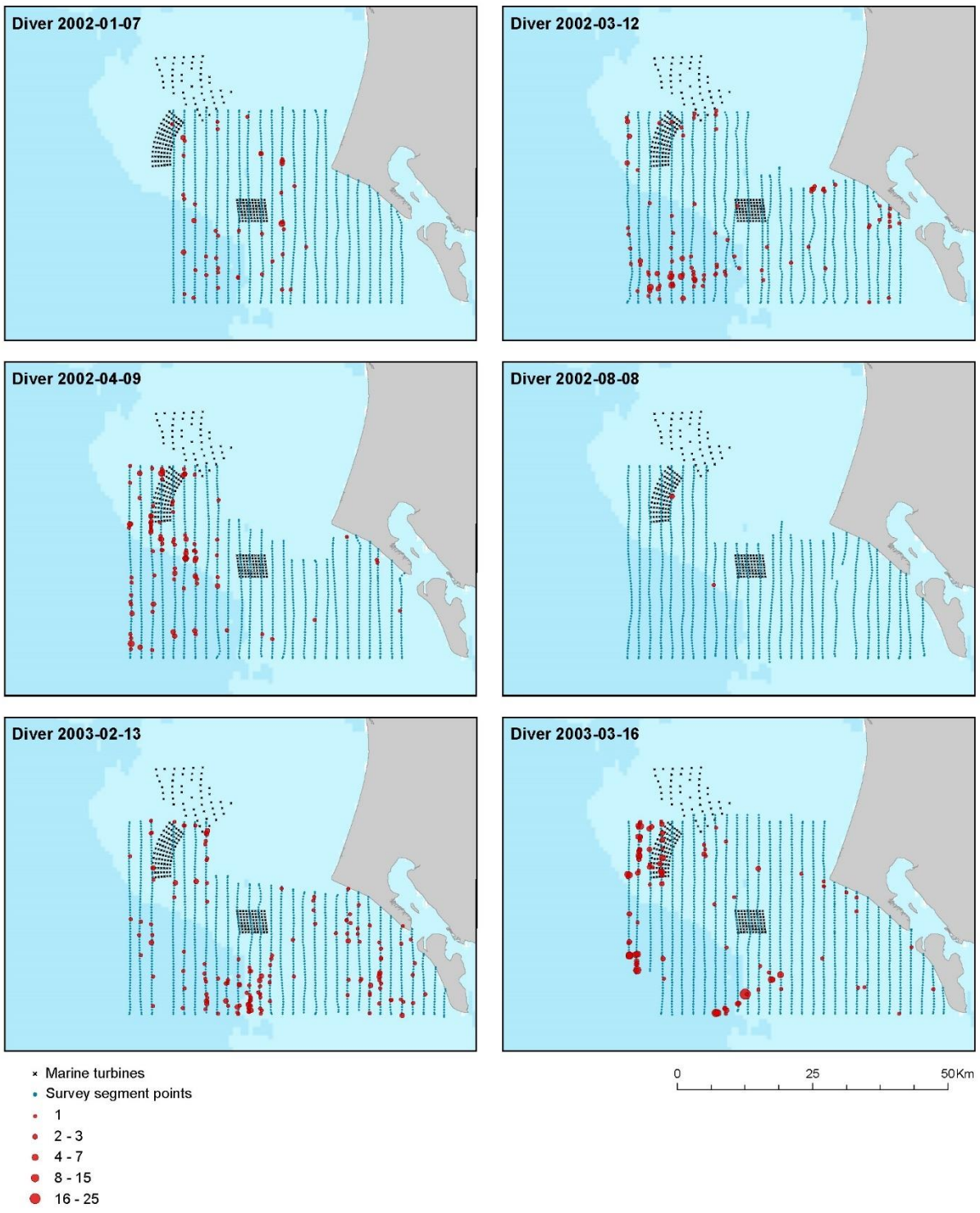

Figure 8.13. The distribution of observed red-throated diver/black-throated diver during six surveys from January 2002 to March 2003.

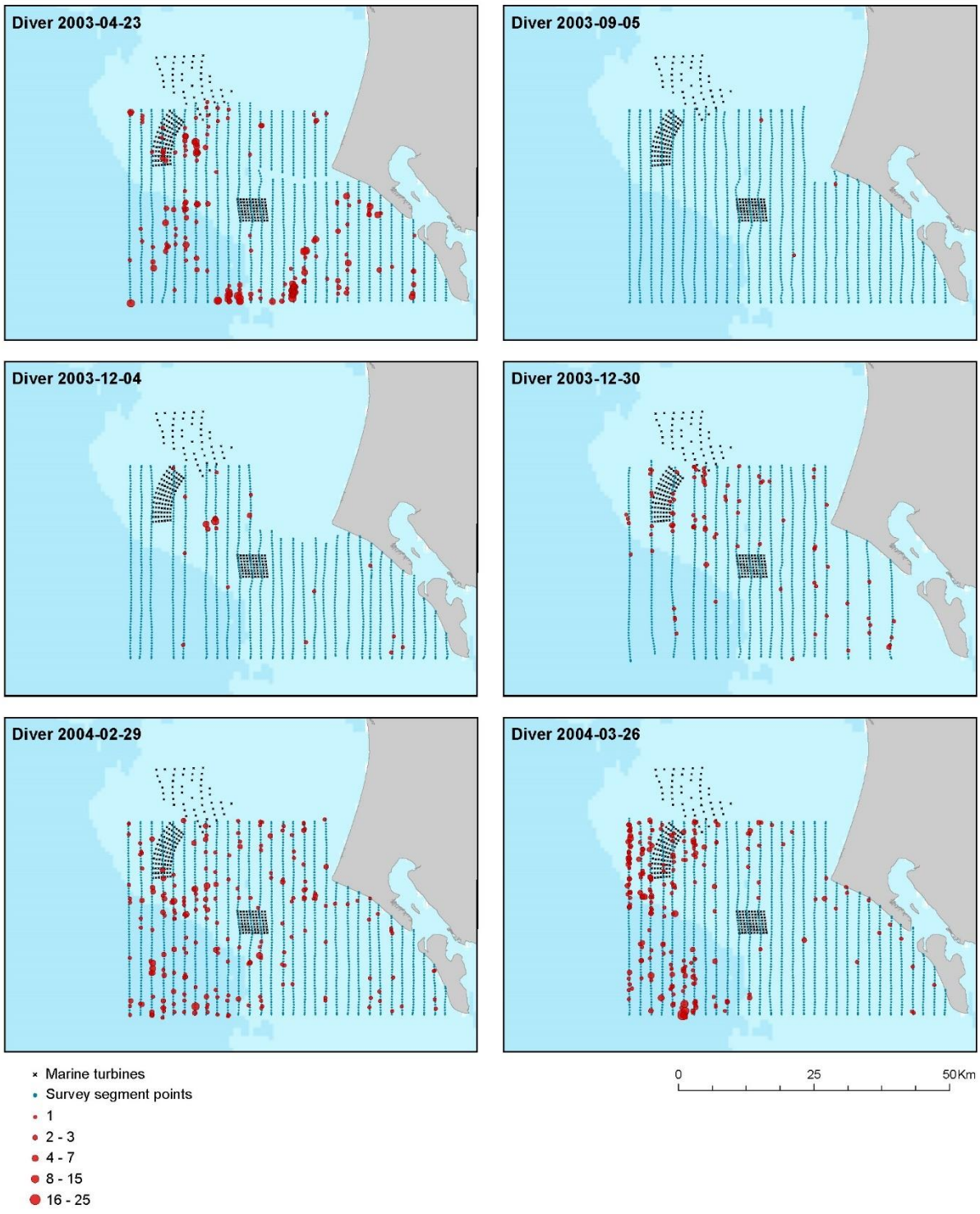

Figure 8.14. The distribution of observed red-throated diver/black-throated diver during six surveys from April 2003 to March 2004.

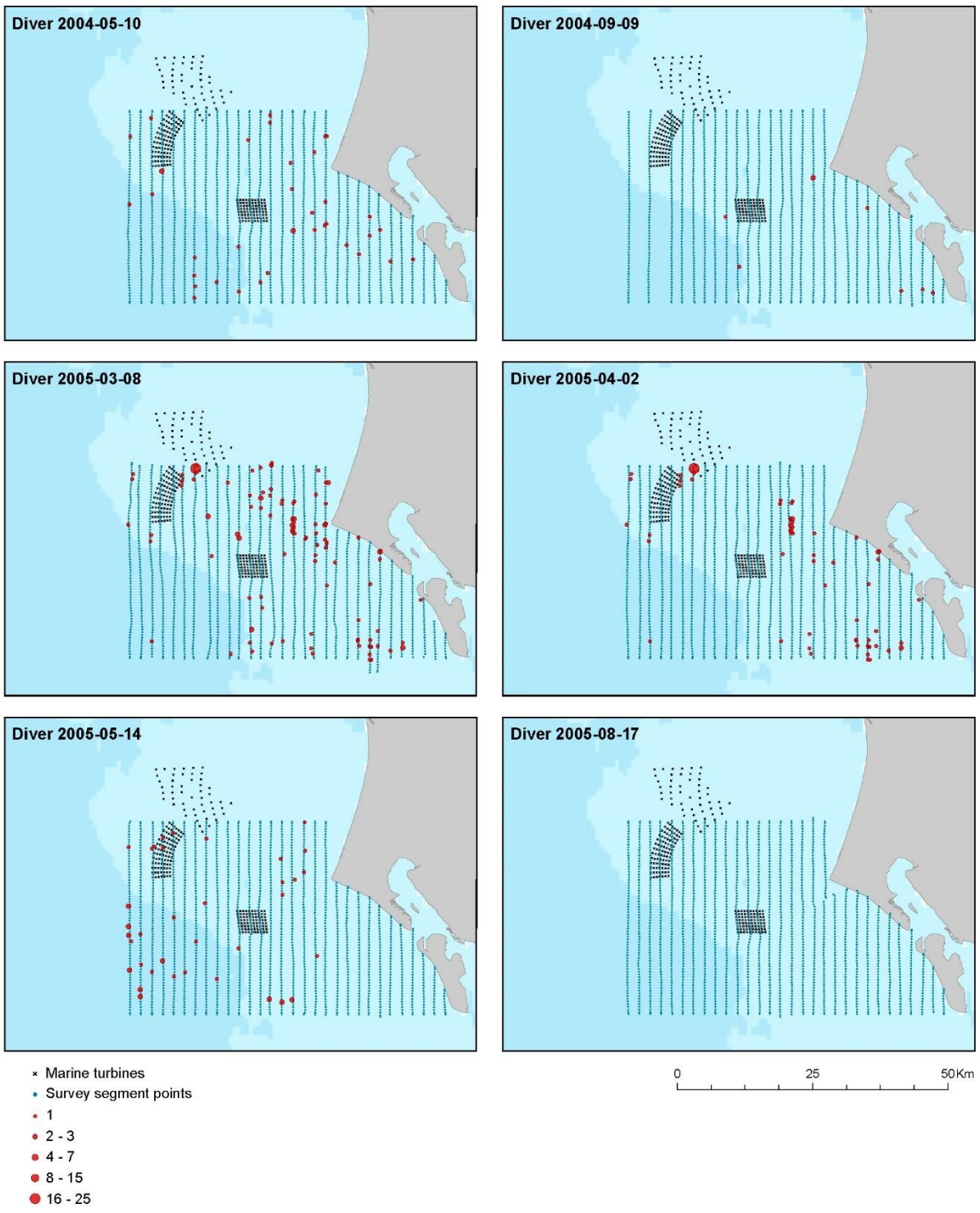

Figure 8.15. The distribution of observed red-throated diver/black-throated diver during six surveys from May 2004 to August 2005.

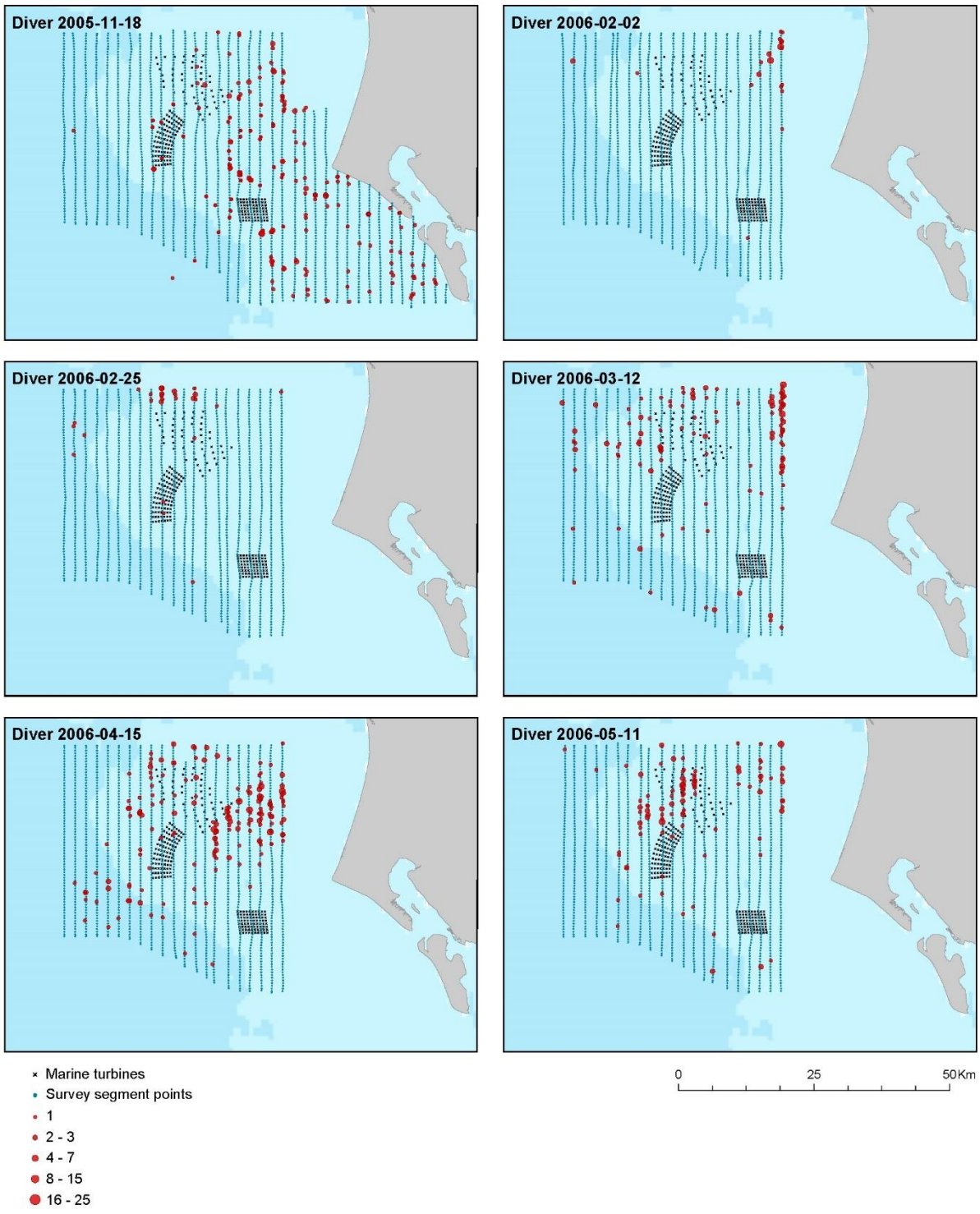

Figure 8.16. The distribution of observed red-throated diver/black-throated diver during six surveys from November 2005 to May 2006.

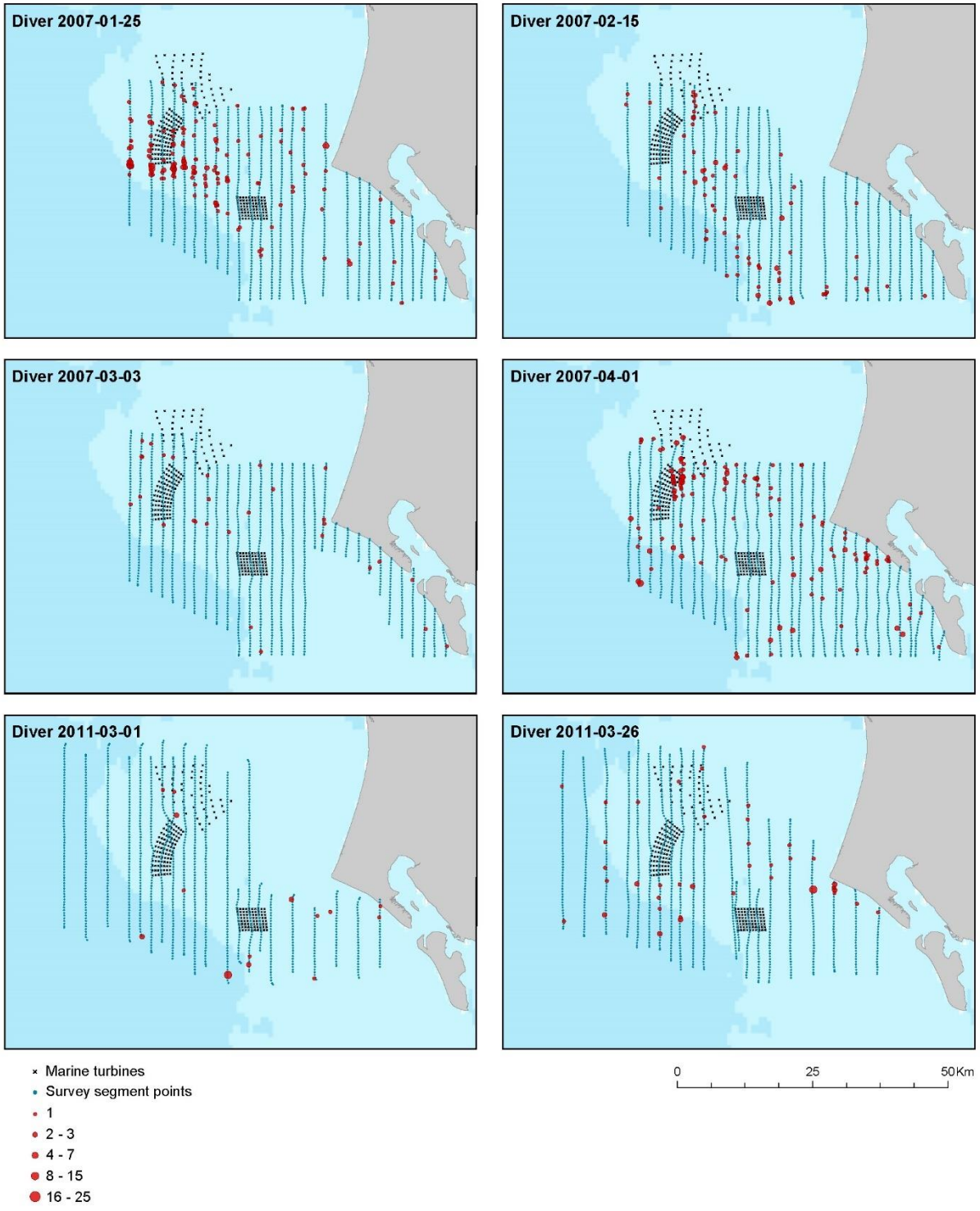

Figure 8.17. The distribution of observed red-throated diver/black-throated diver during six surveys from January 2007 to March 2011.

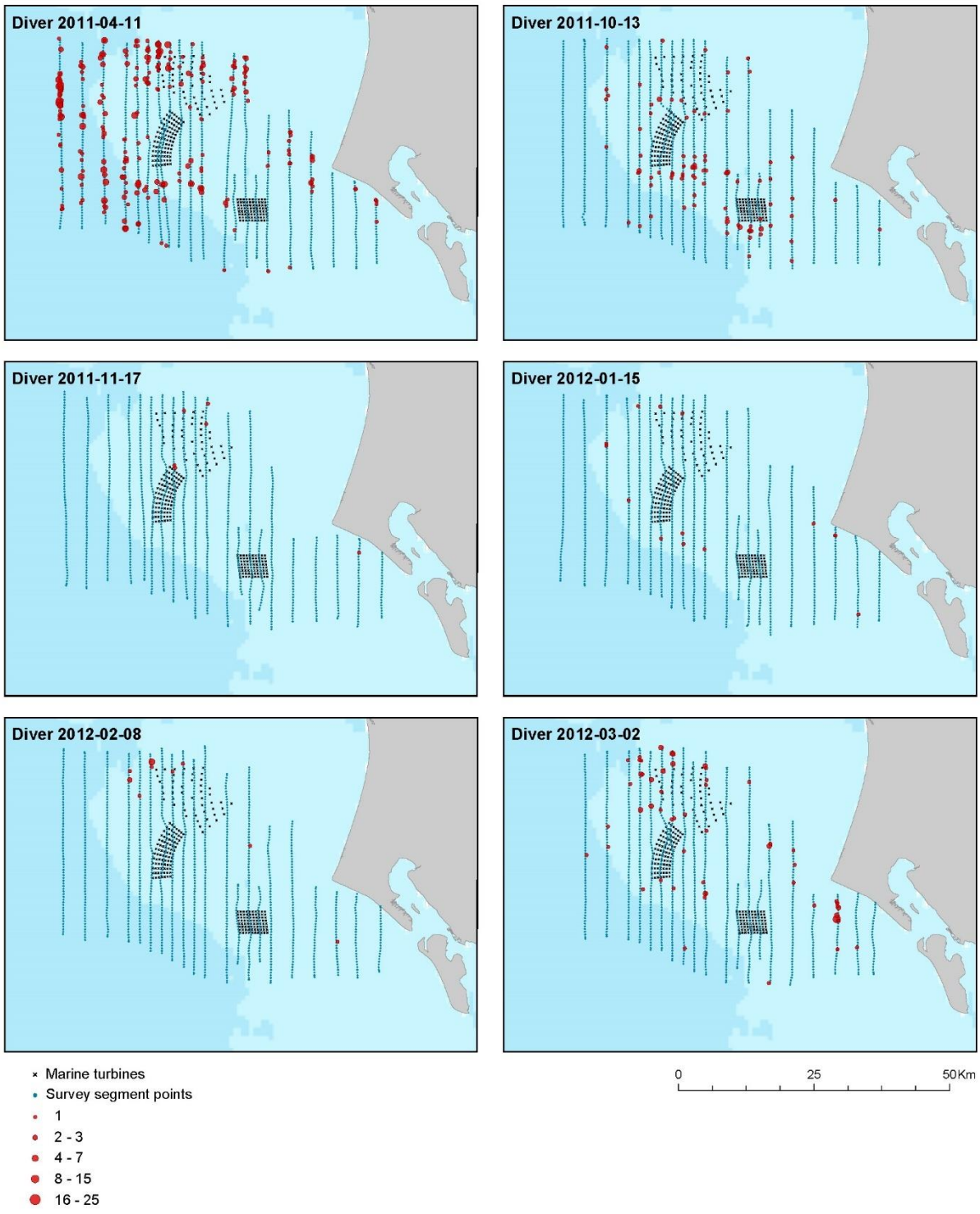

Figure 8.18. The distribution of observed red-throated diver/black-throated diver during six surveys from April 2011 to March 2012.

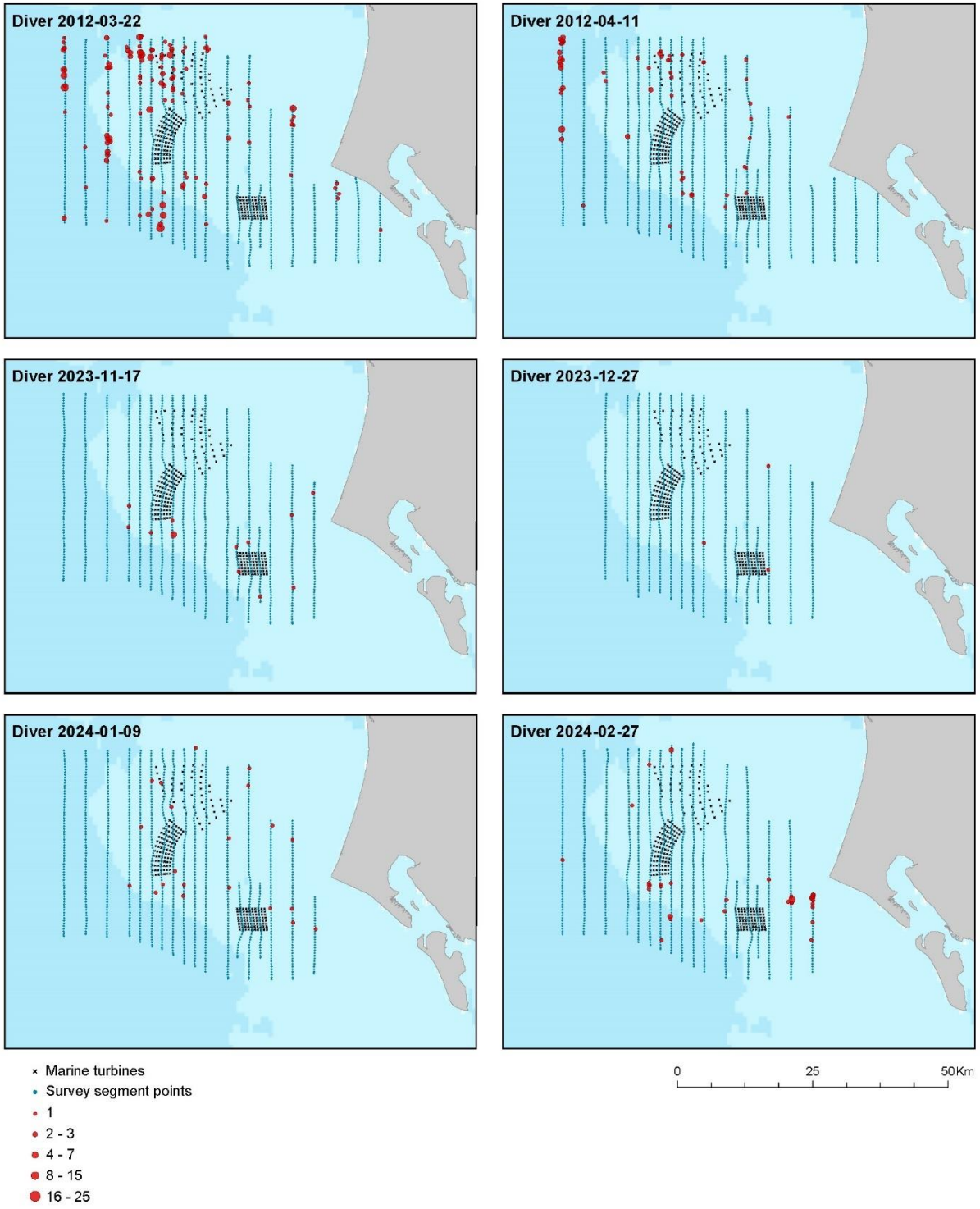

Figure 8.19. The distribution of observed red-throated diver/black-throated diver during six surveys from March 2012 to February 2024.

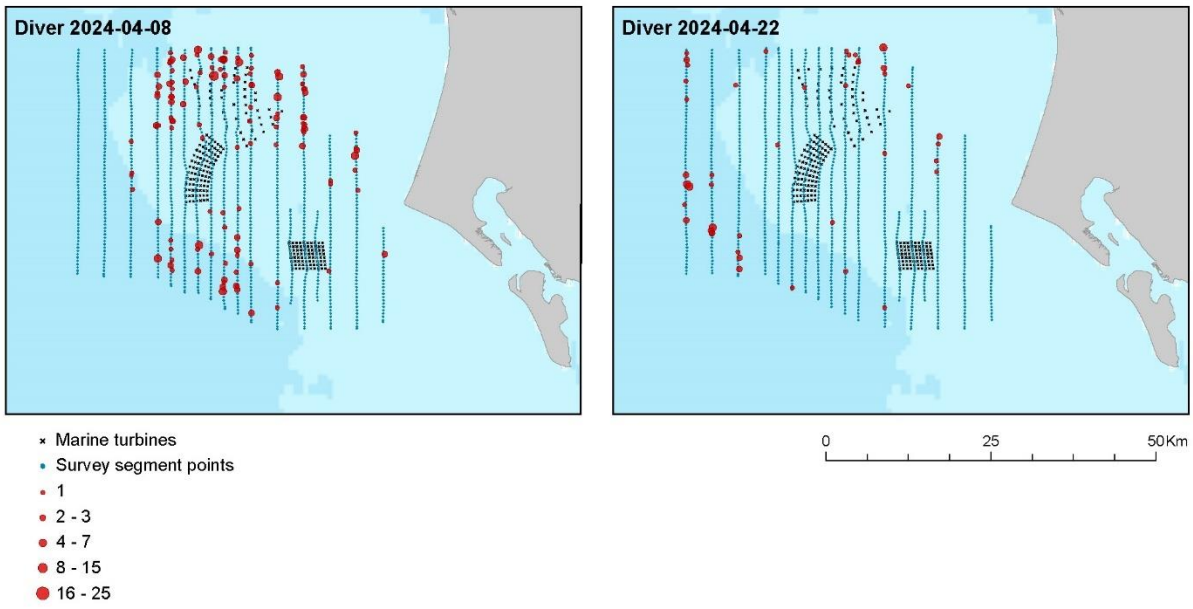

Figure 8.20. The distribution of observed red-throated diver/black-throated diver during two surveys in April 2012.

Appendix 2

Additional details for modelling methods

8.2 Additional spatial analysis details

The response variable for the spatial models under analysis here, are bird counts in a small area (segment) which have been corrected for detectability. This response was modelled using a Tweedie framework, which includes an estimated dispersion parameter (ϕ) and Poisson-Gamma mixing parameter (ξ) to return an appropriate mean-variance relationship in each case. The mixing parameter takes on values from 1 (equivalent to quasi-Poisson) and 2 (equivalent to Gamma). If the estimated parameter was close to one, the models were considered quasi-Poisson. A set of candidate explanatory variables were associated with each segment to model the signal, and in this study each of the 56 surveys was analysed separately, including covariate selection, for each species. The candidate environmental covariate was water depth (bathymetry, Figure 8.21) while distance from coast (Figure 8.22) (as a one-dimensional term) was also considered in each model, in the unlikely case there was compelling evidence for consistent spatial patterns with distance from coast which were the same in all directions. Additionally, to account for more realistic (and localised) surface patterns (due to perhaps unmeasured covariates) a spatial surface was also fitted to each model. Specifically, a two-dimensional CReSS-based surface using a Gaussian radial basis function was included in the model (Scott-Hayward, Oedekoven, et al. 2014).

As an illustration, the following equation represents an example of a Tweedie model with log link function and fitted with a one-dimensional smooth term (e.g., bathymetry) alongside a two-dimensional spatial smooth:

$$y_{ij} \sim Tw(\mu_{ij}, \phi, \xi)$$

$$\mu_{ij} = e^{\left(\beta_0 + s_1\left(\text{Bathymetry}_{ij}\right) + s_2\left(\text{XPos}_{ij}, \text{YPos}_{ij}\right)\right)}$$

where y_{ij} is the estimated count for transect i segment j and s_1 represents either a quadratic B-spline or natural cubic spline smooth of depth. Here, s_2 is a two dimensional smooth of space (with coordinates XPos and YPos in UTMs). Implicit in this model are also coefficients for the intercept (β_0) and any spline-based coefficients associated with the smooth terms. The effort associated with each observation varied depending on the associated segment area and so segment area was included as an offset term (on the log scale).

A globally applicable depth or distance to coast term and a more flexible spatial term were trialed for inclusion in each model, to indicate how best to model spatial patterns in each case. In particular, this quantifies if any spatial patterns are sufficiently described by the one-dimensional covariates (which applies the same across the surface) or if a more considered approach to spatial patterns was required for each survey and for each species. For example, if depth was selected and a two-dimensional spatial element was not deemed necessary (as determined by the model selection procedure governed by objective fit criteria) then this signals that any spatial patterns are primarily a function of the depth, regardless of the geographical location of this depth in the survey area.

If the two-dimensional spatial term was selected for inclusion in a model, then the spatial density patterns (over and above any environment-related terms) were accommodated using a spatially adaptive term which permits different amounts of flexibility across the surface in a targeted and yet parsimonious way (hence, relatively complex spatial patterns can be accommodated with very few parameters).

Selection between competing models was undertaken using an information criterion metric, BIC, which has a penalty related to the extent of the data supporting the model.

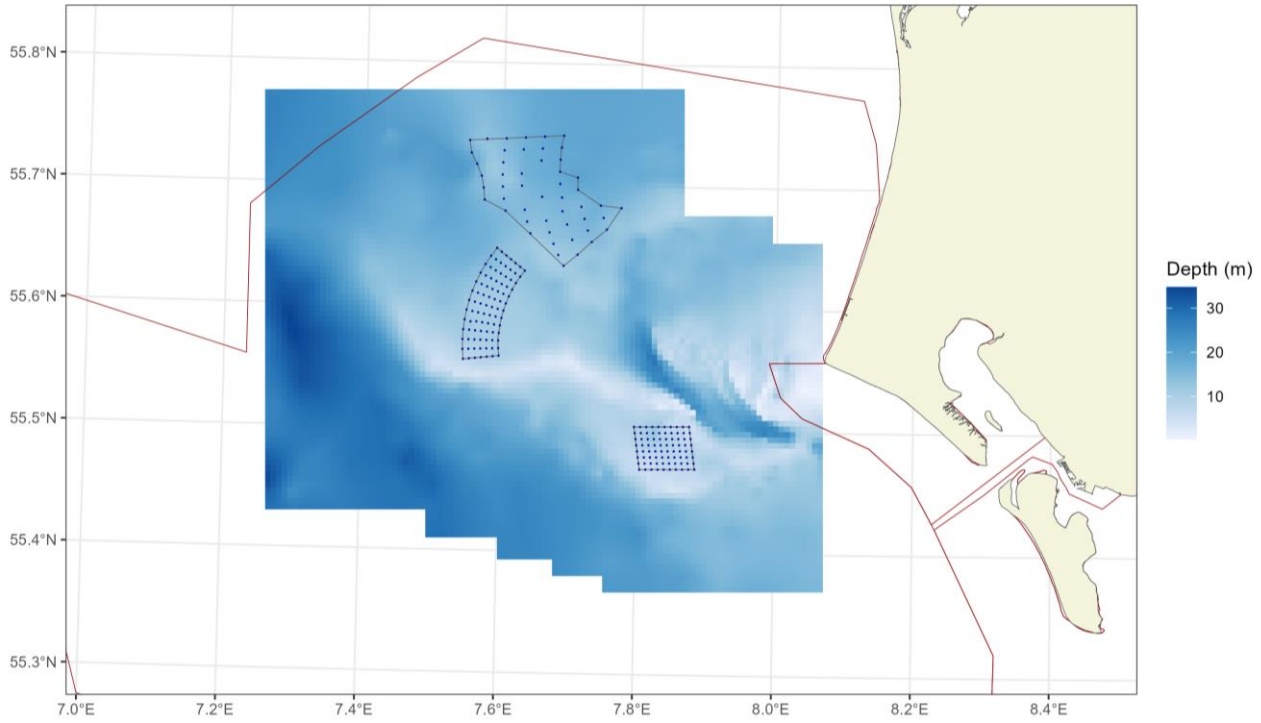

Figure 8.21. Visual representation of bathymetry (water depth).

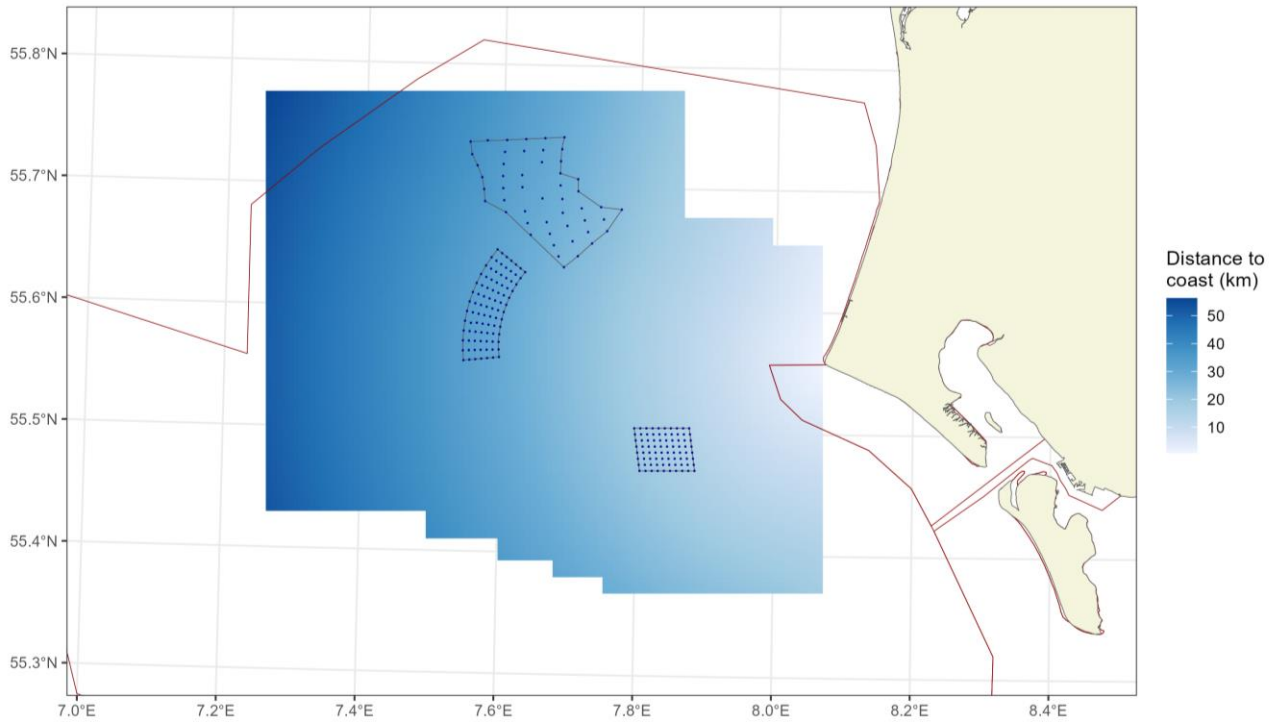

Figure 8.22. Visual representation of distance to coast.

The 1D smooth terms (for depth or distance to coast) were specified to be either a quadratic (degree 2) *B*-spline (*df* = 3,4,5) or a natural cubic spline (*df* = 2,3,4). In cases where these degrees of freedom boundaries were reached, however, a broader range of parameters were trialled instead. The degrees of freedom for these terms determine the flexibility of these smooth (and nonlinear) relationships - the more degrees of freedom, the more flexible the relationship can be.

The location of this flexibility (along the x-axis) in these terms (e.g., depth) was also determined as part of the model selection process. This permitted the relationship in some areas of the covariate range to be relatively complex (e.g., in shallow waters) and in other areas (e.g., in deep waters) to be relatively simple. In both smooth types, a maximum of three internal knots and the spline-specific number of boundary knots were permitted. An objective fit criterion determined the number and location of knots.

The spatial patterns in each analysis were based on a two-dimensional spatial term (of variable complexity). The flexibility of the spatial element constituted part of the model selection procedure and, for each survey, was determined using a Spatially Adaptive Local Smoothing Algorithm (SALSA). While this model selection element technically occurred between limits (*df* = [2,100]), the flexibility chosen in each case was not bounded in practice by those values since the selection procedure occurred well within the bounds of the specified range.

The *MRSeaPP R* package, designed to fit both CReSS and SALSA-type models when quadrature points are included, was used for model fitting. For computational reasons, BIC was used to determine the flexibility of the smooth terms (knot number and placement), while the more computationally intensive 5-fold cross-validation (CV) was used to govern the inclusion/exclusion of covariates (R Core Team 2022; Scott-Hayward, Mackenzie, and Walker 2023). The CV procedure attempts to balance the fit to data unseen by the model while minimising the number of parameters (parsimony). Note that this cross-validation was predicated on preserving correlated blocks of survey data (transect lines) so that any residual autocorrelation present was not disrupted when choosing folds. This was considered necessary to ensure independent sampling units under the scheme.

The assumed mean-variance relationship under the model was assessed visually using plots of the model's fitted values against the residuals' variance. In this analysis, Tweedie models were employed, which assume a nonlinear mean-variance relationship:

$$Var(y) = V(\mu)\phi = \mu^{\xi}\phi$$

ϕ is the dispersion parameter. The dispersion parameter was estimated for each model, and this estimate was used in the visual assessment of this mean-variance relationship assumed to hold under the model. ξ is the power parameter and is estimated before model fitting using a maximum likelihood profile approach. Based on the nature of the response data, the values of ξ were permitted between 1 (Quasi-Poisson) and 2 (Gamma).

QQ plots and residuals against predicted values plots were assessed to ascertain the level of agreement between the data and the model. These plots were created using the *DHARMa R* package and using simulated residuals.

Regarding interpretation (e.g. Figure 2.6), the left panel is a uniform QQ plot, and the right panel shows residuals against predicted values, with outliers highlighted in red. Given these outputs, we would expect that a correctly specified model shows:

a straight 1-1 line, and no compelling evidence against the null hypothesis of a correct overall residual distribution, as indicated by the *p*-values for the associated tests in the QQ-plot.

visual homogeneity of residuals in both the vertical and horizontal directions, in the residuals against predictor plot.

Pearson residuals for each model were also spatially visualised to ensure no areas of consistent bias across the survey area. This would be indicated by clusters of negative or positive residuals in spatially similar locations.

Residual independence was not assumed to hold under the model, and instead, model inference proceeded under robust standard errors. As described, Auto Correlation Function (ACF) plots (e.g. Figure 2.4) were instead used to check the suitability of this blocking structure via a "decay to zero" trend within blocks.

Appendix 3

Executive summary of modelling methods

8.3 Extra plots

8.3.1 Common scoter extra plots

The figures in this section are outputs for if the full Phase 1 set of surveys is used. No interpretation of these plots is provided.

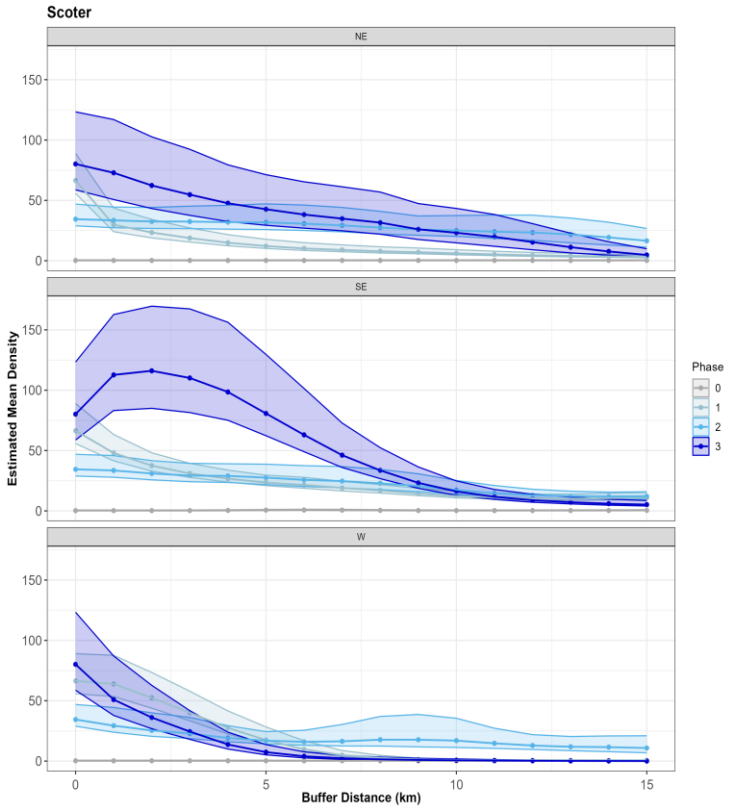

Figure 8.23. Figure showing the estimated densities in a sequence of 1 km buffers around the HR II windfarm.

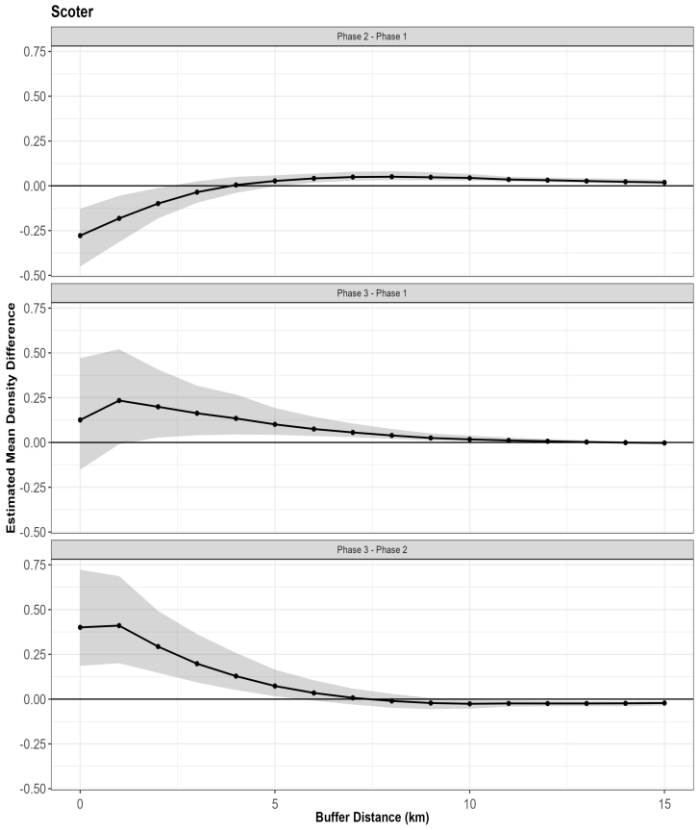

Figure 8.24. Changing density with distance from the wind farm footprint.

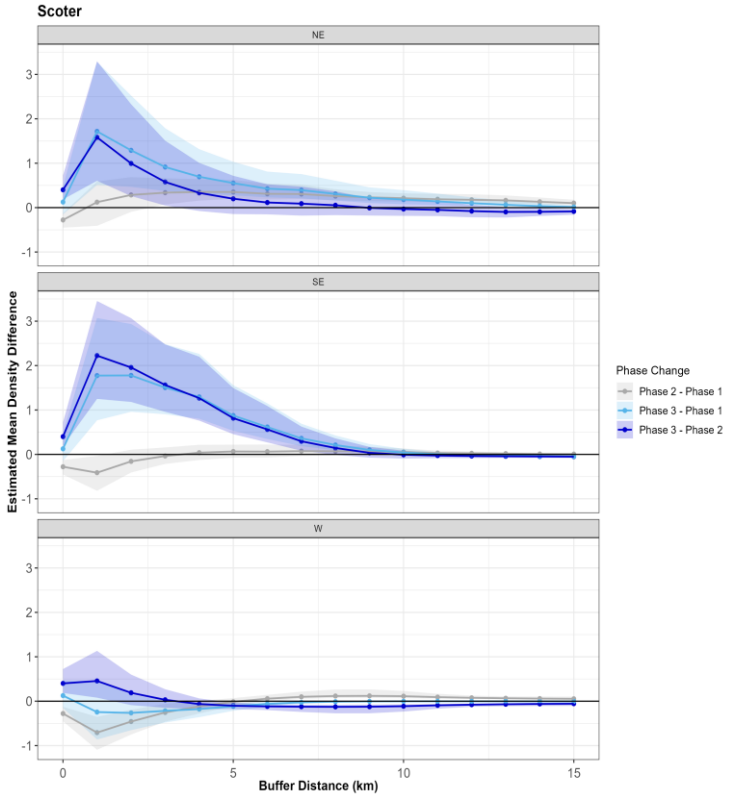

Figure 8.25. Figure showing the differences with distance to footprint by phase change and by sector.

8.3.2 Diver extra plots

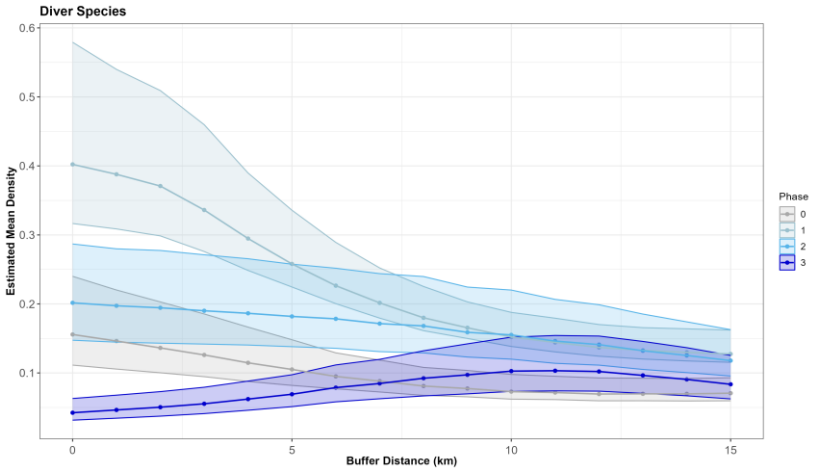

Figure 8.26. Figure showing the estimated densities in a sequence of 1 km buffers around the HR II windfarm.

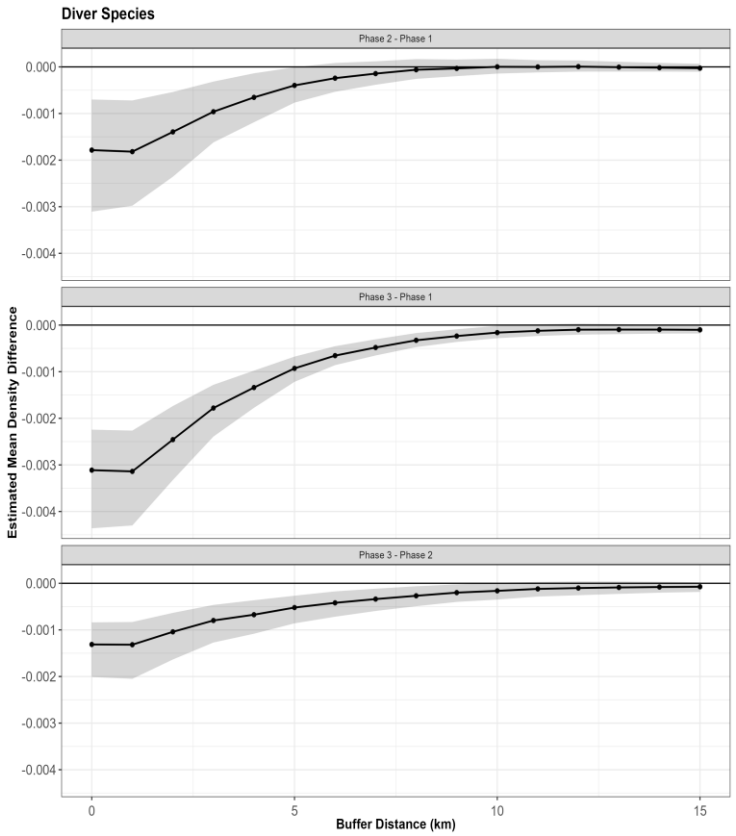

Figure 8.27. Changing density with distance from the wind farm footprint.

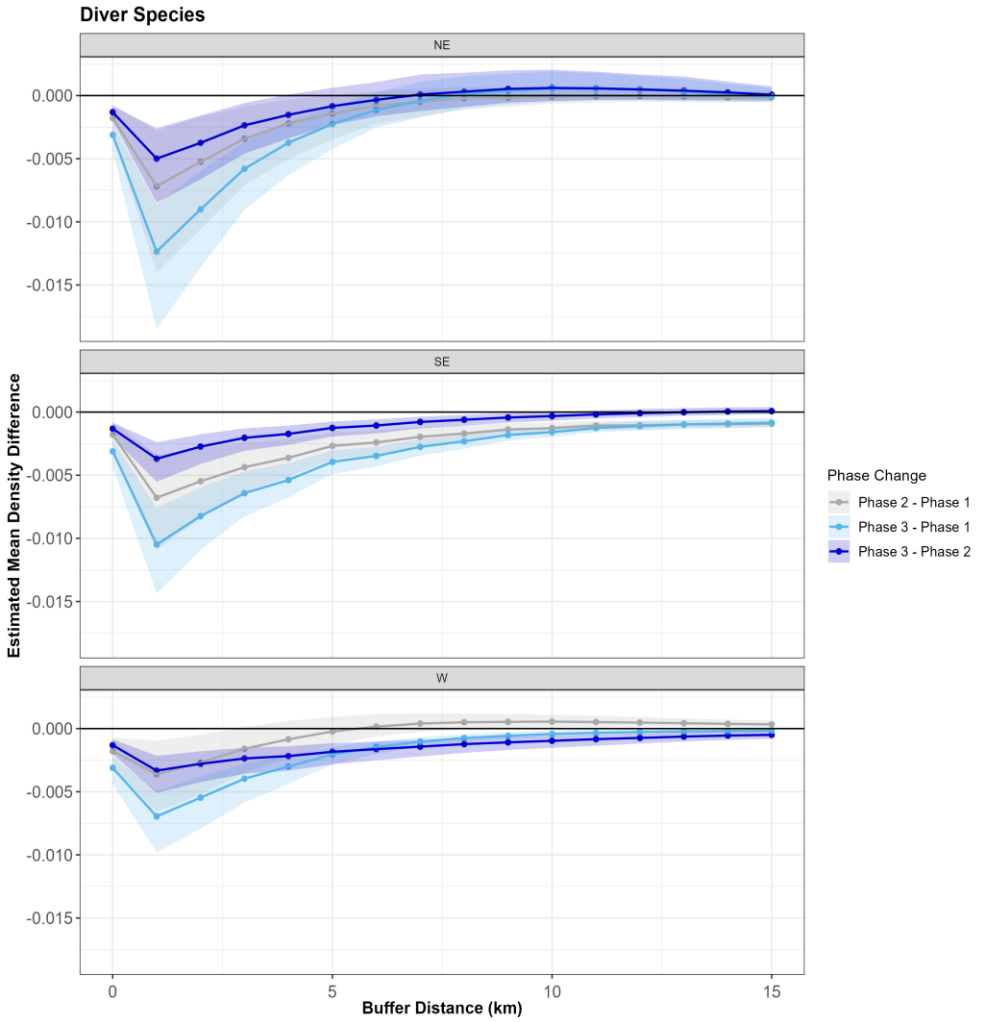

Figure 8.28. Figure showing the differences with distance to footprint by phase change and by sector.